THERMAL STUDIES OF FRUIT TREES IN RELATION TO LOW TEMPERATURE TRUNK SPLITTING

Dissertation for the Degree of Ph. D.

MICHIGAN STATE UNIVERSITY
ERIC RICHARD NORRIS

1976

This is to certify that the

thesis entitled

Thermal Studies of Fruit Trees in Relation
to Low Temperature Trunk Splitting

presented by

Eric Richard Norris

has been accepted t
of the requi

Ph.D. degre

Date August 6, 1976

ABSTRACT

THERMAL STUDIES OF FRUIT TREES IN RELATION TO
LOW TEMPERATURE TRUNK SPLITTING

By

Eric Richard Norris

The overall objective of the study was to ascertain the cause of low temperature trunk splitting in fruit trees. Based on the hypothesis that trunk splitting is caused by temperature extremes resulting in thermal stress in the trunk, investigations were carried out in the following specific areas:

1. Temperatures were measured in the trunks of fruit trees during two winters. On cold, clear days, it was found that the trunk was heated by the sun's radiation to temperatures well above ambient. Rapid cooling in the evening resulted in steep temperature gradients near the trunk surface.

2. Using a quartz tube dilatometer, the sub-freezing radial and tangential coefficients of thermal expansion of fresh Montmorency cherry wood were determined. Measurements were also made of the tangential coefficient of thermal expansion of Montmorency cherry bark. It was found that the coefficient of thermal expansion in the tangential direction was greater than in the radial direction in both sapwood and heartwood. Also, the corresponding coefficients of

thermal expansion were greater in sapwood than in heartwood. The thermal expansion determined was greater than could be explained based on the properties of wood or ice.

3. Fresh, frozen sections of Montmorency cherry sapwood were observed under the microscope. Extracellular ice was observed and the cells exhibited a shrunken appearance.

4. The temperature data and the coefficients of thermal expansion were used as input data to a finite element thermal stress analysis model of the tree trunk. The model was set up for plane strain in a cylindrical anisotropic material. The model predicted trunk surface tensile tangential stresses of the same order of magnitude as known tangential failure stresses in fresh wood.

Approved B A Stout, June , 1976
Major Professor

Approved D.R. Heldman, June , 1976
Department Chairman

THERMAL STUDIES OF FRUIT TREES IN RELATION TO LOW TEMPERATURE TRUNK SPLITTING

By

Eric Richard Norris

A DISSERTATION

Submitted to
Michigan State University
in partial fulfillment of the requirements
for the degree of

DOCTOR OF PHILOSOPHY

Department of Agricultural Engineering

1976

ACKNOWLEDGMENTS

The author wishes to thank his research director, Dr. B. A. Stout, for his many hours of advice, guidance and patient encouragement during the course of this study. The other members of the guidance committee, Dr. G. L. Cloud, Dr. L. J. Segerlind, Dr. F. W. Bakker-Arkema and Dr. R. A. Mecklenburg, were always willing to provide assistance during this work.

All of the faculty, technical and clerical staff and graduate students of the Department of Agricultural Engineering must be thanked for their help, advice and encouragement.

The author is indebted to Dr. C. R. Olien for the use of his laboratory facilities and his freely-given help and advice. The support of Dr. C. Van Den Brink and the Environmental Science Services Administration in the form of field laboratory facilities is gratefully acknowledged.

The people of Michigan, who provided funds and facilities for the execution of this study must also be thanked. The author is also indebted to McGill University for the study leave which made it possible to carry out this study.

Finally, the author wishes to dedicate this work to his wife, Bonnie, for her unending patience and understanding.

TABLE OF CONTENTS

LIST OF TABLES

LIST OF FIGURES

LIST OF SYMBOLS

B_i = body force in "i" direction, lb/in^3

E = modulus of elasticity (Young's modulus), lb/in^2

e = first invariant of strain tensor, in/in

e_{ij} = deviatoric strain component, in/in

i,j,k = indices indicating Cartesian coordinate directions (also, node numbers for finite elements)

K = bulk modulus, lb/in^2

n_j = unit normal in the "j" direction

R = index indicating radial direction

r = radius dimension

s = first invariant of stress tensor, lb/in^2

s_{ij} = deviatoric stress component, lb/in^2

T = change in temperature from a set point, °F

u_i = displacement in "i" direction, in

x_i = coordinate designation in the "i" direction

Z = index indicating axial direction

α = coefficient of thermal expansion (in/in)/°F (also, coefficient in displacement equation of finite element)

γ_{ij} = shear strain, in/in

δ_{ij} = Kronecker delta

ε = strain component, in/in

λ = first Lamé constant, lb/in^2

G (or μ) = second Lamé constant (shear modulus), lb/in^2

ν = Poisson's ratio, dimensionless

σ = stress component, lb/in^2

θ = index indicating angular measurement

Note: Other symbols may be defined within the text where utilized.

1. INTRODUCTION

1.1 Winter Injury

One of the problems facing many of the fruit industries in North America today is winter injury of the tree. A broad, comprehensive definition of winter injury is given by Jensen et al. (1970): "Winter injury is the generalized term which applies to damage to the tissue of a tree caused by an unfavorable temperature environment."

Winter injury in fruit trees can be divided into several more specialized types of damage, such as (1) crown injury, (2) crotch injury, (3) sunscald, (4) bark splitting, (5) trunk splitting, and (6) black heart. The specific injury on which this thesis is focused is trunk splitting. This injury is manifested by a vertical split in the tree trunk which extends through the bark and cambium and into the woody tissue. This wound is an open invitation for infestations of rots and cankers which, if left untreated, may eventually kill the tree. The trunk of a peach tree with a typical case of trunk splitting is shown in Figure 1.1. Notice the secretion of resin and the generally unhealthy appearance of the bark tissue surrounding the wound. If the tree is not killed this damage will seriously impair production for the rest of its life.

1.2 Extent of the Problem

Many fruit species are affected by trunk splitting. Some of the most severaly affected are the stone fruits such as peaches,

Figure 1.1 Typical case of trunk splitting (Photo No. 68-52)*

*Negative number, filed with Dr. B. A. Stout, Agricultural Engineering Department, Michigan State University.

cherries, plums and apricots. Larsen (1968) estimated that 25 percent of the peach trees planted in Michigan orchards do not reach bearing age because of this affliction. Jensen et al. (1970) reported that the average life of a peach orchard in Georgia is eight years, with an average of only five years of production. The major cause of this is winter injury of some type.

Trunk splitting is prevalent in the northern U.S. At the turn of the century, the state of Michigan boasted 12.5 million peach trees. In 1974, that figure stood at 1.48 million (Michigan Agricultural Statistics, 1975). Larsen (1968) stated that a major reason for this reduction is that farmers have gone out of the peach business because of repeated losses from trunk splitting. The five-year average peach production in Michigan from 1964 through 1968 was 118 bushels/acre. Larsen (1968) estimated that a good economic level of production would be 300 bushels/acre. A part of this depressed yield can be attributed to the decimation and general lowering of vigor of the orchard due to trunk splitting.

1.3 A Brief History of the Problem

Winter injury of fruit trees is not a new affliction for the fruit producers of North America. The problem has been here as long as the industry and has been responsible for the demise of certain segments of the fruit industry, especially in the northern regions. Larsen (1968) estimated that in the period from 1845 through 1925, ten of the 80 winters caused an "oustanding" amount of damage to fruit trees in the U.S. Almost all winters resulted in noticeable injury in Michigan orchards.

Tingley (1937) reported the loss of almost a complete orchard in the winter of 1933-34 due to a sharp drop in temperature to -31°F on December 30. Rawlings and Potter (1936) reported heavy injury to McIntosh apple trees in New Hampshire when a week of above-freezing weather was followed by a sharp drop in temperature. Anthony et al. (1936) reported severe injury in Pennsylvania orchards after a heavy frost in the winter of 1935-36. Brierley et al. (1950) reported damage to shoots, fruiting spurs, crotches and trunks of apple trees in Minnesota due to "seasonal peculiarities in the winter of 1947-48. Simons (1970) reported on the development of callus and phloem tissue around the cracks which developed in the trunks of Delicious and Starking apple trees in the winter of 1968-69. Distortion of tissues and necrotic areas restricted and often blocked the flow of metabolites in the phloem. As a result, the function of the transporation system of the tree was impaired.

From the above survey it is apparent that the problem of winter injury is widespread and has occurred over a long period of years. There are some very obvious common factors which are almost always mentioned in connection with winter injury. These are:

1. Tree immaturity: Winter injury occurs most often in younger orchards in the three- to seven-year age. The younger, weaker wood tissue is more susceptible to the problem.

2. Prior heavy crop: Winter injury is often observed in trees which have borne a particularly big crop during the

preceding season. Presumably, the strain of heavy fruiting leaves the tree in a weakened condition.

3. Early frost: If there is a sharp freeze early in the fall before "hardening off" occurs, the tree is more susceptible to injury.

4. Excess and/or late fertilizing: Application of large amounts of nitrogen late in the growing season can prevent "hardening off" and increase susceptibility to winter injury.

5. High winds: This is a factor that was mentioned less frequently but high winds are suspected of increasing the rate of heat transfer from the tree trunk and therefore developing larger and steeper temperature gradients.

6. Heavy pruning: A tree which has been heavily pruned is in a weakened condition and more susceptible to damage.

7. Thaw followed by a freeze: In almost all reported cases of trunk splitting, a prolonged thaw period in the middle of the winter was followed by a sharp freeze. It is believed that the tree takes up water during the thaw period and loses some winter hardiness. The subsequent heavy freeze finds the tree in a weakened, more vulnerable condition and the high moisture content is believed to result in greater tissue contraction upon freezing.

At this point it should be emphasized that in the many cases of winter injury cited in the literature, not all of the above conditions were present. In all cases, there was a similar type of situation. First, there was some combination of cultural and/or environmental factors which weakened the tree or decreased

its winter hardiness. Secondly, there was a sharp temperature drop which caused a high temperature gradient with respect to position and time in the tree tissue. Some combination of the above two general conditions was present in all cases cited in the literature.

1.4 Statement of Purpose

Judging from the wide impact of fruit tree trunk splitting and the long history of the problem, it would have been foolhardy to make the ultimate solution of the problem the goal of this study. In fact, the actual mechanism by which the splitting occurs is open to conjecture. Thus, the study was initiated with the goal of shedding more light on how and why trunk splitting occurs. With this overall goal in mind, more specific objectives and areas of study were formulated as follows:

1. Assuming that trunk splitting was a temperature-related problem, a knowledge of the temperatures within the fruit tree trunk during winter became necessary. Therefore, one part of the study was devoted to the study of tree trunk temperatures. This part of the study took the form of a survey of published data and also a field study in which trunk temperatures under Michigan conditions were obtained.

2. A plausible hypothesis was that trunk splitting occurs as a result of thermal contraction. Therefore, a portion of the study focused on the determination of the sub-freezing coefficient of thermal expansion of fresh fruit tree trunk materal. Factors considered were type of tissue (sapwood, heartwood or bark) and orientation within the tissue.

3. Since the tree trunk is made up of biological material, the thermal expansion phenomenon was likely to be a more complex process than that occurring in ordinary engineering materials. Therefore, a portion of the study was devoted to the visual, microscopic inspection of wood material at sub-freezing temperatures. The purpose of this portion of the investigation was to determine any physical processes which occur in living wood tissue during freezing and thawing. It was hoped that any observed changes in the tissue could be related to and help explain the thermal expansion data.

4. Keeping the overall goal of the study in mind, it was necessary to attempt to predict the stresses which occur in the tree trunk. Therefore, the final portion of the study was devoted to a thermal stress analysis of the tree trunk cross-section. Using temperature data from the field studies, and the coefficients of thermal expansion determined in the laboratory, a finite element model of thermal stresses in the tree trunk was developed.

2. REVIEW OF LITERATURE

2.1 Anatomy of the Tree Trunk

The gross anatomy of a tree trunk typical of a growing fruit tree is shown in cross-section in Figure 2.1. The part of the trunk which is known as "wood" is made up of tissue falling within the broad classification of xylem. The xylem serves two purposes--to provide structural strength and to conduct water upward for the use of the tree. When the tree reaches a certain age, the central portion of the xylem begins to die, forming a cylinder of "heart wood" which increases in diameter as the tree grows and matures.

Just outside the woody xylem is a thin layer of cells forming a complete ring around the trunk--the cambium. The cambium is made up of meristematic cells and the division of these cells is responsible for the increase in girth of the tree trunk. Cambium, being the trunk tissue primarily capable of cell division, is a most important part of the tree trunk.

The outer layer of the tree trunk is the bark. It is this layer which contains the phloem tissue which is responsible for conduction of the products of anabolism downward for the use of the roots. The bark also serves as a protective shield or cushion for the underlying cambium.

Far from being a uniform system within themselves, the tissues described above each are a very complex system at the cellular

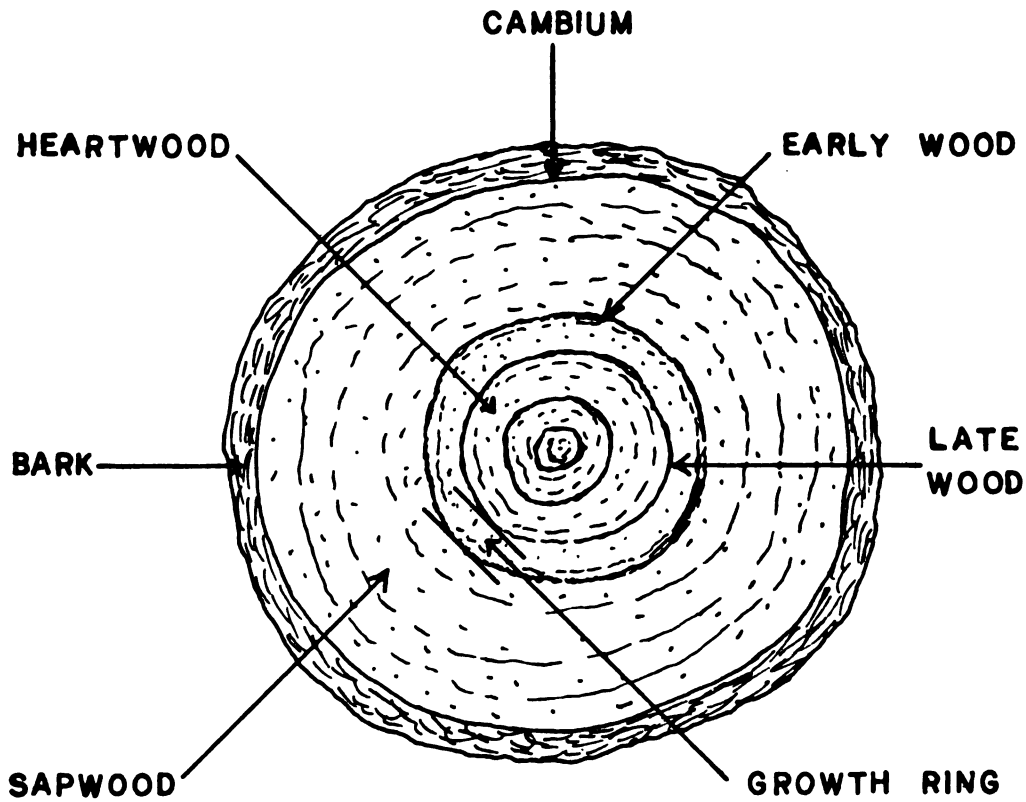

Figure 2.1.--Cross-section of a typical hardwood tree trunk.

level and some description of this diversity will shed some light on the physical properties associated with the tissues.

A diagrammatic representation of the structure of hardwood xylem as given by Sylvester (1966) is shown in Figure 2.2. The structure is made up mainly of fibers, vessels and parenchyma cells. The fibers are long, thick-walled cells with their long axes parallel to the trunk axis. They are coaxially arranged, overlapping each other longitudinally in a random pattern with their tapered ends forming overlapping butt joints. The vessels are very long cells parallel to the trunk axis which form the actual conduction tubes for water transport. They are surrounded by much shorter parenchyma cells. Perpendicular to the vessels and fibers, running in the radial direction, are the rays. These are bundles of parenchyma cells interspersed at random positions throughout the regular arrangement of the axial cells.

From an engineering point of view, this structure may be represented by the idealized schematic diagram of Figure 2.3 as given in Sylvester (1966). Due to the pattern of the growing season in temperate climates, the xylem is of a "ring porous" nature (Essau, 1965). The "growth rings" are formed as a result of a flush of growth in the spring followed by a slowing of growth in the summer with resulting alternate concentric rings of large, thin-walled cells (early or spring wood) and smaller, thick-walled cells (late or summer wood).

Bark is the non-technical term commonly applied to all tissues outside the vascular cambium (Esau, 1965). Since bark is of

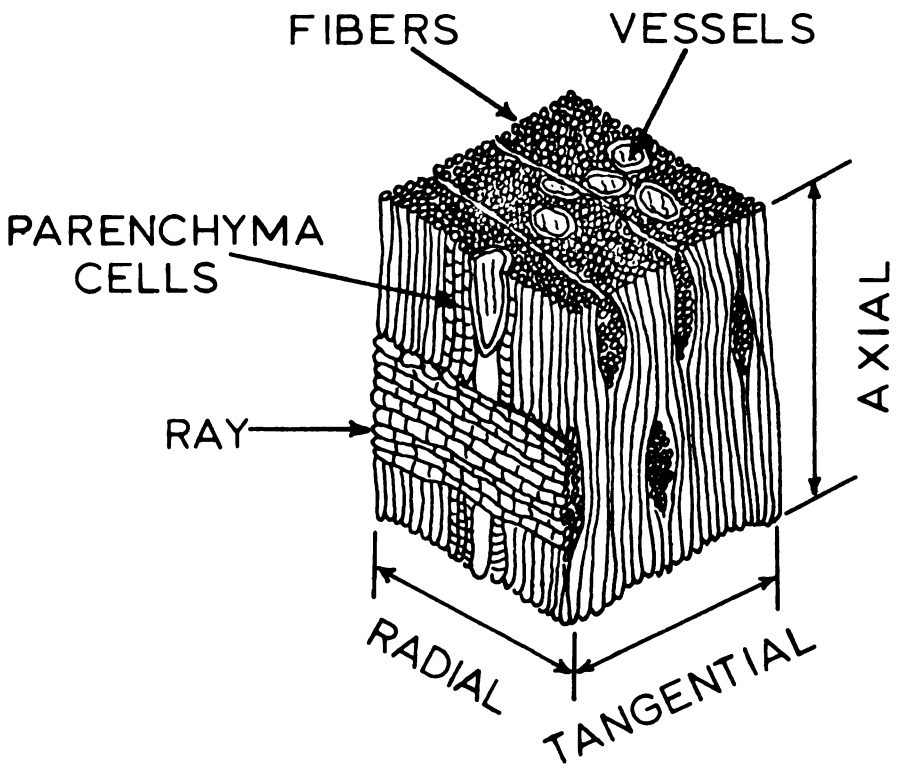

Figure 2.2.--Diagram of the structure of hardwood xylem (Sylvester, 1966).

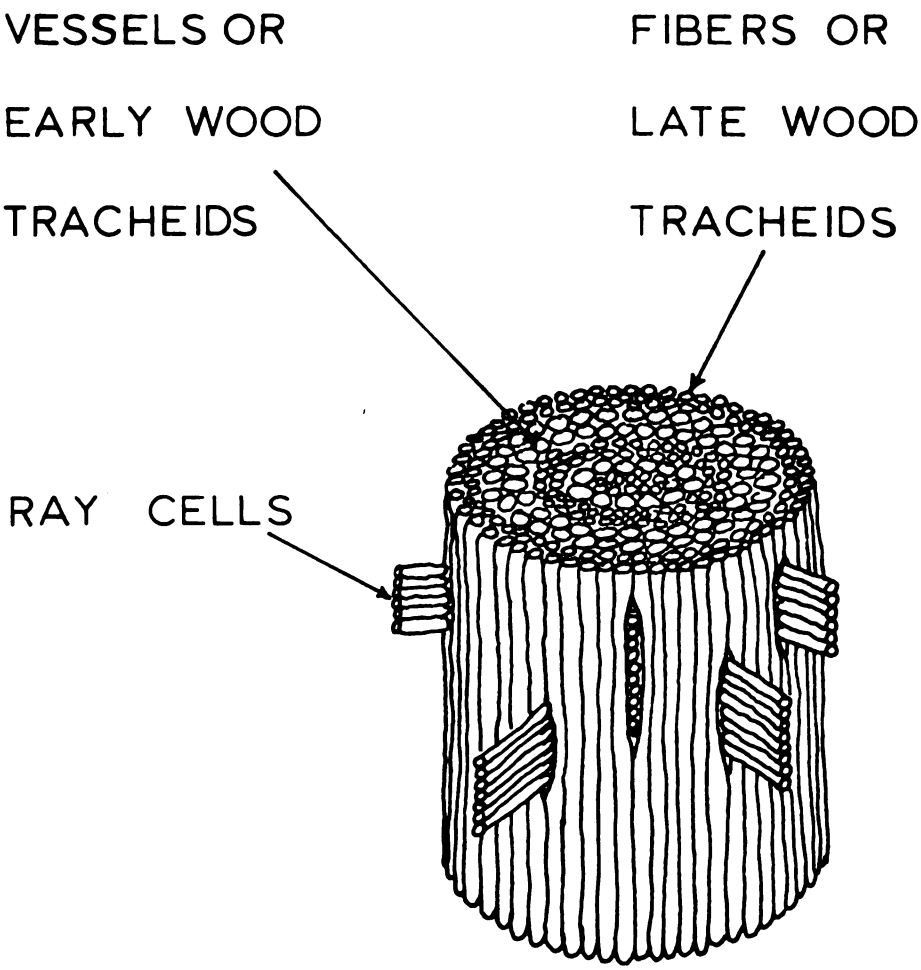

Figure 2.3.--Idealized diagram of the structure of a hardwood tree trunk (Sylvester, 1966).

less economic importance than wood, information on its anatomy and physiology is less abundant. In plants in a secondary state of growth such as a maturing tree, bark includes primary and secondary phloem, cortex and the periderm. Phloem is made up of sieve elements, parenchyma cells, fibers and sclereids. The structural strength of the phloem is concentrated in the sieve elements and fibers, whose long axes are parallel to the tree trunk axis. This was demonstrated by Diener et al. (1968b) who found that the inner bark of peach and cherry trees was much stronger in the axial rather than the tangential direction.

Periderm is a secondary, protective tissue (Esau, 1965). Peach and cherry trees possess a very distinctive periderm in that its fibers are quite specifically oriented in the tangential direction. Thus, the periderm, unlike the inner bark, has its strength concentrated in the tangential rather than the radial direction (Diener et al., 1968b).

2.2 Physical and Thermal Properties of Wood and Bark

The nature of the problem suggested that data on the directional strength properties and thermal expansion characteristics of fresh wood and bark would be necessary in this study.

2.2.1 Mechanical Properties

Since wood is one of the oldest structural materials, many studies have been made on its mechanical properties. Wangaard (1950) presents a compilation of data on a great number of species.

Included in his list is black cherry wood in the fresh condition which would be likely to have properties similar to domestic cherry wood. As in all data pertaining to wood, attention is paid to its anisotropic structure; values of properties are given for the directions parallel, perpendicular and tangential to the grain. This is in keeping with the engineering approximation of wood as an orthotropic material. Of interest in Wangaard's data are the comparatively low values of ultimate tensile strength perpendicular to the grain, in particular black cherry with a value of 570 psi. Kunesh (1968) reports an ultimate stress in radial compression of 450 psi for Douglas fir in the "green" condition. These values are in line with the range of 250 to 1,000 psi for hardwoods in tension transverse to the grain given by Stamm (1969).

Wangaard (1950) indicates that the strength of wood is increased by freezing; however, little quantitative information is given. Vorreiter (1938) reports a 50 percent increase in the bending strength of spruce timber when it is in the frozen condition.

The modulus of elasticity of wood is another important property. Wangaard (1950) gives a value of 1.31×10^6 psi for the modulus of elasticity (E) of fresh black cherry in the axial direction. The U.S. Wood Handbook (1974) indicates that estimates of the moduli of elasticity in the radial and tangential directions of wood can be obtained by multiplying the value for the axial direction by 0.10 and 0.05, respectively. These estimates are in line with Kennedy (1968) who measured modulus of elasticity for dry woods in transverse compression. Kennedy's values for E

had a range of 35,000 psi to 85,000 psi in the tangential direction and 65,000 psi to 105,000 psi in the radial direction. Kunesh (1968) found a modulus of elasticity in radial compression of approximately 30,000 psi for Douglas fir and Western hemlock in the "green" condition. Gerhards (1970) reported a decrease of 23 percent in the axial modulus of elasticity of Southern Pine in the green condition as compared with the dry condition.

The viscoelastic nature of wood and bark is an area which has received some study. The following paragraphs are a summary of studies in this area.

Bach and Pentoney (1968) studied the creep and recovery in longitudinal tension of hard maple in the air-dry to kiln-dry conditions. Even at these low moisture contents (4-12 percent d.b.), it was concluded that the mechanical behavior was nonlinear viscoelastic, and that the nonlinearity became more significant with increased moisture content, temperature or stress.

Diener et al. (1968a) performed static and dynamic bending tests on fresh Montmorency cherry wood and represented the material by a spring-Maxwell-Bingham (SMB) model. Good data fit indicated that the wood was, indeed, much more complex than a simple elastic material.

Mechanical properties of bark have been the subject of very little investigation since bark has been of marginal economic importance in the forest industry. Martin and Crist (1968) investigated the density, drying shrinkage, toughness, hardness, tensile, compressive and shear strength of various pine and hardwood barks.

Wide variations of physical and mechanical properties were found both between and within species. In general, the mechanical properties of bark displayed less anisotropy between the longitudinal and transverse directions than did those of green wood. This was explained on the basis of anatomy, since bark contains fewer longitudinal fibers and must gain its strength from the weaker sieve and parenchyma cells.

Diener et al. (1968b) investigated the directional strength properties of cherry, apple and peach bark. It was found that in all cases, the bark was strongest in the longitudinal direction and weakest in the tangential direction. The peach bark was much stronger in the tangential direction than the apple or cherry because of the presence of a strongly oriented periderm. The failure curves were quite dependent upon rate of deformation, that is, the behavior was viscoelastic.

2.2.2 Coefficient of Thermal Expansion

Most materials expand when heated and contract when cooled. Often, for a wide range of temperature, this change in dimension is directly proportional to the temperature change. The proportionality is expressed by the coefficient of linear thermal expansion, α, defined as the change in length per unit length for a temperature change of one degree (Johns, 1965). That is, it is the ratio of unrestrained strain because of temperature change (thermal strain) to the change in temperature causing that strain. The units of α are in/in/deg = deg^{-1}.

As opposed to the well-behaved case described above, the coefficient of thermal expansion of many materials is a function of temperature (Hoyle, 1964). Therefore, the value of α reported in experimental studies should be accompanied by the temperature range over which the measurement was made.

An early investigation of thermal expansion of woody material was reported by Joule (1859). He observed that the "expansibility" of bay wood in the transverse direction was approximately ten times that in the longitudinal direction. This is a conclusion borne out by the work of more recent researchers. Joule also observed that the thermal expansion of wood was increased by the application of a constant tensile force, and that heating relieved various types of mechanically-induced permanent sets in wood. These observations are some of the first indications of the viscoelastic nature of wood and the temperature dependence of its mechanical properties.

Joule also made observations regarding the effect of moisture content on thermal expansion. It is likely that some contraction phenomena which he reported were actually due to drying of the specimen because of poor moisture content control. Thus, he pointed out the strong relationship between moisture content change and dimensional change.

Values for the coefficient of thermal expansion of "dry" wood are available in handbooks. Marks (1964) gives values of 3.39, 25.7 and 34.8 x 10^{-6} $°C^{-1}$ for the coefficient of thermal expansion of wood in the longitudinal, radial and tangential directions, respectively. Perry (1950) states a range of 2.57 to

9.51 x 10^{-6} $°C^{-1}$ for the longitudinal direction and 32.5 to 61.4 x 10^{-6} $°C^{-1}$ for the transverse direction for various species of wood. Weatherwax and Stamm (1947) measured the axial, radial and tangential coefficients of thermal expansion between -50°C and +50°C of nine species of commercially important wood and reported the following ranges of values:

axial	(2.89 to 4.28) x 10^{-6} $°C^{-1}$
radial	(21.8 to 30.7) x 10^{-6} $°C^{-1}$
tangential	(29.7 to 42.7) x 10^{-6} $°C^{-1}$

Stamm (1969) gives a method of approximating the coefficient of thermal expansion in the tangential and radial directions by the following formulae:

$$\alpha_R = 45\ \rho_0 \times 10^{-6}\ °C^{-1} \qquad \text{(radial)}$$

$$\alpha_\theta = 58\ \rho_0 \times 10^{-6}\ °C^{-1} \qquad \text{(tangential)}$$

where ρ_0 is the dry specific gravity of the wood.

For the purposes of this study, the above values are of marginal value. They are often given for simply "wood" with the species unspecified, or if the species is known, it is for some species which is important to the forest industry. Also, these values are given for "dry" lumber. The concern of this study is with moist, living tissue of fruit tree trunks. Information in this specific area is quite sparse.

In the usual sense, thermal expansion and contraction is considered to be that dimensional change resulting from changes in

atomic excitation for different temperatures. In the case of living wood tissue there is evidence to suggest that temperature-related dimension change arises both from the above cause and from thermally induced water absorption and desorption within the cell structure. In general, the swelling and shrinking because of moisture migration are of such a magnitude as to overshadow the effects of the usual thermal expansion phenomenon.

2.2.3 Moisture Movement and Dimensional Change

The movement of water within wood and the process of drying has been the object of considerable research by investigators interested in the utilization of forest products. Their main interest has been the investigation of stresses that develop within wood as drying takes place under various conditions of temperature, pressure and humidity.

Skaar and Simpson (1968) made a comprehensive survey of moisture sorption phenomena in woody tissue. Water occurs in wood in three forms--free water, water vapor and hygroscopic (bound) water in the cell walls. When there is only hygroscopic water present in sufficient quantity to saturate the cell walls, the wood is at the so-called "fiber saturation point."

Choong and Fogg (1968), from measurements of water sorption in wood in the hygroscopic range, concluded that moisture movement occurred in the form of both vapor and bound water in all moisture content ranges. Radial movement was more readily achieved than

tangential movement. Movement in the form of vapor predominated in the axial direction.

Kass (1965) measured the stresses developed in wood specimens when externally restrained while drying. His observations led to the conclusion that water tension forces in the wood fibers played a distinct role in the development of drying stress.

Youngs and Bendtsen (1964) used a stress function approach similar to the Airy stress function to predict drying stresses in oak wood.

Erickson et al. (1968) showed a greater shrinkage of wood material when freeze-dried than when dried by conventional means. In their study on Sitka spruce, the total radial and tangential shrinkage of wood samples subjected to different drying treatments was determined. The study showed that prefreezing of the wood samples decreased the total shrinkage in both grain directions, regardless of the subsequent drying treatment. Also, freeze-drying resulted in greater total shrinkage in both grain directions regardless of previous or subsequent treatments. Further studies by Erickson and Petersen (1969) on black walnut indicated a significant decrease in wood shrinkage during drying, if the wood were first prefrozen. No explanation was offered.

Skaar and Simpson (1968) outlined the various factors which interact to define the complex temperature-moisture-expansion phenomenon in wood. First there is the usual thermal expansion effect which occurs because of the change in excitation of the atoms of the material with temperature. For wood in the hygroscopic

range, the water within the cellulose also expands with increasing temperature, adding another component to the system. When wood is heated in water, there is a water loss from the cell wall to the free water since the vapor pressure of the hygroscopic water increases more quickly than that of free water. In general, it has been found that this last effect predominates and wood will actually shrink when heated in water, as has been demonstrated by Yokota and Tarkow (1962).

Martin (1968) has reported the only data available on the expansion of bark material. In the hygroscopic range, the volumetric change of bark with changing moisture content is in the same range as that for wood.

2.3 Tree Trunk Temperatures in Winter

Based on the premise that winter injury occurs because of some extreme conditions of temperature, the temperature field existing in the living tree trunk during the course of a winter day became of interest. A pioneer investigator in this area was Harvey (1923). His observations from miniature thermocouples embedded in the cambium and sapwood of apple and plum trees in a Minnesota orchard can be summarized as follows:

1. The highest cambium temperatures occurred on surfaces perpendicular to the incoming rays of the sun.

2. A direct wind of 50 fpm cooled the heated cambium to ambient temperature in a matter of two to three minutes.

3. Passing clouds caused a wider variation in cambium temperature than in air temperature.

4. A short halt in temperature rise or fall was experienced at the point of freezing or thawing.

5. Supercooling of approximately 5°C was observed before the trunk moisture froze.

6. The variation of sapwood temperature lagged that of cambium temperature and was less extreme.

7. Cambium temperatures on the northerly exposure of the trunk of 2 to 3°C lower than ambient were observed.

8. Cambium temperatures of 13°C above ambient on the southern exposure were observed.

9. A rise of cambium temperature of 10°C in three minutes was observed upon sudden exposure to direct sunlight.

Eggert (1944) measured cambium temperatures of peach and apple trees in New Hampshire. His findings generally corroborate those of Harvey with these differences and additions:

1. In peach trees, the peak cambium temperature occurred between 12 noon and 2:00 P.M. Cambium temperatures of 60 to 80°F were common with the temperature rise above ambient on the order of 50 to 55°F.

2. In apple trees, the peak cambium temperature occurred between 3:00 P.M. and 5:00 P.M. Temperatures as high as 60°F were observed with a usual temperature rise over ambient of 30-35°F.

3. A north wind had little lowering effect on the peak cambium temperature whereas a very weak south wind caused a sharp temperature drop.

4. A "hazy" atmosphere sharply decreased the peak cambium temperature.

6. An application of white paint to the tree trunks decreased the peak temperature to approximately 10°F above ambient.

Jensen et al. (1970) measured cambium and mid-trunk temperatures, and soil temperatures as well as wind velocity and direction in a Georgia peach orchard. Some pertinent observations from this work are:

1. Cambium temperatures on the south side of the trunk were higher in February (95°F) than in May (85°F). This was because of a greater incident radiation resulting from the lower angle of incidence of the sun's rays and the lack of protective foliage in the winter.

2. At night, a drop in cambium temperature of 70 to 80°F in a matter of a few hours was quite common.

3. Protective coatings attenuated the temperature peaks and decreased the rate of change of temperature. Fiberglas batting with a bonded aluminum reflector was most effective followed by a single layer of aluminum foil and white paint.

4. The maximum cambium temperature moved around the tree from southeast to southwest as the day progressed.

5. The peak mid-trunk temperature was reached after the temperature of all parts of the cambium and the ambient temperature had begun to drop.

6. A "strong" wind reduced the mid-trunk temperature rise from 15 to 20°F to approximately 2°F.

Konstantinov and Batalov (1972), in a study of winter hardiness, measured the temperatures at various heights at the surface and at various depths on the north and south sides of apple, birch and pine trees. Their results were similar to those of Harvey and Eggert; they also found that the height above snow level was a significant factor. On clear, sunny days, the temperatures in the lower portion of the trunk were elevated because of the additional load of radiation reflected from the snow surface.

From the above observations, it is obvious that many factors affect the temperature pattern in a tree trunk. Derby and Gates (1966) performed a comprehensive study of this problem and developed a finite difference computer solution for the prediction of temperatures under various conditions. The program considered boundary conditions of the combined effects of direct solar radiation, reflected solar radiation, long wave thermal radiation, air temperature and wind speed. Material properties considered were bark absorptivity, specific heat and thermal conductivity. Provision was made for radial differences in specific heat and conductivity to account for the differences in properties of bark, sapwood and heartwood. Because of the anisotropic nature of wood, thermal conductivity was varied in both the radial and tangential directions. The only factor not considered was the effect of translocation of water and metabolites within the trunk. Comparisons were made with the experimental work of Eggert (1944). Predicted maximum cambium temperatures fell within the range of the measured temperatures despite the many approximations which were made. Eggert's

measurements indicated a range of maximum cambium temperature from 10°C to 16°C, occurring between 3:00 P.M. and 5:00 P.M. The maximum cambium temperature predicted by the program was 12.5°C occurring at approximately 2:00 P.M. (This was using input data to simulate a tree and climatic situation equivalent to that reported by Eggert.)

Derby and Gates (1966) also made a limited number of measurements on a living aspen tree with results which corresponded quite well with predicted values. For example, the data for a particular day reported by Derby and Gates shows an actual maximum cambium temperature of 15°C on the southernmost point of the tree occurring at 12:30 P.M. The computer simulation predicted a temperature of 17°C occurring at 1:00 P.M.

The physiological implications of elevated temperatures occurring in woody tissue during winter are a new area of research. Konstantinov (1971) and Konstantinov and Batalov (1972) compared the winter hardiness of tissues from the north and south sides of apple, birch and pine. In all cases, when the trunk had been subjected to a number of days during which the south side reached elevated temperatures, the winter hardiness of the tissue was reduced. One of the physiological features of frost-hardy cells is the development of a thick layer of protoplasm with a resultant decrease in vacuole size (Krasavtsev and Tutkevitch, 1971). This is believed to have an effect on the mechanism of ice formation in plant tissues.

2.3.1 Ice Formation in Plant Tissues

Parker (1963) reviewed the question, "Does ice form inside or outside plant cells?" His assessment at that time was that there was no general agreement by researchers on this question. Most researchers reported that ice formed exclusively in the intercellular spaces, and tended to dehydrate the protoplasm within the cells. Generally, it was agreed that intracellular ice occurred only upon "fast" freezing; however, no dividing line between "fast" and "slow" was proposed.

In 1970, Weiser indicated that researchers in the field of frost hardiness were still concerned about the amount, location and physical nature of ice formation in plant tissues, and had not yet reached complete agreement.

Krasavtsev (1968) from microcalorimetric studies, determined that there was an increase in the amount of ice in woody cells as the temperature was depressed further below the freezing point. Since his samples survived freezing to -60°C, he concluded that the ice formed was extracellular and that the cells dehydrated as the temperature is lowered.

Olien (1964), in studying the freezing of the barley plant, concluded that a movement and change of phase of the water had to take place to equilibrate the vapor pressure of intracellular material, extracellular water, and extracellular ice.

Further work by Krasavtsev (1970) showed that the rate of water outflow from woody cells as the temperature was lowered was

directly related to the frost hardiness of the species. He concluded that a physiological difference affecting cell wall permeability was the reason for these differences. This conclusion was substantiated by Evert and Weiser (1971), Ishmukhametova and Khokhlova (1971), and Glerum (1973) who showed differences in the electrical properties of plant tissues of the same species but varying in winter hardiness.

Krasavtsev and Tutkevich (1970) and Krasavtsev (1973) performed microscopic investigations of ice formation in elder and apple shoots. They found that intracellular ice formed when the rate of cooling of the tissue exceed 3°C/min. Their conclusion was that the formation of intracellular ice was always fatal, and occurred when the rate of cooling was too fast for moisture migration out of the cell to prevent ice formation.

These observations conflict somewhat with those of Sakai and Otsuka (1967) who demonstrated that cortical parenchyma of mulberry could survive rapid cooling by immersion in liquid nitrogen, followed by rapid thawing in 30°C water. However, Sakai and Otsuka first "precooled" their specimens slowly to -30°C before immersion in the liquid nitrogen. The slow "precooling" is very similar to the procedure used by Krasavtsev and Tutkevich (1970) and would result in a major portion of the cell's freezable water leaving the cell before the rapid cooling. Further work by Pogosyan (1971) and Pogosyan and Sakai (1972) on freezing and thawing of grapevines showed that there was really no disparity between the work of Krasavtsev and Sakai.

McLeester et al. (1969) and Quamme et al. (1973) studied the exotherms of woody tissues as the temperature was lowered slowly. Both studies showed three distinct temperature "rebounds" during the cooling process, indicating the rapid freezing of some portion of the water in the tissue. Two exotherms occurred above -20°C; a third occurred at approximately -40°C. Both studies concluded that the first exotherm occurred because of the freezing of supercooled extracellular water; the second exotherm resulted from the freezing of supercooled water extracted from the cells; the third exotherm, which was associated with tissue injury or death, was explained as resulting from the freezing of intracellular water. These results are similar to those of Brown et al. (1974) who found "plateaus" in the freezing curves of fruit and vegetable tissues.

The freezing of water in a plant material is an example of the Stefan problem originally formulated by Stefan in 1889 and studied comprehensively by Rubenstein (1971). The original problem considered by Stefan was the analysis of freezing of groundwater. The general Stefan problem includes any situation in which there is a diffusion of heat accompanied by a change of phase or state. Rubenstein (1971) has compiled the major recent solutions of particular cases of the Stefan problem. Closed form analytical solutions are available for only problems with relatively simple geometry. Irregular geometry or time varying boundary conditions make numerical solution of the problem the only feasible method of attack.

2.4 The Theory of Thermal Stress

2.4.1 General Theory-- Thermoelasticity

In order to develop an understanding of the stresses which can occur in a body as a result of a temperature field, it is necessary to consider the theory of thermal stresses. The assumptions basic to the theory of linear isotropic thermoelasticity are outlined by Boley and Weiner (1960) as follows:

(1) Temperatures are independent of deformations (i.e., no thermal coupling).

(2) The deformations are small (infinitesimal).

(3) The deformations are elastic.

In the case of tree trunks, assumption (2) is open to some question; assumption (3) must be seriously questioned. Modified theory will be considered in Section 2.4.3 to account for the viscoelastic nature of wood materials.

Thermal stresses in isotropic materials can arise from two causes:

(1) External constraints on a thermally expanding body,

(2) A non-uniform temperature field within the body.

For the problem under consideration, (1) does not come into play. Thermal stresses which may develop will be the result of a non-uniform temperature distribution. In order to visualize this type of stress, consider the body to be made up of infinitesimal cubical elements. A uniform temperature rise causes equal expansion of each cube. As a result, the cubes fit together with no stress,

regardless of temperature. However, with a non-uniform temperature field, each cube tries to expand to a size different than its neighbor. The constraint of adjacent cubes prohibits free expansion. The result is a thermal stress.

In order to describe the stress field, one must consider the components of strain at a point. From the above discussion it is apparent that the strain at any point in a body subjected to a non-uniform temperature field is made up of two parts. First, there is the strain due to uniform thermal expansion which can be represented by $\alpha T\delta_{ij}$. Secondly, there is the strain required for continuity as defined in linear isothermal elasticity. Thus, the strain at a point can be written as

$$\epsilon_{ij} = \frac{1 + \nu}{E} \sigma_{ij} - \frac{\nu}{E} \sigma_{kk} \delta_{ij} + \alpha T \delta_{ij} \tag{2.1}$$

Expressing the stress in terms of strain, equation (2.1) becomes

$$\sigma_{ij} = [\lambda e - (3\lambda + 2\mu)\alpha T]\delta_{ij} + 2\mu\epsilon_{ij} \tag{2.2}$$

As in isothermal elasticity, the conditions of equilibrium must hold. These are represented by

$$\frac{\partial \sigma_{ij}}{\partial x_j} + B_i = 0 \tag{2.3}$$

By the same token, the same relationship exists between strain and displacement as in isothermal elasticity.

$$\epsilon_{ij} = \frac{1}{2} \gamma_{ij} = \frac{1}{2} \left(\frac{\partial u_i}{\partial x_j} + \frac{\partial u_j}{\partial x_i} \right) \tag{2.4}$$

The general thermoelastic problem is, therefore, to determine $6\sigma_{ij}$, $6\varepsilon_{ij}$ and $3u_i$ (15 unknowns) from the above 15 relations (6 stress-strain equations, 3 equilibrium equations and 6 strain-displacement equations). The specification of the problem is completed by the physical boundary conditions and a known temperature distribution. For a thermoelastic problem with no surface tractions, the boundary conditions are specified by

$$\sigma_{ij}n_j = 0 \tag{2.5}$$

2.4.2 Plane Polar Formulation

From the general equations of the preceding section, the plane problem can be formulated by appropriate simplifying assumptions. There are two general types of plane problem, namely, plane stress and plane strain. For "thin" prismatic bodies ("small" uniform dimension in one coordinate direction), the concept of plane stress is appropriate. The restriction of the general theory to a theory of plane stress is defined by the equation

$$\sigma_{i3} = 0 \tag{2.6}$$

where the 3-direction is the coordinate direction in which the body is thin. This relationship restricts the stress field to that existing in a plane plate of constant thickness acted upon only by forces in the plane of the plate.

Plane strain is the concept used to consider "long" (theoretically infinite) bodies acted upon by loads uniformly distributed in the infinite direction and having no components normal to the

finite planes. In the non-isothermal case, plane strain requires that the temperature field be uniform in the infinite direction. This is an assumption which would seem reasonable for the temperature field in the tree trunk, taking the axial dimension as infinite. Plane thermal strain is defined by

$$T = T(x_1, x_2) \tag{2.7}$$

and

$$u_i = u_i(x_1, x_2) \tag{2.8}$$

With the above restrictions in mind the equations for the plane polar formulation may be written explicitly. Three of the six stress-strain relations remain.

$$\left.\begin{aligned} \varepsilon_{RR} &= \frac{1}{E}(\sigma_{RR} - \nu\sigma_{\theta\theta}) + \alpha T \\ \varepsilon_{\theta\theta} &= \frac{1}{E}(\sigma_{\theta\theta} - \nu\sigma_{RR}) + \alpha T \\ \varepsilon_{R\theta} &= \frac{1+\nu}{E}\sigma_{R\theta} \end{aligned}\right\} \tag{2.9}$$

The equilibrium equations are

$$\left.\begin{aligned} \frac{\partial\sigma_{RR}}{\partial r} + \frac{\sigma_{RR} - \sigma_{\theta\theta}}{r} + \frac{1}{r}\frac{\partial\sigma_{R\theta}}{\partial\theta} + B_R &= 0 \\ \frac{\partial\sigma_{R\theta}}{\partial r} + \frac{2\,\sigma_{R\theta}}{r} + \frac{1}{r}\frac{\partial\sigma_{\theta\theta}}{\partial\theta} + B_\theta &= 0 \end{aligned}\right\} \tag{2.10}$$

The three remaining strain-displacement relations are:

$$\left.\begin{aligned} \varepsilon_{RR} &= \frac{\partial u_R}{\partial r} \\ \varepsilon_{\theta\theta} &= \frac{u_R}{r} + \frac{1}{r}\,\frac{\partial u_\theta}{\partial \theta} \\ \varepsilon_{R\theta} &= \frac{1}{2}\left[\frac{\partial u_\theta}{\partial r} - \frac{u_\theta}{r} + \frac{1}{r}\,\frac{\partial u_R}{\partial \theta}\right] \end{aligned}\right\} \qquad (2.11)$$

In the case of plane strain, however, the usual material constants must be replaced by the following modified constants:

$$E' = \frac{E}{1 - \nu^2}, \quad \nu' = \frac{\nu}{1 - \nu}, \quad \alpha' = \alpha(1 + \nu) \qquad (2.12)$$

The shear modulus, G, remains unchanged. Also, for the case of plane strain there is an accompanying axial stress

$$\sigma_{ZZ} = \nu(\sigma_{RR} + \sigma_{\theta\theta}) - \alpha E T \qquad (2.13)$$

This might be considered a restraining stress which maintains the material in a state of plane strain.

In the general case of plane stress, an axial strain is present as a result of the Poisson effect.

$$\varepsilon_{ZZ} = -\frac{\nu}{E}(\sigma_{RR} + \sigma_{\theta\theta}) + \alpha T \qquad (2.14)$$

Equations (2.13) and (2.14) above are not, however, a part of the plane thermal stress problem requiring solution. When the solution to the problem defined by equations (2.9), (2.10) and (2.11) is

found, the results of this solution may be applied to equations (2.13) or (2.14) (whichever is applicable) to completely define the stress-strain field. Thus, the solution to the plane polar problem has been reduced to eight equations in eight unknowns (σ_{RR}, $\sigma_{\theta\theta}$, $\sigma_{R\theta}$, ε_{RR}, $\varepsilon_{\theta\theta}$, $\varepsilon_{R\theta}$, u_R, u_θ).

This is still a formidable problem, particularly if $T(r,\theta)$ is an arbitrary function or the result of experimental measurement.

2.4.3 Thermal Stress in Viscoelastic Materials

As outlined in the last two sections, the theory of thermal stresses applied to elastic materials is quite well defined. Theoretical consideration of thermal stresses in a viscoelastic material is not nearly as advanced. Herein consideration will be given to the general principles to be applied to a thermoviscoelastic problem (Nowacki, 1962).

If the term $(-\frac{s}{3}\delta_{ij})$ is added to both sides of equation (2.2) in section 2.4.1, the equation can be split into two separate equations,

$$s_{ij} = 2\mu e_{ij} \tag{2.15}$$

and

$$s = 3K\,(e - 3\alpha T) \tag{2.16}$$

where

$$s_{ij} = \sigma_{ij} - \frac{1}{3}s\delta_{ij} \tag{2.17}$$

$$e_{ij} = \varepsilon_{ij} - \frac{1}{3}e\delta_{ij} \tag{2.18}$$

and

$$K = \frac{2\mu\ (1 + \nu)}{3\ (1 - 2\nu)} \tag{2.19}$$

In equations (2.15) and (2.16) above, s_{ij} and e_{ij} denote the deviatoric components of the stress and strain tensors, respectively, s and e denote the isotropic (or hydrostatic) components of stress and strain, respectively. The material behavior defined by these equations is that of an elastic Hookean body. In linear viscoelastic theory, it is usually assumed that the material behaves elastically with respect to isotropic compression or tension but viscoelastically with respect to the deviatoric stress and strain. Therefore, equation (2.16) remains unchanged and equation (2.15) is modified to describe the properties of the material under consideration. In general, the equation relating the deviatoric components of stress and strain in a viscoelastic material takes the form

$$P_1(D)s_{ij} = P_2(D)e_{ij} \tag{2.20}$$

where $P_i(D)$ are linear differential operators of the form

$$P_i(D) = \sum_{n=0}^{N_i} a_i{}^{(n)} D^n \ , \ a_i{}^{(n)} \neq 0, \ i = 1, 2, \ldots$$

and

$$D^n = \frac{\partial^n}{\partial t^n}$$

denotes the n^{th} time derivative.

Direct solution of the problem defined by equations (2.16) and (2.20) is very difficult. Nowacki (1962) outlines a method of solution for the problem in which variables are transformed by means of Laplace transforms, a solution is found for the transformed problem and the reverse transform is taken. This system works for well-behaved functions and temperature distributions which are amenable to Laplace transformation. As in the elastic case, ill-behaved functions or experimental temperature distributions are very difficult to solve.

Hammerle (1968), in his study of stress-cracking of the horny endosperm of corn kernels considered the material to be a thin viscoelastic slab subjected to temperature and moisture gradients. The assumption of the thin slab configuration reduced the problem to one of plane stress. He accounted for the effect of temperature and moisture gradients on the viscoelastic parameters by the use of "shift factors." For example, the effect of changing temperature was modeled by the time-temperature shift factor

$$a_T = t_T/t_0$$

where

t_T = time required to observe some phenomenon at temperature T

t_0 = time required to observe the same phenomenon at reference temperature T_0.

That is, a_T is the factor required to superimpose line segments of data, each segment being from observations at a constant temperature above the reference temperature. A similar time-moisture shift factor, a_m, was employed to account for the effect of changes in moisture content on the time of occurrence of phenomena.

Experimental values of a_T and a_m were obtained by Hammerle (1968) by graphical manipulation of data to superimpose data from various moisture content and temperature conditions on data for standard conditions.

2.4.4 Orthotropic Thermoelasticity

Sections 2.4.1 through 2.4.3 have dealt with the theory of thermal stresses in isotropic materials. Wood, however, is orthotropic; that is, its material properties are different in each of the longitudinal, radial and tangential directions. If the modulus of elasticity, Poisson's ratio, shear modulus and coefficient of thermal expansion are different in each of the three principal directions, then from Lekhnitskii (1963) the system of equations represented by equation (2.1) becomes, in expanded form:

$$\left.\begin{aligned}
\varepsilon_{11} &= \frac{\sigma_{11}}{E_1} - \frac{\nu_{21}\sigma_{22}}{E_2} - \frac{\nu_{31}\sigma_{33}}{E_3} + \alpha_1 T \\
\varepsilon_{22} &= -\frac{\nu_{12}\sigma_{11}}{E_1} + \frac{\sigma_{22}}{E_2} - \frac{\nu_{32}\sigma_{33}}{E_3} + \alpha_2 T \\
\varepsilon_{33} &= -\frac{\nu_{13}\sigma_{11}}{E_1} - \frac{\nu_{23}\sigma_{22}}{E_2} + \frac{\sigma_{33}}{E_3} + \alpha_3 T
\end{aligned}\right\} \qquad (2.21)$$

$$\left.\begin{aligned} \gamma_{12} &= \frac{\sigma_{12}}{G_{12}} \\ \gamma_{23} &= \frac{\sigma_{23}}{G_{23}} \\ \gamma_{31} &= \frac{\sigma_{31}}{G_{31}} \end{aligned}\right\} \tag{2.21}$$

where

$$\left.\begin{aligned} E_1\nu_{21} &= E_2\nu_{12} \,, \\ E_2\nu_{32} &= E_3\nu_{23} \,, \\ \text{and} \\ E_3\nu_{13} &= E_1\nu_{31} \end{aligned}\right\} \tag{2.22}$$

For the case of cylindrical anisotropy (Lekhnitskii, 1963), these equations become (using cylindrical coordinates)

$$\left.\begin{aligned} \varepsilon_{RR} &= \frac{\sigma_{RR}}{E_R} - \frac{\nu_{\theta R}\sigma_{\theta\theta}}{E_\theta} - \frac{\nu_{ZR}\sigma_{ZZ}}{E_Z} + \alpha_R T \\ \varepsilon_{\theta\theta} &= -\frac{\nu_{R\theta}\sigma_{RR}}{E_R} + \frac{\sigma_{\theta\theta}}{E_\theta} - \frac{\nu_{Z\theta}\sigma_{ZZ}}{E_Z} + \alpha_\theta T \\ \varepsilon_{ZZ} &= -\frac{\nu_{RZ}\sigma_{RR}}{E_R} - \frac{\nu_{\theta Z}\sigma_{\theta\theta}}{E_\theta} + \frac{\sigma_{ZZ}}{E_Z} + \alpha_Z T \\ \gamma_{R\theta} &= \frac{\sigma_{R\theta}}{G_{R\theta}} \\ \gamma_{\theta Z} &= \frac{\sigma_{\theta Z}}{G_{\theta Z}} \\ \gamma_{ZR} &= \frac{\sigma_{ZR}}{G_{ZR}} \end{aligned}\right\} \tag{2.23}$$

For the case of plane strain, the strain is a function of radius and angle only. Therefore, $\gamma_{\theta Z} = \gamma_{ZR} = \varepsilon_{ZZ} = 0$. Using these relationships and solving for stress, we obtain, using matrix notation,

$$\begin{Bmatrix} \sigma_{RR} \\ \sigma_{\theta\theta} \\ \sigma_{R\theta} \end{Bmatrix} = \frac{1}{(1 - \nu_{R\theta}\nu_{\theta R} - \nu_{\theta Z}\nu_{Z\theta} - \nu_{ZR}\nu_{RZ} - \nu_{R\theta}\nu_{\theta Z}\nu_{ZR} - \nu_{\theta R}\nu_{Z\theta}\nu_{RZ})}$$

$$\times \begin{bmatrix} E_R(1 - \nu_{Z\theta}\nu_{\theta Z}) & E_R(\nu_{\theta R} + \nu_{ZR}\nu_{\theta Z}) & 0 \\ E_\theta(\nu_{R\theta} + \nu_{Z\theta}\nu_{RZ}) & E_\theta(1 - \nu_{ZR}\nu_{RZ}) & 0 \\ 0 & 0 & G_{R\theta} \end{bmatrix}$$

$$\times \begin{Bmatrix} \varepsilon_{RR} - (\nu_{ZR}\alpha_Z + \alpha_R)T \\ \varepsilon_{\theta\theta} - (\nu_{Z\theta}\alpha_Z + \alpha_\theta)T \\ \gamma_{R\theta} \end{Bmatrix} \qquad (2.24)$$

Equation (2.24) will be used in the prediction of thermal stresses by means of finite element analysis later in the thesis.

2.5 Previous Investigations Related to Trunk Splitting

Parker (1963) devoted a section of his extensive review of cold resistance in woody plants to some of the ideas, observations,

investigations and theories which have appeared regarding tree trunk splitting. Generally, it was agreed that the reason for trunk splitting was a massive contraction (or expansion) which could not be explained by the coefficient of thermal expansion of either wood or ice. Parker noted that there was some disagreement on whether cracking occurred upon heating or cooling of the tree trunk. One school of thought maintained that sapwood experienced a much greater tangential contraction than heartwood upon cooling, resulting in sufficient tangential stress to initiate a crack extending from the exterior of the trunk inward. This theory was substantiated by reports of sharp cracking noises at sunset. Others were of the opinion that, upon heating, the sapwood expanded faster than the heartwood and caused sufficient tangential stress in the heartwood to initiate an internal crack which eventually spread outward to the surface. This theory was substantiated by reports of muffled cracking noises occurring in the morning at sunrise and by the fact that frost cracks often occurred on the southern side of the tree trunk--the side warmed by the sun's radiation. Depending on circumstances, both explanations were deemed plausible. Herrington et al. (1964) determined the tangential coefficient of thermal expansion of Acer rubrum L. at 0.4 percent moisture d.b., 28 percent d.b. (fiber saturation) and 119 percent d.b. (saturated). At the two lower moisture contents, thermal contraction with decreasing temperature was continuous and yielded a coefficient of thermal expansion of approximately 41 x 10^{-6} $°C^{-1}$. The saturated samples behaved similarly down to the freezing point where a small expansion

was experienced. Below 0°C, a coefficient of thermal expansion of $380 \times 10^{-6}\ °C^{-1}$ was measured. Herrington did not explain the large change in thermal expansion below the freezing point but postulated that a migration of water from the saturated cell wall into the cell lumen was causing the shrinkage due to a dehydration of the cell wall.

Kübler (1962) used an electrical resistance strain gauge mounted on a clip gauge to measure the sub-freezing radial and tangential dimensional changes of beechwood at various moisture contents. Results similar to those of Herrington (1964) were recorded. The coefficient of thermal expansion in the tangential direction was greater than that in the radial in a proportion similar to that occurring above the freezing point. Reswelling occurred upon reheating but a distinct hysteresis effect was evident. Kübler's explanation of the massive shrinkage was that the vapor pressure of the ice within the cell cavities decreased more quickly than the vapor pressure of the hygroscopic water in the cell walls, resulting in dehydration and shrinkage of the fibrils of cellulose in the cell walls.

Schirp and Kübler (1968) carried the above work further by investigating five species of wood at a variety of moisture contents. Distinct differences between species and moisture contents were observed. From this study, it was concluded that, depending upon moisture content, four components influence to varying degrees the change in dimension of wood with temperature. These are (1) thermal

expansion of the wood material, (2) movement of moisture from cell walls to cell cavities, (3) formation of ice layers in the tissue, and (4) the volumetric expansion of freezing water.

3. THE INVESTIGATION

3.1 Field Experiments

The occurrence of widely varying and quickly changing temperatures within the tree trunk is documented in Section 2.3. It was felt, however, that a measure of the magnitude of these temperature changes for the Michigan situation was required. The following two sections outline the field experiments carried out to this end.

3.1.1 Winter of 1968-69

During the winter season of 1968-69, internal temperature measurements were made on a peach tree in the orchard of the Michigan State University Horticultural Experiment Farm. The tree selected was in its fourth growing season and was of typical size for the population of the orchard. Care was taken to find a tree with a trunk which was straight, vertical and close to a circular cross-section. The tree chosen was atypical in that it was in the outside guard row of the orchard.

It was suspected that more severe temperature fluctuations might be experienced by a tree in this exposed position. Also, it was feared that the considerable boring required to insert temperature probes into the tree might injure or kill the tree. This would be of less consequence to other experiments in the orchard since the guard row was not used for production experiment purposes. This

concern was unjustified since the tree survived and produced a heavy crop the following summer.

Thermocouples were installed in the tree trunk approximately 15 inches above ground level and in the 16 positions indicated in Figure 3.1. The preponderance of thermocouples in the southwest quadrant of the trunk was used to detect a suspected high temperature gradient in that area.

Two types of thermocouples were used in the installation. For the temperatures at the cambium level, a thermocouple of the type shown in Figure 3.2a was employed. Six-inch lengths of copper and constantan wires of diameter 0.003 inches were soldered together at one end to form the junction. The other ends were joined to standard polyvinyl-coated 24-gauge thermocouple lead wire. The small wire and its joint with the lead wire were coated by dipping in an epoxy resin preparation.

These thermocouples were installed by cutting a vertical slit approximately 1/2-inch long in the bark with a sharp pocket knife. The knife blade was then worked under the bark on one side of the slit to a depth of 3/8 inch. The thermocouple junction was then inserted in the cavity behind the blunt edge of the knife, and the knife was withdrawn allowing the bark to close down tightly on the thermocouple function. The injury to the bark was slight and a few weeks of healing left the junction firmly implanted in the cambium. The lead wire was taped firmly to the trunk to prevent breakage of the thermocouple. As a result of this method of placement of the junction, the thermocouple wires ran at least 100 wire diameters in

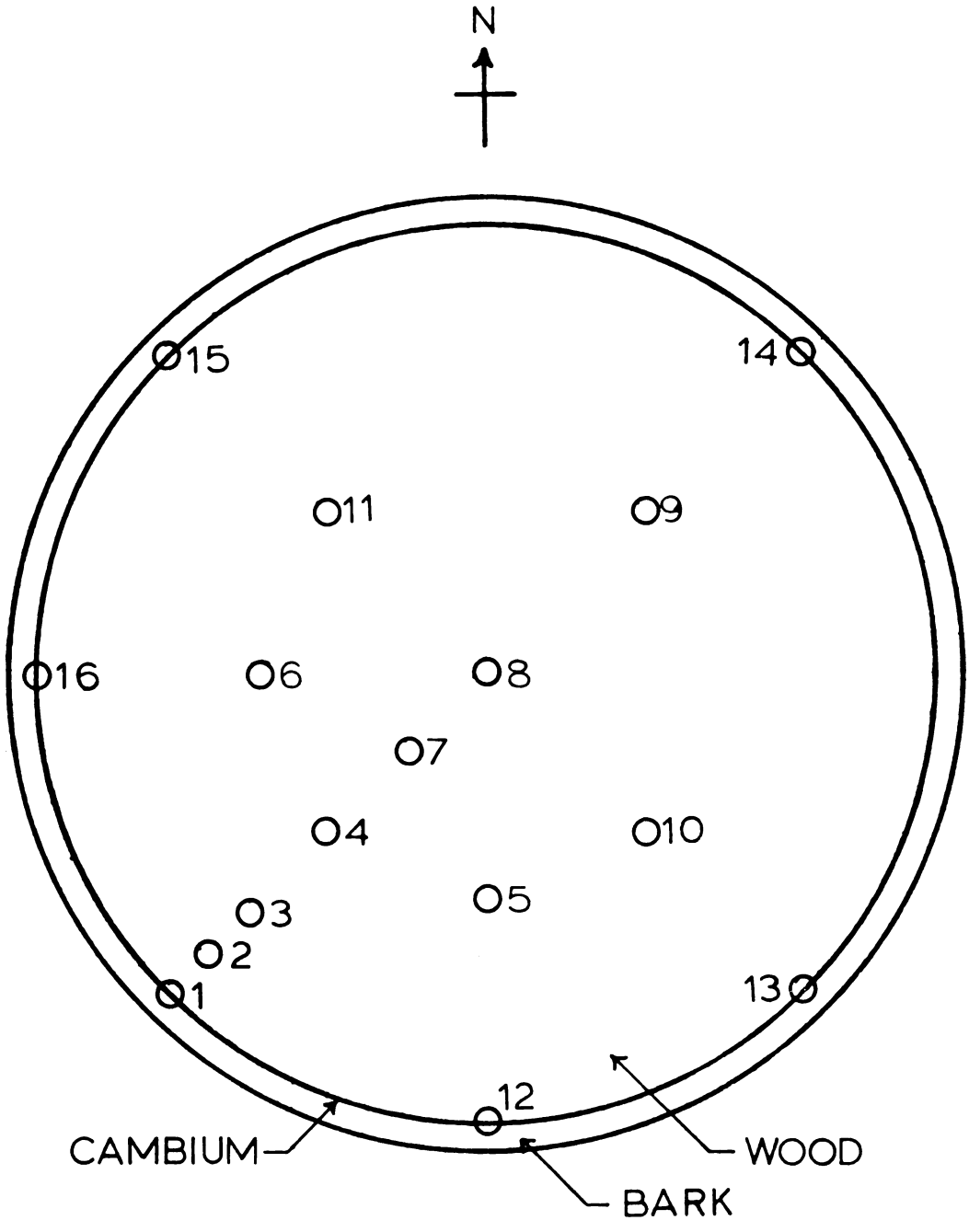

Figure 3.1.--Points of location of thermocouples in tree trunk, winter 1968-69. (Scale 1.5X actual.)

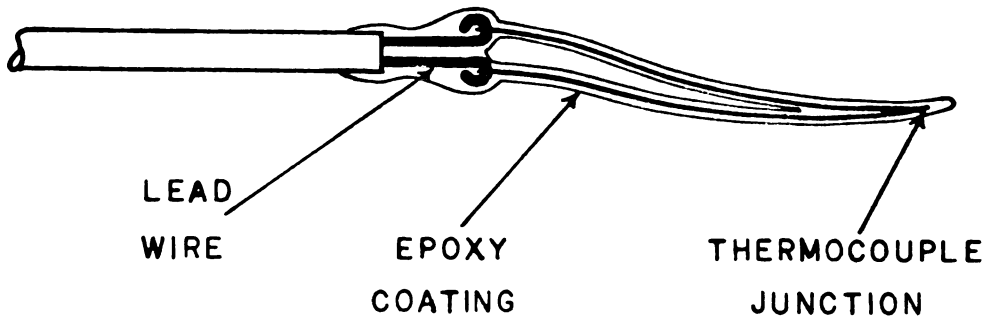

Figure 3.2a.--Diagram of thermocouple used to measure cambium temperature.

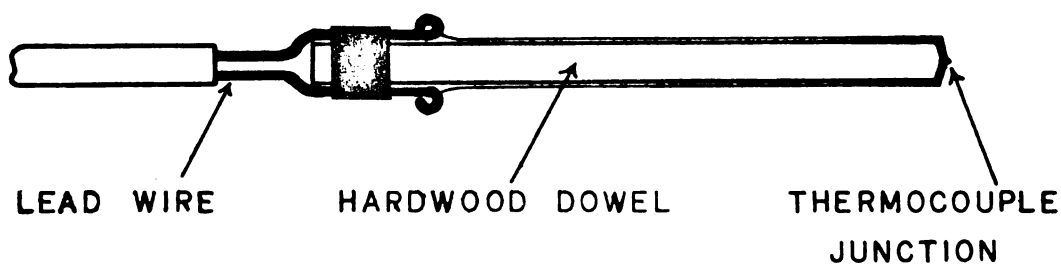

Figure 3.2b.--Diagram of thermocouple probe used to measure internal wood temperature.

the circumferential direction at cambium level, before emerging from the trunk. This condition was assumed to provide ample protection against errors due to heat conduction along the wire.

The thermocouple probes embedded in the wood were of the type shown in Figure 3.2b. The actual junction was made with 0.003-inch diameter copper and constantan wires. The probe was made of 1/8-inch hardwood dowel material. The junction was placed at the end of the dowel and the two wires ran back opposite sides of the dowel. Two coats of an acrylic spray served to bond the wires to the wooden dowel. Lead wires were soldered to the fine thermocouple wire and taped firmly to the end of the dowel.

A tree of exactly circular cross-section could not be found; the one selected was slightly elliptical in shape with the major axis aligned with the N-S direction. At thermocouple installation level, the major axis was 3.5 inches and the minor axis 3.3 inches measured from cambium to cambium. In order to install the "internal" thermocouples without any of the probes intersecting, it was necessary for their level of installation to vary over a 3-inch range in height; also, to minimize the disturbance of incoming radiation, all "internal" probes were inserted from the northeast segment of the trunk.

Installation consisted of drilling a 9/64-inch hole in the tree trunk and inserting the probe. The drill bit was constrained to enter the trunk in the direction indicated by use of a compass, and by using a jig clamped to the trunk through which the drill was forced to pass. Since all holes were radial, and the trunk was

knot-free, no bending of the bit was expected. Depth was controlled by a collar clamped on the drill bit.

The healing action of the tree tissues soon held the probe firmly in place. Readings were taken beginning five weeks after installation. By that time the bark had healed quite well. It was assumed that the hardwood dowels would equilibrate in moisture content with the surrounding tissues sufficiently to make them similar in their heat transfer properties. The diameter of the actual thermocouple wires (0.003 in) was sufficiently small in comparison to the depth of embedment that errors from heat conduction along the wires was assumed negligible.

The lead wires were run to a meteorological observation trailer located nearby in the orchard where the signals were fed to a 16 point Minneapolis-Honeywell temperature recorder. Using the weather forecast as a guide, temperatures were recorded on days when the days promised to be cold, clear and sunny. Hourly data for 27 January and 5 February 1969 for the thermocouples shown in Figure 3.1 are included in Appendix A.

The records of 5 February 1969 were interesting and typical of those obtained on clear, cold days.

Figure 3.3 shows some of the cambium temperatures and the central trunk temperatures observed in the tree trunk throughout the day. Notice that the temperature is essentially uniform across the trunk until sunrise at which time the temperature in the southeast cambium starts to rise sharply. This is followed by temperature rises at the southernmost point and the southwest point of the trunk.

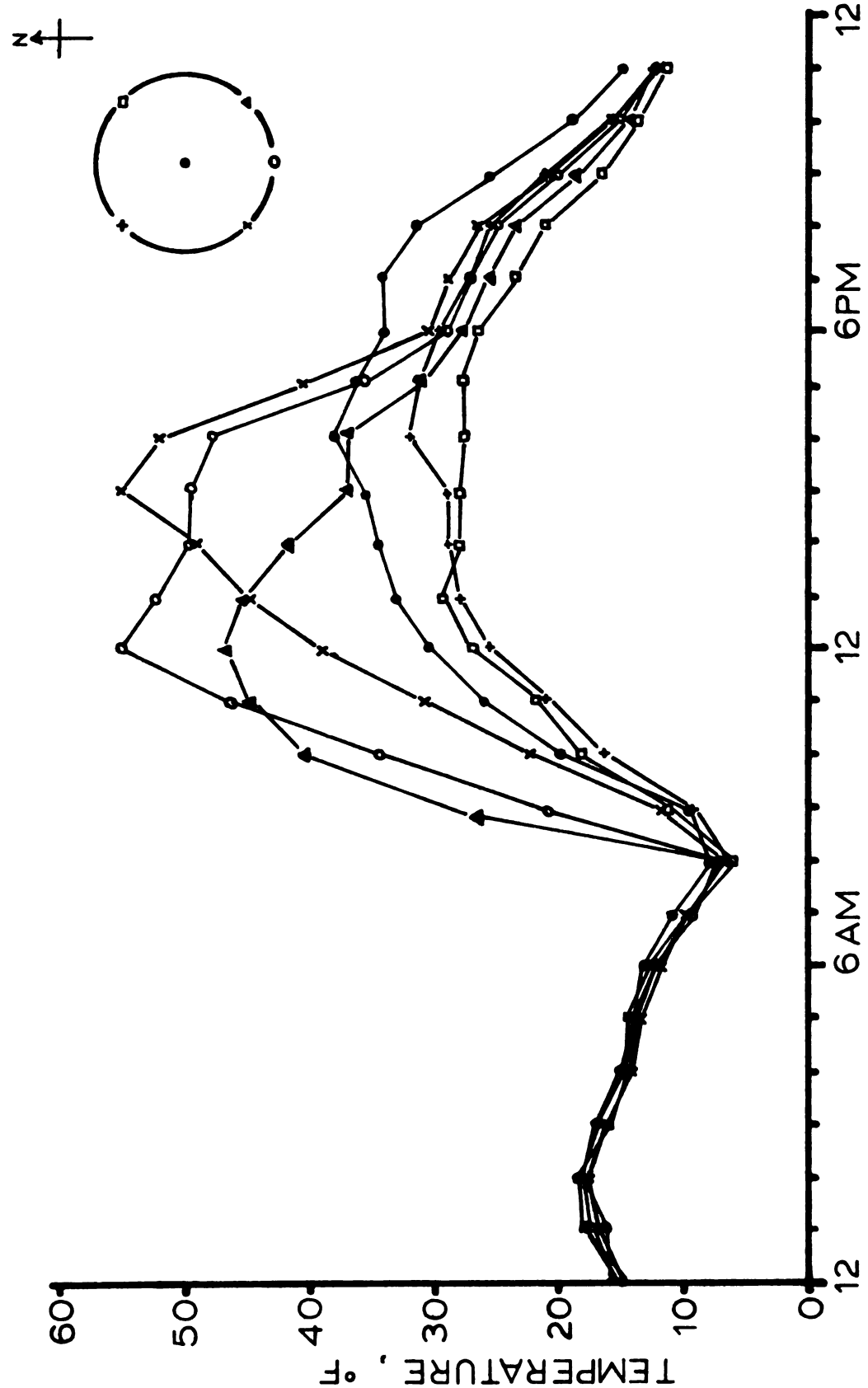

Figure 3.3.--Temperatures observed at various points in tree trunk, 5 February 1969.

These temperatures reach their peaks and fall in turn as the direction of the sun changes throughout the day. The temperatures at the trunk center, northwest cambium and northeast cambium experience rises and falls which are not as extreme and lag in time behind the temperatures on the south side.

Figure 3.4 shows the temperature contours in the trunk at 9:00 A.M., 5 February 1969. Notice the steep temperature gradient in the southeast portion of the trunk, and the relatively level temperature regime in the northwest portion.

Figure 3.5 shows the map of temperature contours for the same tree trunk at 9:00 P.M. of the same day. Notice that the central portion of the trunk is now at the highest temperature with the steep temperature gradients on the southwest and northeast portions of the periphery.

Figures 3.6 and 3.7 show the position of the 32°F isotherm at one-hour intervals throughout the same day. Continuous translation and rotation of this isotherm corresponding to the position and intensity of the incident sunlight is evident. Some thermal lag is shown by the fact that the greatest proportion of the trunk is above 32°F at 4:00 P.M., after the maximum intensity of sunlight and after the highest cambium temperature. Note that at 4:00 P.M., approximately 75% of the tree trunk is at a temperature above 32°F. Weather records for the Environmental Science Services Administration (ESSA), U.S. Department of Commerce, show a maximum temperature in the Lansing, Michigan area (Capital City Airport) of 25°F on 5 February 1969. The minimum temperature was 4°F. Records from

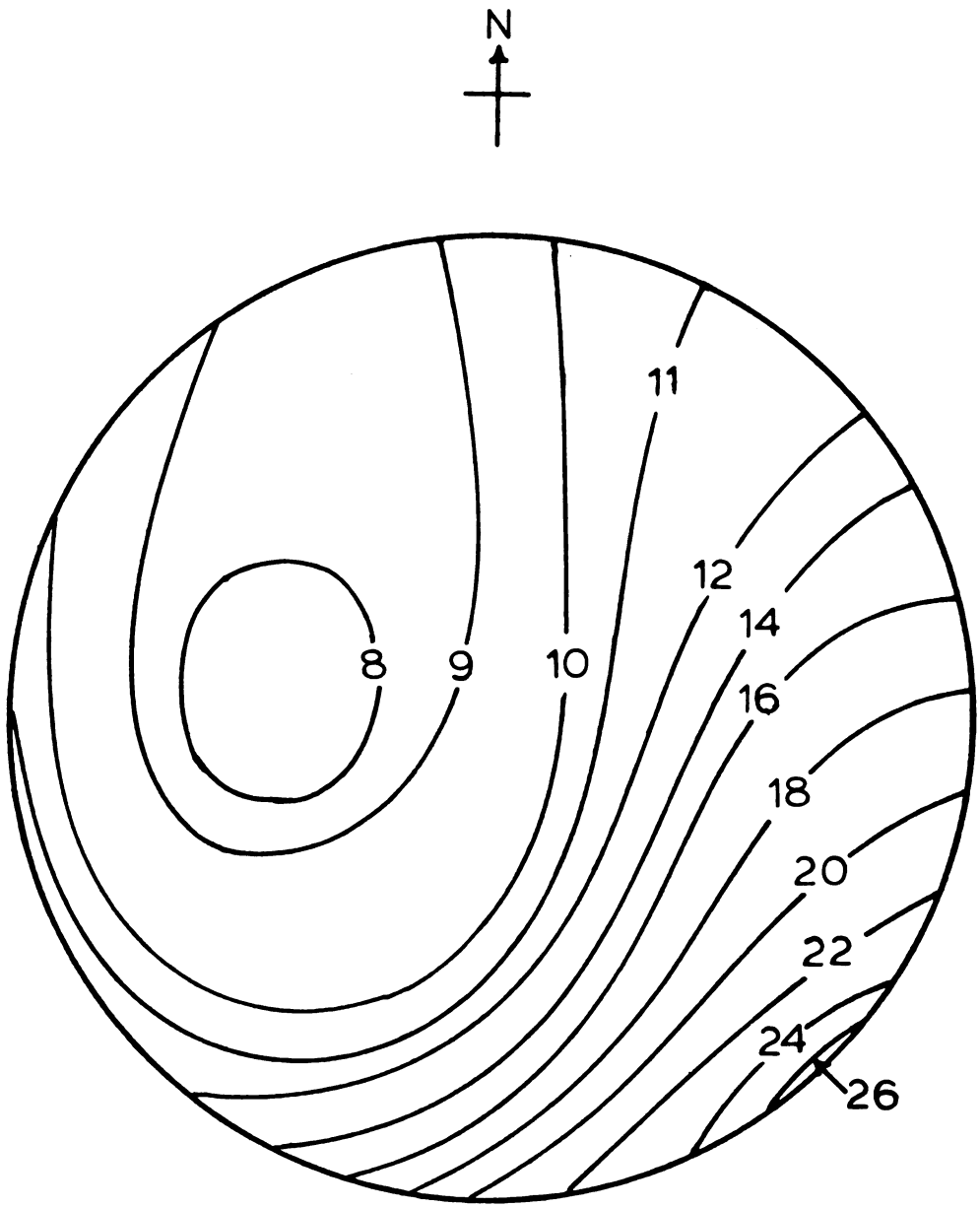

Figure 3.4.--Isothermal map of tree trunk, 9:00 A.M., 5 February 1969. (Scale 1.5X actual, temperatures in °F.)

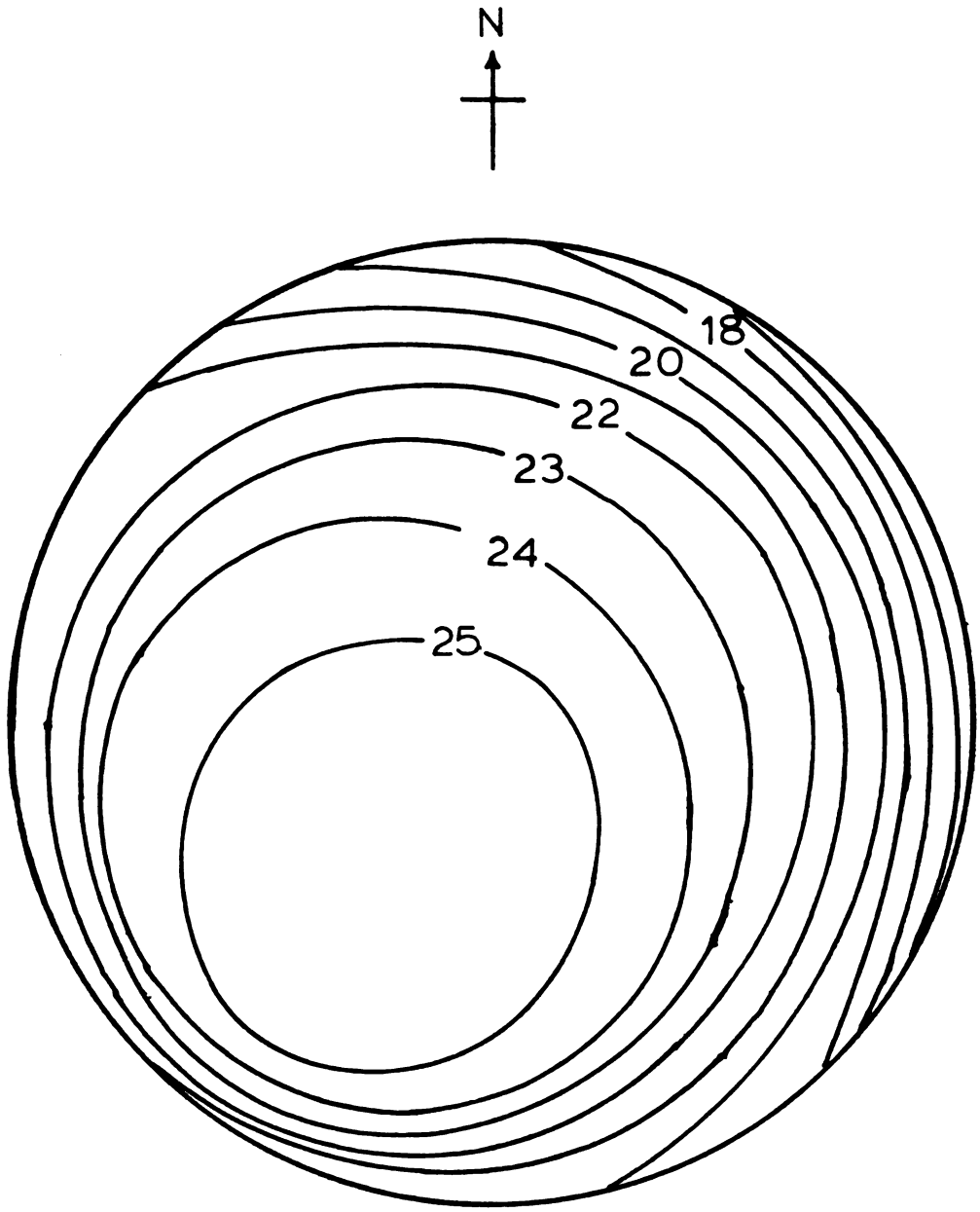

Figure 3.5.--Isothermal map of tree trunk, 9:00 P.M., 5 February 1969. (Scale 1.5X actual, temperatures in °F.)

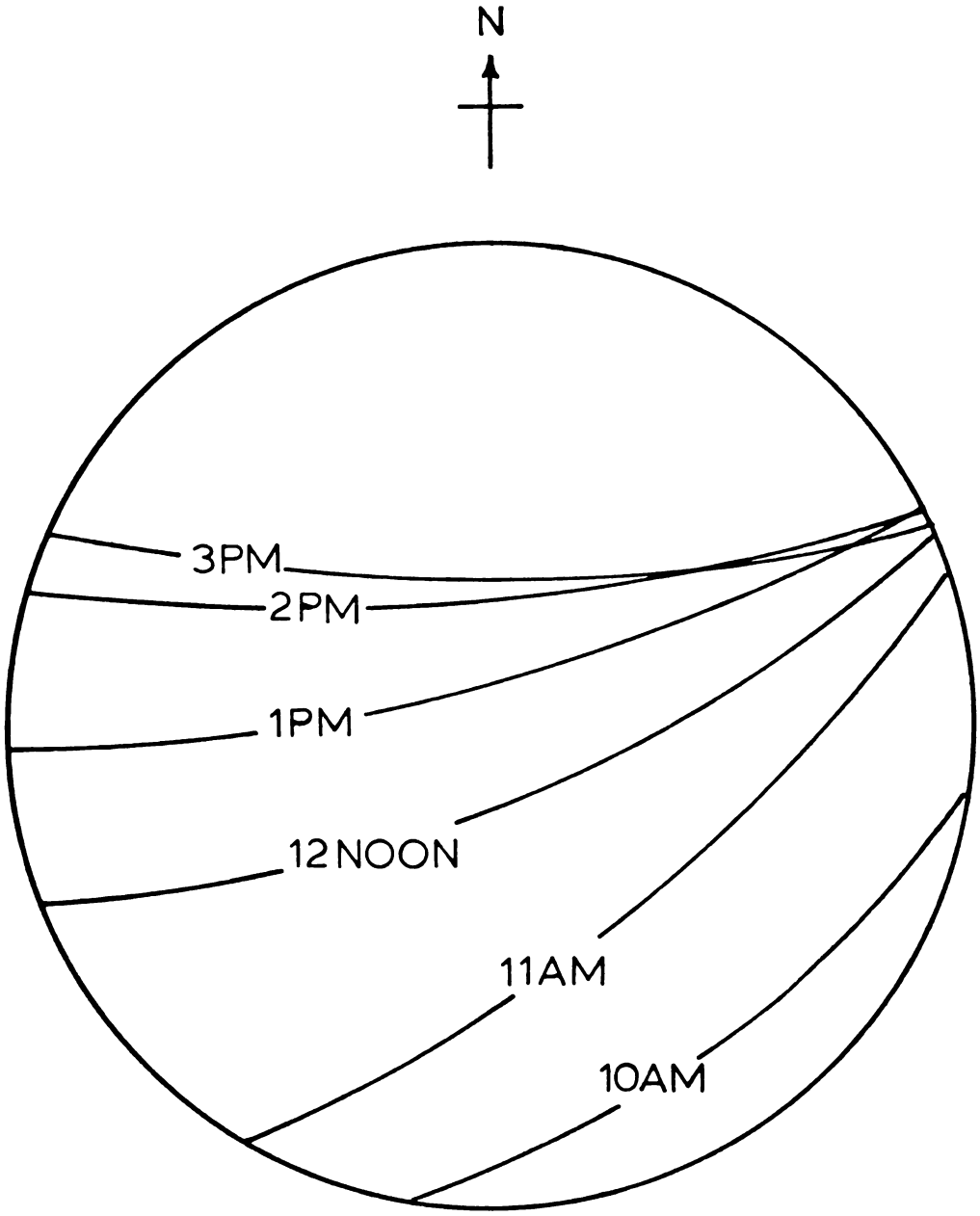

Figure 3.6.--Movement of the 32°F isotherm in a tree trunk, 5 February 1969, 10:00 A.M. to 3:00 P.M. (Scale 1.5X actual.)

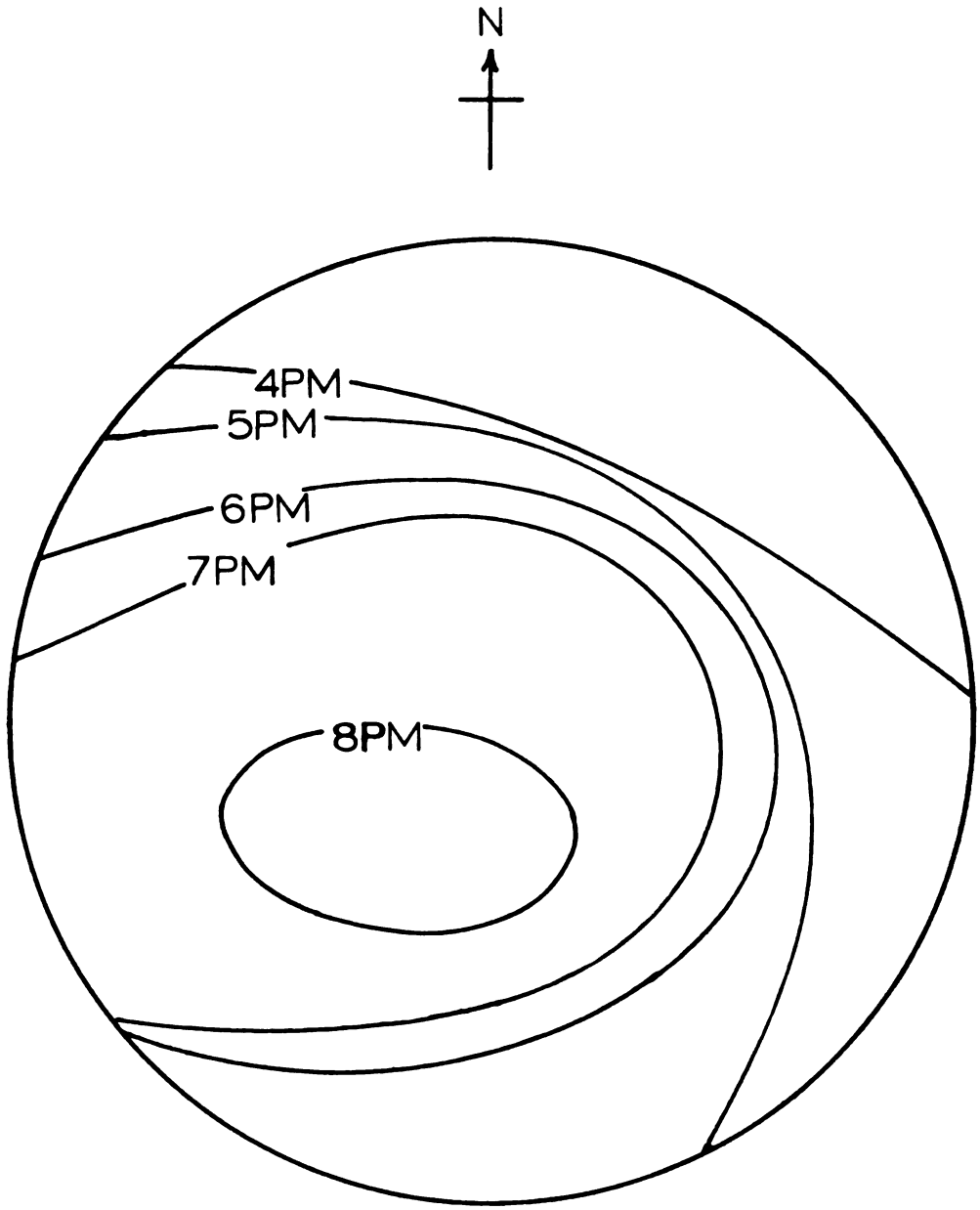

Figure 3.7.--Movement of 32°F isotherm in a tree trunk, 5 February 1969, 4:00 P.M. to 8:00 P.M. (Scale 1.5X actual.)

ESSA show 10.1 hours of sunshine which is 99% of possible hours of sunshine.

One interesting fact is shown in Figure 3.7 by the 32°F isotherm at 8:00 P.M. At this point in time, there is an unfrozen portion of the trunk surrounded by a closed loop of material below 32°F. The significance of this pattern with respect to the results of the laboratory studies will be discussed in Chapter 4.

Comparison of these results with the work reported by Derby and Gates (1966) shows some similarities in spite of the quite different conditions under which the two studies were carried out. (The observations by Derby and Gates were for an aspen tree in April, 1965, near Black Hawk, Colorado, 40°N latitude at an elevation of 9,300 ft. The observations herein reported were for a peach tree in February, 1969, near East Lansing, Michigan, 42°N latitude at an elevation of 800 ft.) Although the temperature values are different, the same general pattern emerges. The isothermal lines tend to translate from the southeast quadrant to the northwest quadrant during the morning, rotate clockwise during the mid-day hours and translate from the northeast quadrant to the southwest quadrant during the evening. There is a tendency for the isothermal lines to close with an area of colder tissue completely surrounding an area of warmer tissue. The highest cambium temperature reported by Derby and Gates occurred earlier (1:00 P.M. rather than 3:00 P.M.) and at the southern cardinal point (rather than at the southeast exposure).

Jensen et al. (1970) reported similar translation and rotation of temperature contours for a peach tree in Georgia, although their work was for a higher range of ambient temperatures.

3.1.2 Winter of 1969-70

During the winter of 1969-70, temperatures within the trunk of another tree were measured. This tree was in the same orchard as for the experiment of the previous year, but was located in the second row from the orchard's edge and approximately 60 feet further south. Temperatures were monitored in several other trees to which various treatments were applied, designed to attenuate the large temperature gradients observed in the previous year. A stepping switch arrangement was devised so that more than one tree could be monitored by one recorder. For the purposes of this study, the tree to which no treatment was applied was the one of interest; therefore, temperature data for selected days for this tree are reported in Appendix B. After the experience of the 1968-69 winter, it was decided that a more uniform placement of thermocouples would be advantageous. The placement of the thermocouples is shown in Figure 3.8. Notice that the thermocouples are placed at 60° intervals around the trunk at the cambium and corresponding "internal" thermocouples are placed at 60° intervals at the half-radius points.

The construction and installation of the thermocouples was the same as in the previous year. Again, all "internal" thermocouples were inserted radially from the northern side of the tree.

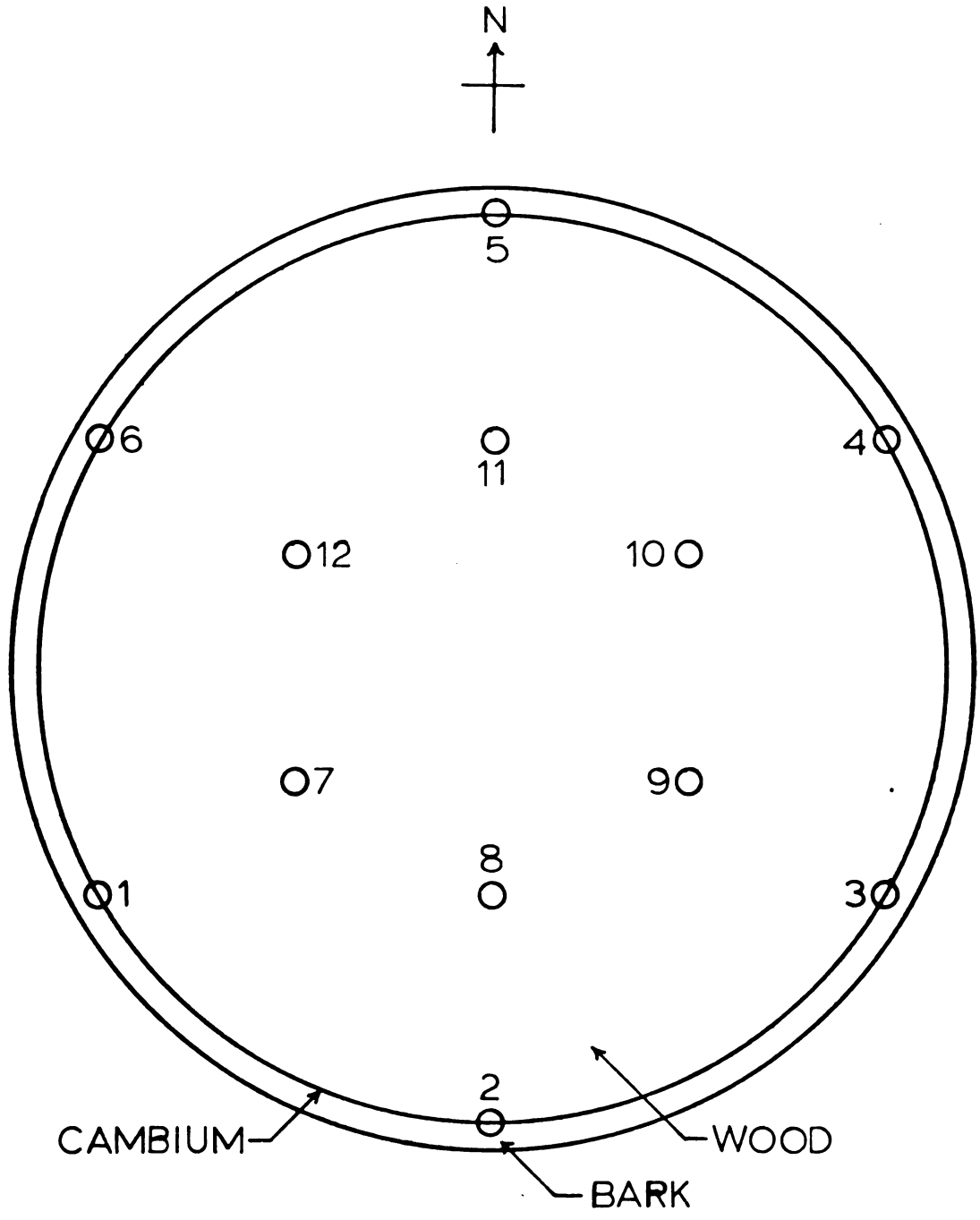

Figure 3.8.--Points of location of thermocouples in tree trunk, winter 1969-70. (Scale 1.5X actual.)

The tree was not a perfect circle. Measurements at the cambium showed the tree to be 3.6 inches between thermocouples 2 and 5, 3.5 inches between thermocouples 1 and 4, and 3.4 inches between thermocouples 3 and 6. On clear, sunny days, the temperatures observed in the tree trunk followed a pattern similar to that reported for the previous winter. Two interesting temperature contour maps from the 1969-70 winter are shown in Figures 3.9 and 3.10. These figures are both derived from temperature data for evenings of relatively cold, clear days. Notice that steep temperature gradients are evident near the surface of the tree trunk in both Figures 3.9 and 3.10. Further reference to these temperature patterns will be made in the analysis in Section 3.3.

3.2 Laboratory Experiments

The laboratory experimentation fell into two categories: (1) the measurement of the low temperature coefficient of thermal expansion of fruit tree wood and (2) a microscopic study of frozen woody tissue to relate the formation of ice crystals to the low temperature expansion phenomenon.

3.2.1 Coefficient of Thermal Expansion

3.2.1.1 Development of apparatus.--A low temperature chamber was required for this study. A standard upright kitchen freezer was modified for this purpose. The experiment required that it be possible to hold a given temperature without the instability inherent to a conventional "on-off" thermostat. Also, it was required that

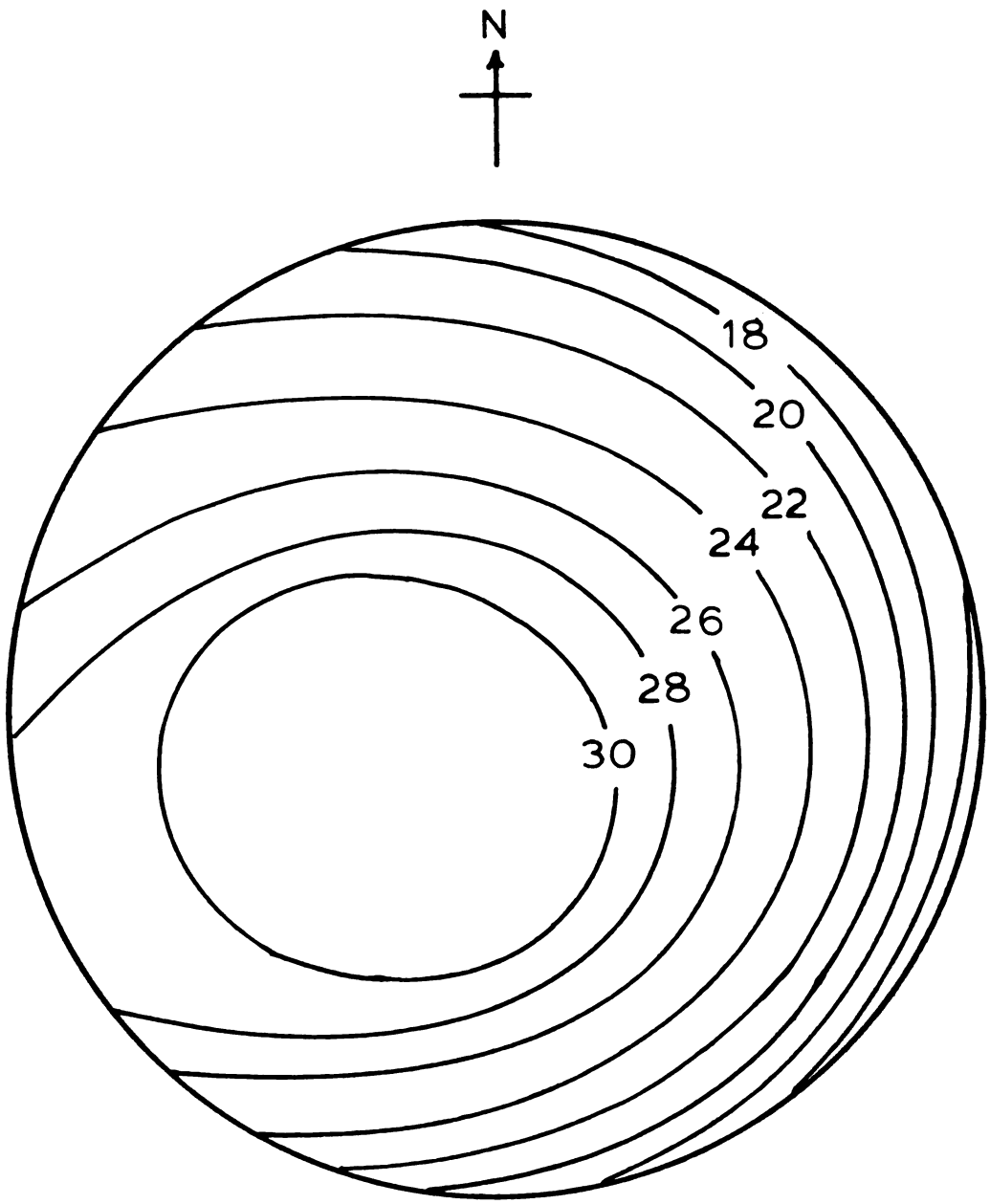

Figure 3.9.--Isothermal map of tree trunk, 5:14 P.M., 14 January 1970. (Scale 1.5X actual, temperatures in °F.)

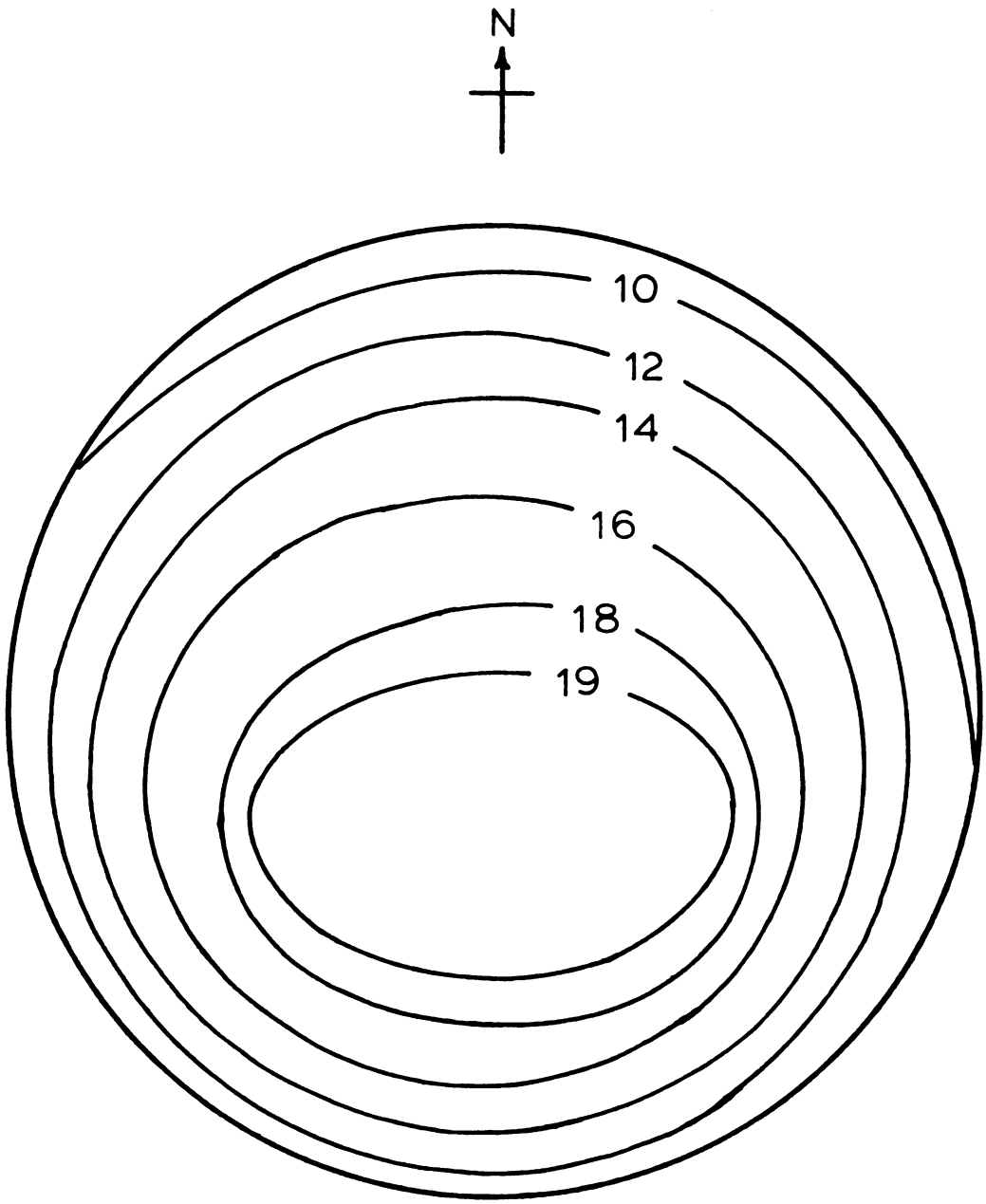

Figure 3.10.--Isothermal map of tree trunk, 7:42 P.M., 18 January 1970. (Scale 1.5X actual, temperatures in °F.)

it be possible for the temperature to be varied upward or downward in a continuous controlled manner. Figure 3.11 shows a schematic diagram of the refrigeration system modified to meet the requirements. The compressor was set to run continuously, eliminating the temperature fluctuation of "on-off" operation. The temperature maintained in the evaporator coils was varied by means of the needle valve which throttled the flow of refrigerant in the system. When the needle valve was fully open, there was continuous normal operation of the freezer and the temperature stabilized at approximately 0°F. This was a function of the characteristics of the refrigerant, in this case Freon -12, and the overall thermal resistance of the freezer cabinet. If the back pressure on the compressor was increased by partially closing the valve, the restricted flow of refrigerant resulted in a lower rate of heat removal and a higher equilibrium temperature.

The position of the needle valve was controlled by a servo motor which was, in turn, controlled by a 10-minute cycle timer. This timer provided power to the servo motor for a period of 5 seconds (or any multiple of 5 seconds) per 10-minute interval. Thus, when the cycle timer was activated, the flow of refrigerant was changed abruptly but by a small amount every 10 minutes. The thermal inertia of the freezer cabinet provided a smoothing effect which resulted in a smooth, gradual temperature change in the system.

The 10-minute cycle timer was controlled by a 24-hour "on-off" time clock and the direction of rotation of the servo motor was controlled by a second time clock and a DPDT relay set up as a

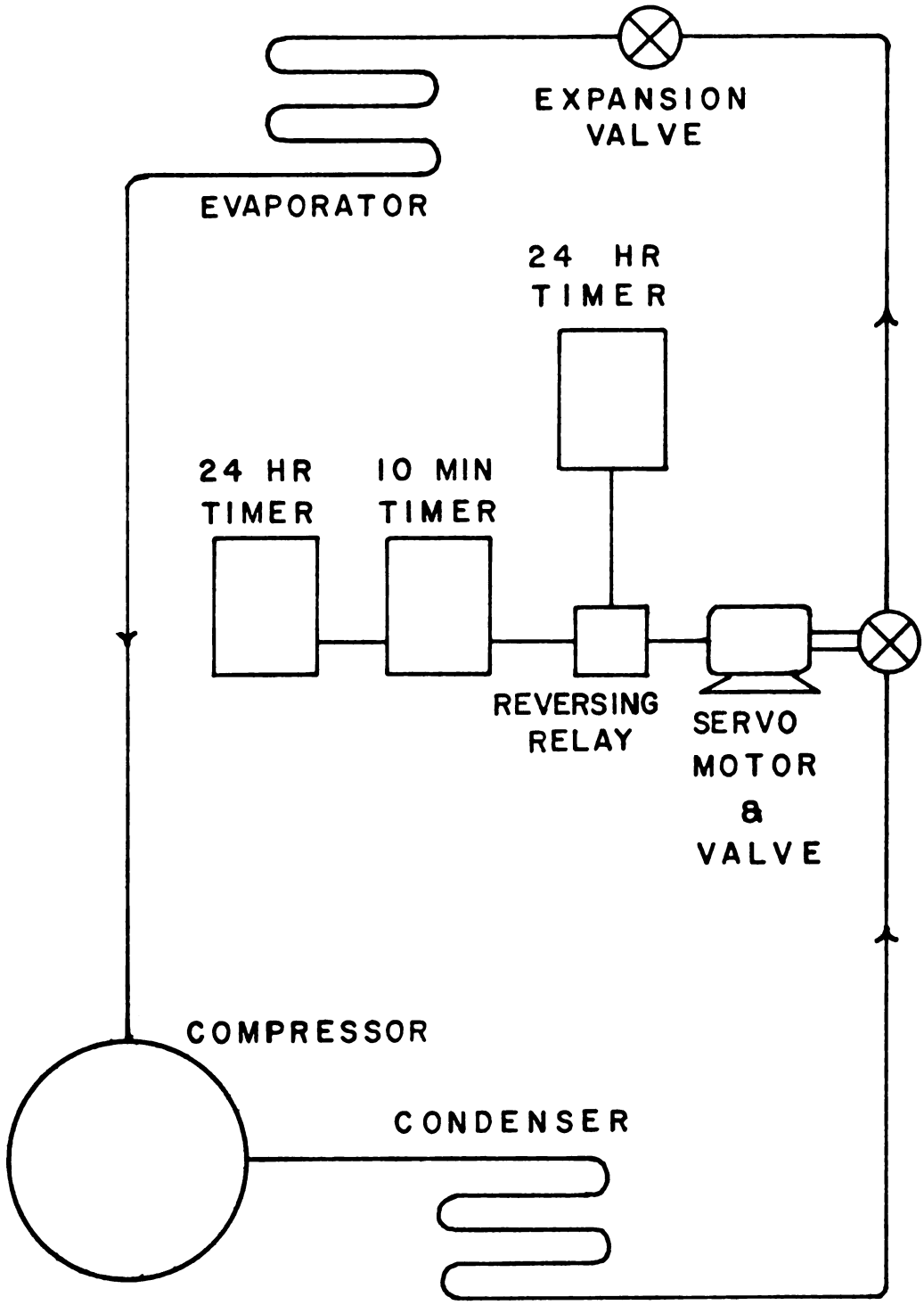

Figure 3.11.--Schematic diagram of control system of modified freezer used in the coefficient of thermal expansion tests.

reversing switch. These controls provided the facility for complete programming of temperature over a 24-hour period.

The determination of the coefficient of thermal expansion required the development of a system for elongation measurement of a sample subjected to changing temperature. The system used in this study is shown diagrammatically in Figure 3.12. This is a modification of the vitreous silica dilatometer recommended in ASTM Designation E 228-66aT (1968). There are two features of this design that are noteworthy. First, the working parts are made of fused quartz which has a very low coefficient of thermal expansion; therefore, the instrument error does not overshadow the displacement being measured. Secondly, the LVDT (displacement transducer) was outside the freezer chamber, and the change in length of the sample was transmitted to it by the relative motion of the quartz tube and rod. This eliminated the problem of thermal error in the displacement transducer.

Since measurements were to be made below 32°F it was necessary to introduce a few drops of ethylene glycol between the quartz tube and rod to prevent freezing and sticking in the apparatus. In order to keep the ethylene glycol from contaminating the sample, vaseline was forced between the lower ends of the quartz tube and rod as a seal.

Internal temperature of the sample was measured with a miniature copper-constantan thermocouple embedded in the sample. A 24-gauge copper constantan thermocouple was placed in the air within 1/2 inch of the sample. The signals from these thermocouples as

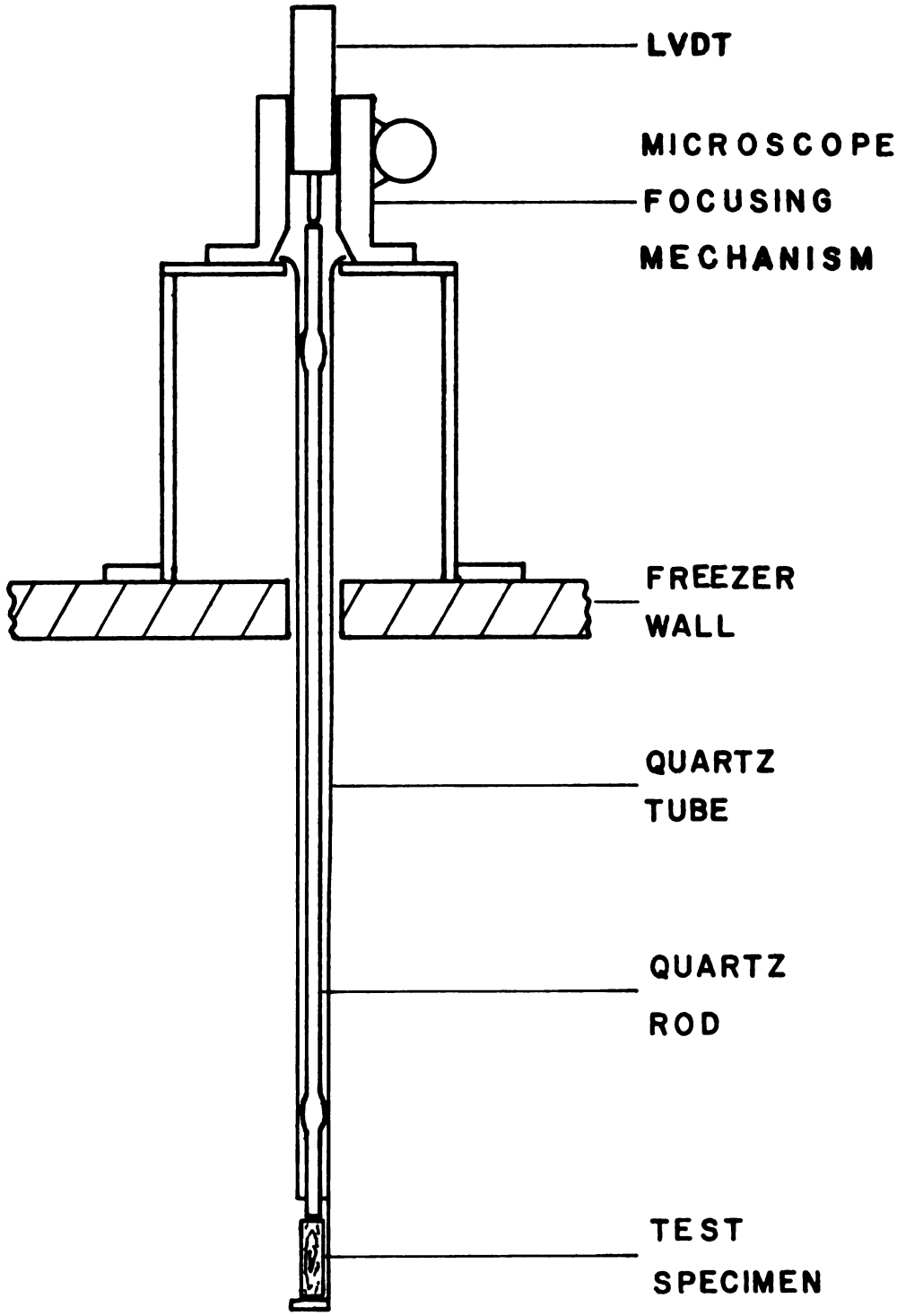

Figure 3.12.--Cross-section of the quartz tube dilatometer.

well as a millivolt signal from the LVDT amplifier were fed to a Texas Instruments Multiriter 24-point recorder. Two dilatometer units were installed in the chamber, thus resulting in six output signals being recorded simultaneously.

3.2.1.2 Experimental procedure.--The directional strength properties and anatomy of wood indicated that the coefficients of thermal expansion of wood for the radial and tangential directions (rather than longitudinal) were of prime importance in this study. Therefore, these were the two general cases of expansion studied.

In general, there were three types of tissue involved--heartwood, sapwood and bark. The thermal expansion of these three tissues was investigated in the radial and tangential directions except for the case of bark where only the tangential expansion was measured.

In all tests, Montmorency cherry tissue was used, with tissue being taken from four separate tree trunks. From each trunk, at least six samples were taken for each of the five cases mentioned above.

During late winter 1970, four mature Montmorency cherry trunks were cut, sealed with grafting compound on the cut faces, transported to the laboratory and stored at 34°F in sealed plastic bags.

At the beginning of a series of tests, transverse slabs approximately 1-1/4 inches thick were cut from a trunk. Each slab

was then subdivided into ten samples as illustrated in Figure 3.13, yielding two samples for each of the five cases specified above. The code used to identify the samples shown in Figure 3.13 was as follows: BT--bark, tangential direction; XT--sapwood, tangential direction; XR--sapwood, radial direction; HT--heartwood, tangential direction; and HR--heartwood, radial direction. In order to keep moisture loss to a minimum, the samples were held in a closed environment at 34°F and 100% R.H. until the time of testing.

A test specimen was a sample approximately 3/8" x 3/8" x 2" cut by a band saw from the middle of the sample as shown in Figure 3.13. The pieces cut from both sides of the test specimen were placed in moisture determination cans, weighed and placed in a drying oven. Moisture content determination was as specified by ASTM (1968). The forced-air drying oven was maintained at 103±1°C until no weight loss in the sample was apparent between two weighings spaced six hours apart. For the size and initial moisture content of samples used in this study, 48 hours of drying was found to be sufficient. Moisture sample weights were determined to the nearest 1/10 milligram by means of an enclosed mechanical pan balance.

The dimensions and fresh weight of the test specimen were determined and recorded. A common pin was then forced into the side of the test specimen. Using the pin as a handle, the specimen was then immersed in molten paraffin wax for less than two seconds. Upon solidification of the film of wax enclosing the specimen, the pin was removed from the specimen. The pin served a dual role in

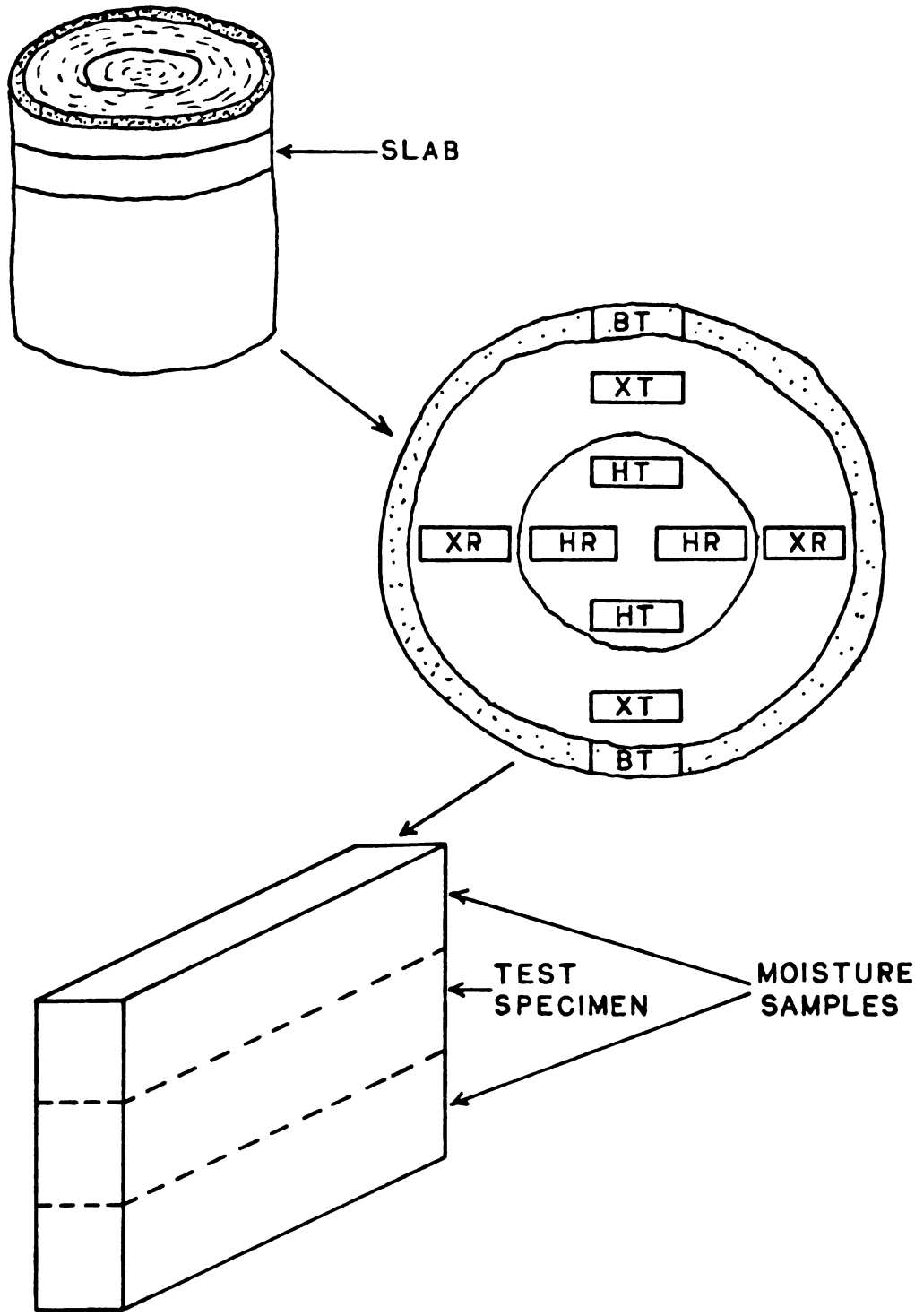

Figure 3.13.--Method of sampling for the coefficient of thermal expansion tests.

that the hole left upon its removal was used for the insertion of a miniature thermocouple into the test specimen.

The test specimen was then reweighed, placed in the dilatometer and the miniature thermocouple was inserted into its center. The time clock controls were then set to provide the following temperature cycle:

1. A 2-hour "hold" period in which the specimen temperature stabilized at approximately 55°F.

2. A 6-hour period of temperature drop during which the specimen temperature was taken down to approximately 0°F.

3. A 2-hour "hold" period at 0°F.

4. A 6-hour period of temperature rise to approximately 55°F.

5. A 2-hour "hold" period at 55°F.

At the end of this cycle, the recorder was automatically shut off. Since the entire test required 18 hours plus the additional time for specimen preparation and installation, the tests were performed on a daily basis, beginning in the morning of one day and terminating early in the morning of the following day.

A test specimen was then removed from the dilatometer and reweighed to determine any moisture loss during the test. The chart was removed from the recorder and displacement transducer readings at 3°F intervals from 40°F to the lowest specimen temperature attained were tabulated.

3.2.1.3 Results.--A typical time-temperature-strain record for the coefficient of thermal expansion tests is shown in Figure 3.14. The thermal strain shown is quite large; so large, in fact, that it is not explained on the basis of the characteristics of dry wood, water, ice, or any combination thereof.

A noteworthy feature of the time-temperature record is the "spike" in the curve at point P. This sudden rise in specimen temperature indicates that water within the specimen has supercooled and then transformed abruptly to the solid phase. The sudden release of heat resulting from this transformation has caused a sharp temperature rise to 32°F. This supercooling effect is consistent with observations reported by Harvey (1923). Occasionally, there was a small, abrupt expansion of the specimen at the time of this temperature rise, followed by rapid contraction. In all cases, however, the rate of specimen contraction increased drastically at this point.

Figure 3.15 shows the same data plotted as thermal strain versus temperature. It is apparent that the thermal strain below 32°F is quite large. There is a marked hysteresis effect between both the curves for temperature rise and fall as well as the initial and final strain values. This indicates that the wood-water-ice combination was behaving as a viscoelastic material.

Coefficients of thermal expansion were calculated for all specimens by dividing the strain experienced between 32°F and the lowest temperature attained by the temperature change. This is in accordance with Hoyle (1964) who stated that in most cases the coefficient of thermal expansion is a function of temperature and

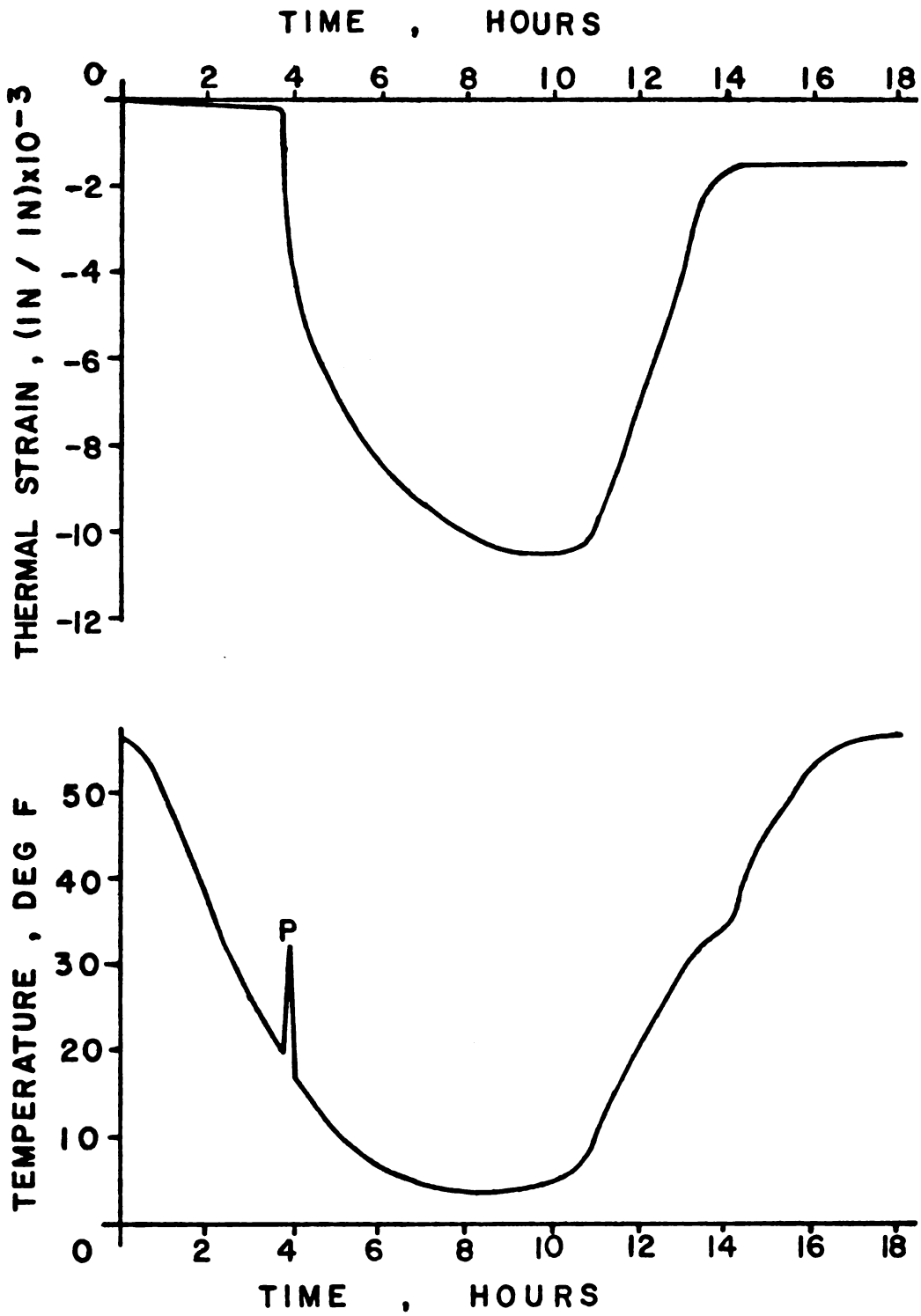

Figure 3.14.--Time-temperature-strain record for a typical coefficient of thermal expansion test.

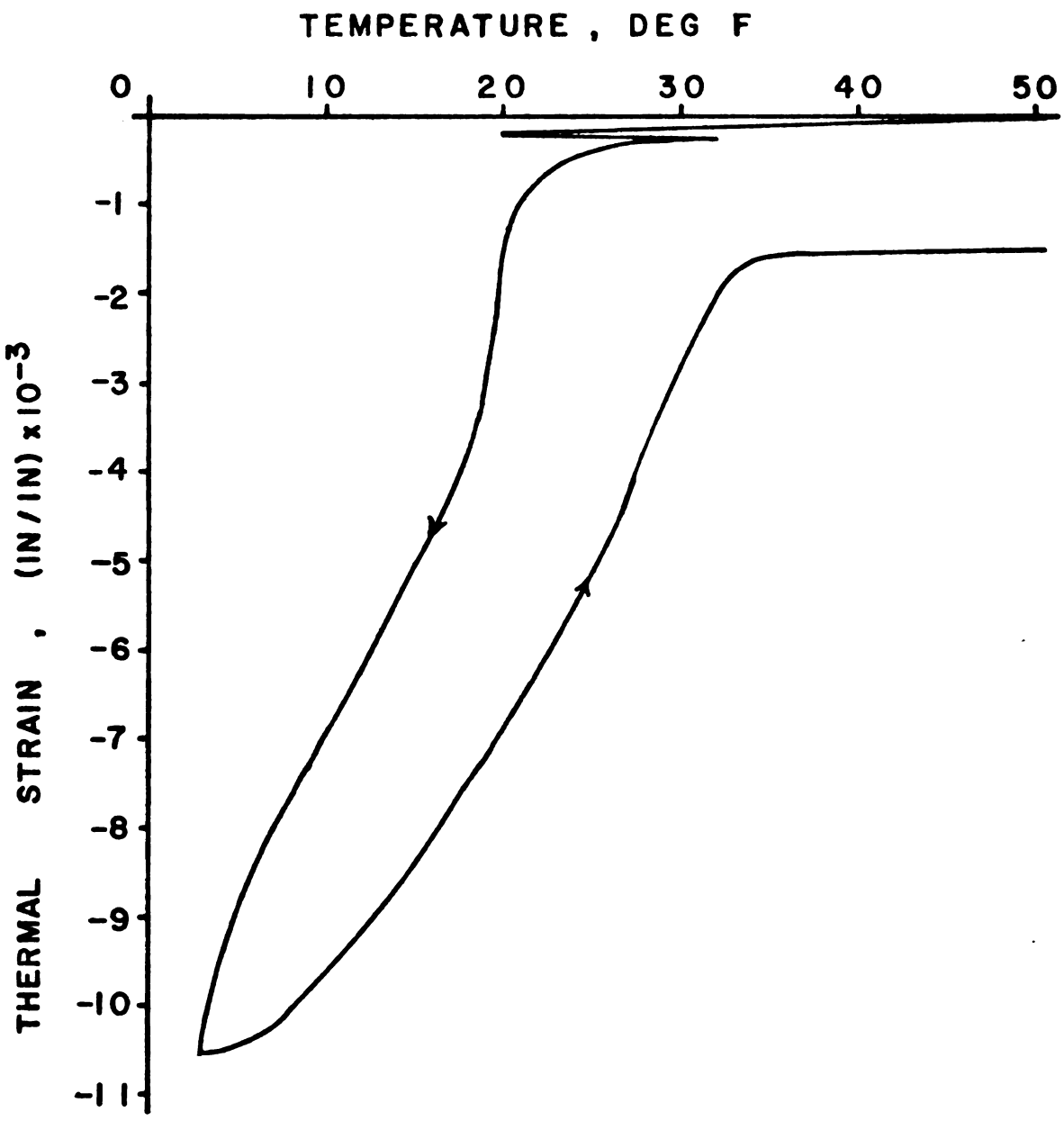

Figure 3.15.--Typical temperature-thermal strain cycle in a coefficient of thermal expansion test.

that a mean coefficient for a temperature range can be calculated in this way, as long as the temperature range is reported.

The cases of falling and rising temperature were considered separately. Tables C.1 through C.4 in Appendix C show the coefficients of thermal expansion, lowest temperature attained, moisture content and dry matter density for the test specimens in this part of the study.

A summary of the coefficients of thermal expansion is given in Table 3.1. Each value shown is the average value for each of the tree-grain direction/temperature-direction combinations. A split plot analysis of the data in Table 3.1 was carried out to isolate effects of the individual trees, the type of tissue, the direction of temperature change and grain orientation on the observed coefficients of thermal expansion. The analysis of variance is shown in Table 3.2.

Comparison of the calculated F-values and tabulated F-values indicates the following:

1. No significant difference among the trees tested.
2. A significant difference between directions of temperature change at $P = 0.01$.
3. A significant difference among specimen types at $P = 0.01$.
4. A significant interaction between specimen types and direction of temperature change at $P = 0.01$.

Least significant differences for the various cases were calculated and comparisons on this basis are shown in Table 3.3.

TABLE 3.1.--Results of the coefficient of thermal expansion study (average coefficient, μ in/in-°F).

Tree No.	1		2		3		4	
Temperature Direction	Fall	Rise	Fall	Rise	Fall	Rise	Fall	Rise
Bark tangential	378 (6, 66)	255 (6, 65)	400 (4, 71)	269 (6, 59)	354 (8, 26)	205 (8, 27)	410 (6, 60)	230 (6, 46)
Sapwood tangential	303 (7, 51)	288 (6, 39)	280 (6, 35)	276 (6, 39)	312 (6, 50)	300 (6, 52)	235 (6, 70)	209 (6, 50)
Sapwood radial	136 (6, 20)	121 (5, 13)	147 (6, 27)	138 (6, 38)	132 (4, 37)	172 (6, 17)	162 (6, 11)	146 (4, 8)
Heartwood tangential	120 (6, 18)	134 (6, 18)	169 (6, 16)	156 (6, 14)	119 (4, 18)	134 (4, 20)	176 (4, 31)	168 (4, 2)
Heartwood radial	79 (7, 13)	77 (7, 9)	80 (5, 7)	73 (5, 5)	75 (5, 14)	66 (5, 13)	70 (4, 18)	71 (4, 5)

Note: The numbers in parentheses are sample size and standard deviation, respectively.

TABLE 3.2.--Analysis of variance for results of the coefficient of thermal expansion study.

Source of Variation	Degrees of Freedom	Sum of Squares	F Calculated	F Tabulated	
				5% (P=.05)	1% (P=.01)
Main plots	7	12,473			
Trees	3	1,104	2.11	9.28	29.46
Temperature direction	1	10,844	62.07	10.13	34.12
Error[a]	3	524			
Sub-plots	39	379,829			
Specimen type	4	318,120	113.24	2.78	4.22
Specimen type x temperature direction	4	32,381	11.53	2.78	4.22
Error[b]	24	16,855			

TABLE 3.3.--Least significant difference analysis of data from the coefficient of thermal expansion study [least significant differences, (μ in/in)/°F].

Comparison	Probability of Type I Error			
	5%		1%	
(1) Between temperature direction means	13.3 *		24.4 *	
(2) Among means for specimen type	27.3		37.0	
BT - XT	*		*	
BT - XR	*		*	
BT - HT	*		*	
BT - HR	*		*	
XT - XR	*		*	
XT - HT	*		*	
XT - HR	*		*	
XR - HT	-		-	
XR - HR	*		*	
HT - HR	*		*	
(3) Among means for specimen type for each temperature direction	38.7		52.5	
	Fall	Rise	Fall	Rise
BT - XT	*	-	*	-
BT - XR	*	*	*	*
BT - HT	*	*	*	*
BT - HR	*	*	*	*
XT - XR	*	*	*	*
XT - HT	*	*	*	*
XT - HR	*	*	*	*
XR - HT	-	-	-	-
XR - HR	*	*	*	*
HT - HR	*	*	*	*
(4) Between means for temperature direction for same specimen type	37.3		52.8	
BT	*		*	
XT	-		-	
XR	-		-	
HT	-		-	
HR	-		-	

*Indicates significant difference at the given probability level.
Key: B-Bark, X-Sapwood, H-Heartwood, R-Radial, T-Tangential.

If the values being compared are greater than the least significant difference at the top of the column, then it is concluded that these values are significantly different. The probability of erroneously making this conclusion when the values are not truly different is given as a percentage at the top of the column.

Comparison number (1) indicates that there was a significant difference in the coefficient of thermal expansion between the means for the directions of temperature change at P = 0.01. However, the comparisons under number (4) of Table 3.3 show that this difference was basically due to the difference in the coefficients of thermal expansion of the bark for temperature rise and fall. The sapwood and heartwood showed no significant differences in their coefficients of thermal expansion for the two directions of temperature change.

Regarding the comparisons under (2) of Table 3.3, the following observations can be made:

(a) The coefficients of thermal expansion in the tangential direction for bark, sapwood and heartwood are all indicated to be significantly different from one another at P = 0.01.

(b) The coefficients of thermal expansion in the radial direction for sapwood and heartwood are indicated to be significantly different at P = 0.01.

(c) The coefficients of thermal expansion of sapwood in the radial and tangential directions were indicated to be significantly different at P = 0.01.

(d) The coefficients of thermal expansion of heartwood in the radial and tangential directions were indicated to be significantly different at P = 0.01.

(e) The coefficients of expansion of sapwood in the radial direction and heartwood in the tangential direction were not significantly different at either P = 0.01 or P = 0.05.

(f) The other comparisons under (2), Table 3.3, all show significant differences at P = 0.01 but the comparisons have no physical significance. They do emphasize, however, the considerable diversity in the coefficients of thermal expansion of the different components of the tree trunk.

Regarding the comparisons shown under (3), Table 3.3, the following observations should be made:

(a) For both P = 0.01 and 0.05, the coefficients of thermal expansion of bark and sapwood in the tangential direction were not significantly different in the case of rising temperature. On the basis of this comparison, and the corresponding comparison under (2), Table 3.3., where the variation due to direction of temperature change was not considered, it is reasonable to conclude that the significant difference attributed to direction of temperature change is not a property of the material, but a result of apparatus design. In the case of the bark, the weight of the quartz rod and LVDT plunger (3.6 oz) was sufficient to cause significant instrument error. Thus, the values determined for the coefficient of thermal expansion of bark are suspect, especially the values for temperature rise.

(b) All other comparisons indicate the same trends as were found in comparison (2), Table 3.3, where the effect of direction of temperature change was not considered.

3.2.2 Microsopic Investigations

The unique thermomechanical behavior of fresh wood below 32°F prompted an investigation, at the microscopic level, of the physical processes of its freezing and thawing.

3.2.2.1 Apparatus.--Apparatus for this portion of the study was available in the USDA laboratory on the MSU campus where studies of winter hardiness of various field crops were in progress; therefore, apparatus development was minimal.[1] The experimental equipment was kept in a temperature-controlled chamber with a refrigeration system similar to that described in Section 3.2.1.1. There was one variation, however; in this case, there were two chambers--the active chamber in which the experiment was performed and a passive chamber in which the evaporator coils were kept at a slightly lower temperature than those of the active chamber. Air was circulated between both chambers. This feature performed one very important function. Any development of frost would occur first on the evaporator coils of the passive chamber, thus maintaining equipment in the active chamber in a frost-free condition.

The active chamber was equippped with an insulated internal front cover fitted with a viewing window and two plastic armlets.

---

[1]The laboratory was located on the third floor of Agriculture Hall, Michigan State University, and was under the direction of Dr. C. R. Olien.

These features allowed manipulation of equipment and material within the chamber with a minimum disturbance of temperature.

The equipment within the active chamber was typical for general microscopic investigation. For sectioning material, a moving blade microtome was used. This microtome was capable of cutting sections in the range of 20 to 50 microns thickness in woody material.

For viewing the sections a monocular microscope was used. The eyepiece was extended out through one of the armlet holes during viewing. For photographing the sections a camera back and microscope adapter were required. These were kept outside the cold chamber, and attached to the microscope when required.

3.2.2.2 Procedure.--The experimental material was frozen in the same freezer in which the coefficient of thermal expansion tests were performed. The freezing rate was the same as for the coefficient of thermal expansion tests and the size of the specimen was approximately the same. No sealing material was used in this case; rather, the specimen was held above a saturated solution of barium chloride which did not freeze in the range of temperatures used and which provided an atmosphere of approximately 91% relative humidity to reduce evaporation from the specimen.

The specimen was frozen to 15°F and then transferred to a thermos container partly filled with an eutectic slush of a saturated solution of manganese chloride ($MnCl_2 \cdot 4H_2O$). This slush maintained the temperature at 15°F during transfer to the chamber in the USDA laboratory, Agriculture Hall.

Prior to this transfer, the active chamber and all equipment inside it were cooled and held at 15°F. It was essential that all equipment to be used inside the test chamber be placed in the chamber and pre-cooled before the beginning of the experiment. All utensils such as tweezers and needles were equipped with wooden or insulated handles to retard the flow of heat into the utensils from the hands of the operator. All operations were performed while wearing cloth gloves to protect the hands of the experimenter and also to retard the flow of heat from the hands of the experimenter through the equipment to the test specimen.

Temperature in the chamber was indicated at all times by an alcohol in glass thermometer inside the active chamber and also by a copper-constantan thermocouple and a Leeds and Northrup manually balanced potentiometer. It was necessary to limit operations inside the chamber to a maximum of approximately one minute out of five to minimize the disturbance of temperature. In order to reduce accumulation of ice on the evaporator coils, every effort was made to limit exchange of air between room and test chamber during the times that no operations were being performed.

After the temperature in the chamber had stabilized from the disturbance of the material transfer, the specimen was removed from the thermos flask and clamped into the vise of the microtome. Using a scalpel, the part of the specimen to be sectioned was pared away on all sides until a relieved vertical projection approximately one millimeter square remained. This was the portion of the specimen used for sectioning.

The microtome cutting head was then lowered until the blade edge was even with the top of the relieved section. The blade was drawn slowly and steadily through the specimen to cut off a thin slice. The cutting head was lowered by 50 microns and another slice was removed in the same manner. This was repeated several times before actual test sections were cut. It was essential that the cutting edge be extremely sharp and that it be moved as slowly and steadily as possible to minimize disturbance of the ice crystal structure during sectioning.

Using a soft bristle brush, the sections to be studied were carefully transferred from the blade to a glass dish containing mineral oil saturated with water at 15°F. It was essential that the oil be in a saturated condition to prevent dehydration of the wood section which would disturb or destroy the ice crystal structure to be examined. The sections were held in the oil while further sectioning was carried out.

Mounting of the wood sections was achieved by using a small metal spatula to dip a drop of oil containing a section out of the holding dish and depositing it on a glass slide. Several sections could be placed on one slide before a cover slip was installed. The slide was then placed in the microscope and visual inspection of the sections was made. During this operation, the eyepiece of the microscope was projected outside the chamber through one of the armlets. Because of heat conduction along the draw tube, the eyepiece tended to collect condensation in the warm room air. Thus, viewing was a periodic operation interrupted by breaks for re-warming of the

eyepiece. The open end of the tube was sealed with a plastic plug during these breaks, to prevent internal condensation on the objective lens system.

When visual inspection revealed features of sufficient interest, a photograph was taken. The eyepiece was replaced by a Leitz camera adapter and Leica 35 mm camera back. Black and white photographs were taken using Kodak Panatomic-X fine grain film (ASA-16). A light meter calibrated for this film and fitted with an eyepiece attachment provided a means of adjustment of light intensity. Because a low light intensity was used to minimize heating of the chamber, relatively long exposure times were required. Since the experimental material was variable in nature, a wide range of exposure times was used to insure a good photograph. Shutter speeds of 1, 2, 4, 8 and 16 seconds were used.

After inspection at one temperature the chamber was allowed to warm up slowly. Changes in ice crystal structure and cellular condition were noted and photographed up to and above the freezing point.

3.2.2.3 Results.--The results of this part of the investigation are best considered by a discussion of the photographs of Figures 3.16 and 3.17. In Figure 3.16a is shown a cross-section of Montmorency cherry sapwood held at 15°F, sectioned to a thickness of 50 microns and magnified 430X. Ice crystal formation is quite evident in the intercellular spaces, recognized as transparent, angular, crystalline structures running in a continuous manner around the

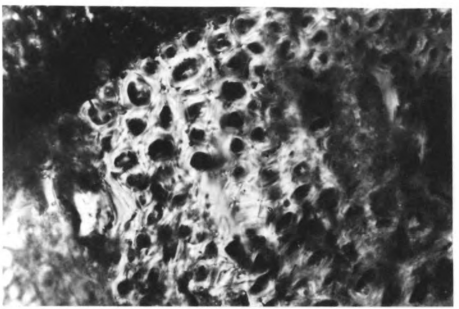

Figure 3.16(a) Lateral cross-section of Montmorency cherry trunk wood at 15°F, magnification 430x (Photo No. 70-191)

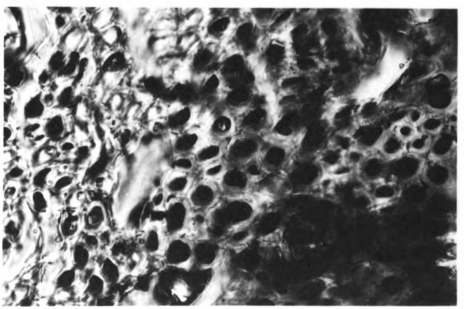

Figure 3.16(b) Lateral cross-section of Montmorency cherry trunk wood at 28°F, magnification 430x (Photo No. 70-196)

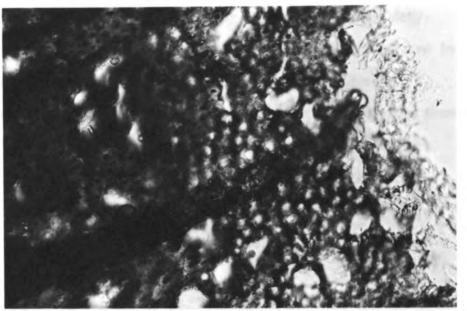

Figure 3.17(a) Lateral cross-section of Montmorency cherry trunk wood at 35°F, magnification 210x (Photo No. 70-198)

Figure 3.17(b) Lateral cross-section of Montmorency cherry trunk wood at 35°F, magnification 430x (Photo No. 70-200)

cells. Also, the cells themselves appear to be shrunken or dehydrated. The cell walls, rather than being tightly stretched, are in irregular shapes around a diminished amount of cell contents.

Figure 3.16b shows a similar section after being warmed from 15°F to 28°F. Ice crystal formation is still evident but it does not fill as large a proportion of the intercellular spaces as before. Also, the cells themselves seem less shrunken than before. This would indicate that the cells have absorbed water as the temperature has risen.

Figures 3.17a and 3.17b show similar cross sections at 35°F and 210X and 430X magnification, respectively. Obviously, no ice is present at this temperature and the living cells at the bottom of Figure 3.17b have lost any shrunken appearance.

These observations are in accord with those of Krasavtsev (1968) who noted severe cellular dehydration in woody material when frozen to -60°C, and those of Olien (1964) who noted the loss of cellular water with the development of intercellular ice in barley crowns.

3.3 Prediction of Thermal Stresses in Tree Trunks

The field portion of this investigation has provided data on interesting temperature regimes in fruit tree tunks. The laboratory investigation has provided data on the sub-freezing radial and tangential coefficients of thermal expansion of cherry wood. In order to link these two types of data, a numerical technique was employed to make a thermal stress analysis of the cross-section of

the tree trunk. The finite element technique was the method chosen to calculate the thermal stress field in a tree trunk subjected to the temperature regimes which were measured. The following sections outline the basic theory and computational procedure used in this analysis.

3.3.1 Basic Theory of Finite Element Analysis

The finite element method is a numerical procedure for the solution of differential equations. The basic premise behind the method is that any function, existing in a region, can be represented by "a set of piecewise continuous functions defined over a finite number of subdomains" (Segerlind, 1976). Consider Figure 3.18 in which the x and y displacements of nodes i, j and k defining the element (e) are represented as shown. If the displacement is assumed to vary linearly within the region, the components of displacement at any point P can be represented by

$$u = \alpha_1 + \alpha_2 X + \alpha_3 Y \tag{3.1a}$$

$$v = \beta_1 + \beta_2 X + \beta_3 Y \tag{3.1b}$$

If the values for the nodal displacements and coordinates are substituted into equations (3.1) one can solve for α_1, α_2, α_3, β_1, β_2 and β_3 in terms of these coordinates and displacements. The final result is

$$u = N_i U_{2i-1} + N_j U_{2j-1} + N_k U_{2k-1} \tag{3.2a}$$

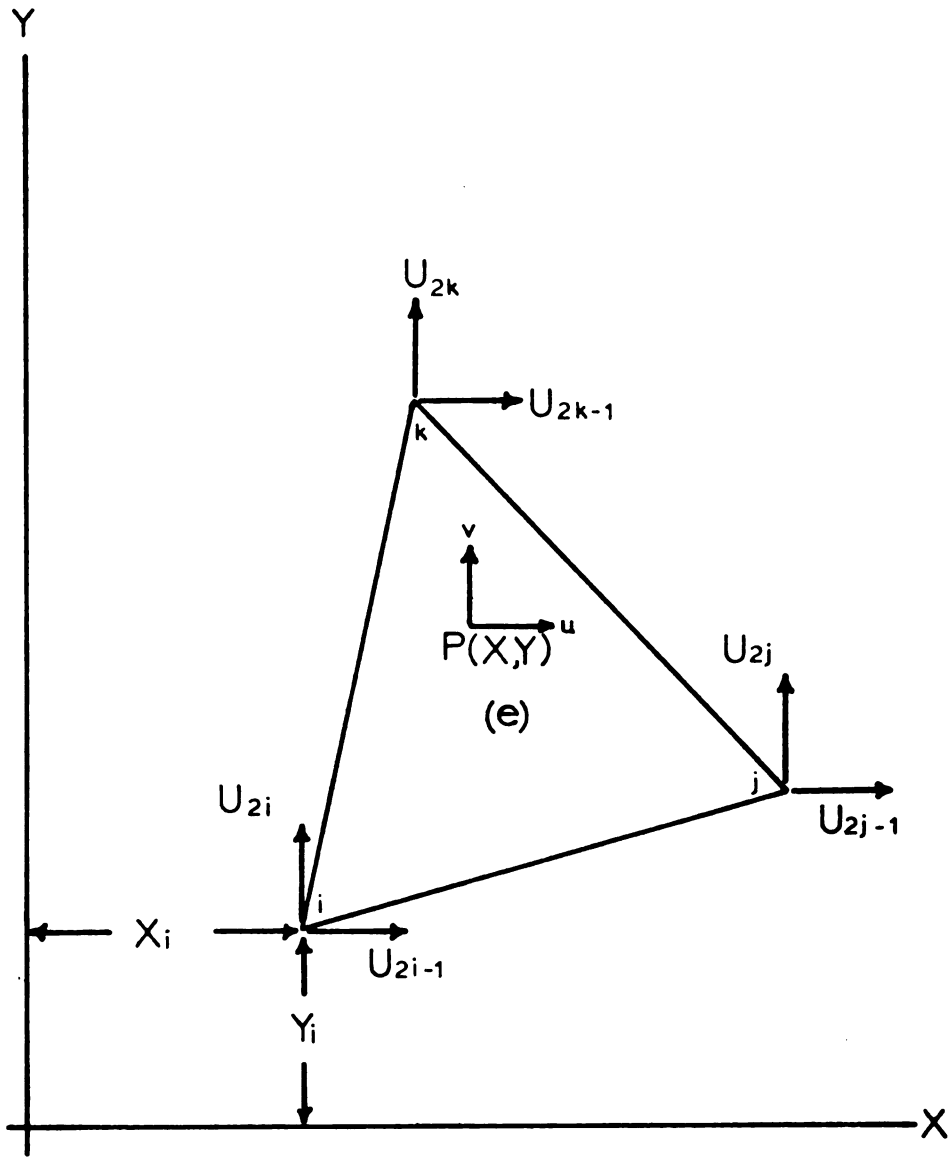

Figure 3.18.--Triangular element showing nodal displacements.

$$v = N_i U_{2i} + N_j U_{2j} + N_k U_{2k} \tag{3.2b}$$

where

$$N_i = (a_i + b_i X + c_i Y)/2A$$

$$N_j = (a_j + b_j X + c_j Y)/2A$$

$$N_k = (a_k + b_k X + c_k Y)/2A$$

and

$$a_i = X_j Y_k - X_k Y_j$$

$$b_i = Y_j - Y_k$$

$$c_i = X_k - X_j$$

The constants a_j, b_j, etc. can be obtained by cycling the subscripts in the equations for a_i, b_i and c_i.

The terms N_i, N_j and N_k are known as the shape functions of the element. Equations 3.2, above, can be written in matrix notation as

$$\{u\} = [N]\{U\} \tag{3.3}$$

where

$$\{u\} = \begin{Bmatrix} u \\ v \end{Bmatrix}$$

$$[N] = \begin{bmatrix} N_i & 0 & N_j & 0 & N_k & 0 \\ 0 & N_i & 0 & N_j & 0 & N_k \end{bmatrix}$$

and

$$\{U\} = \begin{Bmatrix} U_{2i-1} \\ U_{2i} \\ U_{2j-1} \\ U_{2j} \\ U_{2k-1} \\ U_{2k} \end{Bmatrix}$$

Consider the case where a region is divided into several elements as in Figure 3.19. The displacements in each element are given by

$$\{u^{(e)}\} = [N^{(e)}]\ \{U\} \tag{3.4}$$

where $\{u^{(e)}\}$ is the displacement vector of an individual element and $[N^{(e)}]$ is the matrix of shape functions for that element. Since the displacements in the elements are piecewise continuous, this means that the displacements along inter-element boundaries are continuous but their derivatives are not continuous.

The displacement equations for each element can be written in terms of all the nodal displacements by adding zero coefficients to [N] for those displacements not associated with the particular element. This allows all of the element displacements to be written in a single matrix

$$\{u\} = [N^*]\ \{U\} \tag{3.5}$$

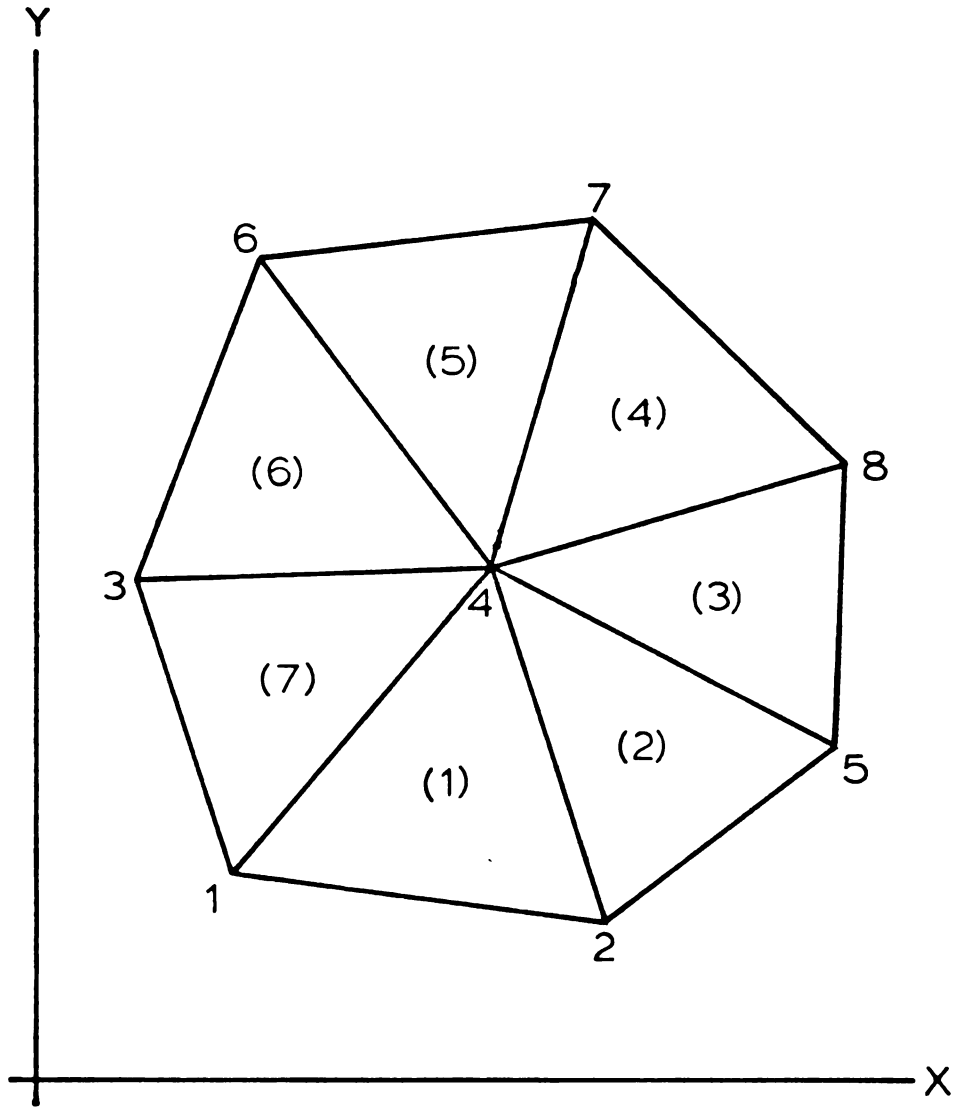

Figure 3.19.--Plane region divided into several elements.

This becomes a sizable system of equations for even a small number of elements. The dimensions of equation (3.5) for the region in Figure 3.19 are

$\{u\}$ 14 x 1

$[N^*]$ 14 x 16

$\{U\}$ 16 x 1

The first row of $[N^*]$ contains the coefficients for $u^{(1)}$ and is

$$[N_1^{(1)} \; 0 \; N_2^{(1)} \quad 0 \; 0 \; 0 \quad N_4^{(1)} \quad 0 \; 0 \; 0 \; 0 \; 0 \; 0 \; 0 \; 0 \; 0]$$

where node i is node 1. The superscript indicates the shape function is to be evaluated in element one.

If one knew the geometry of the region and the nodal values of displacements, equation (3.5) would allow linear interpolation of displacement values at any point in the region. This is not, however, a common type of usage for this method of analysis. The method is most often used to determine the unknown nodal displacements and then these displacements are used to calculate element strains and stresses. The method of solution is outlined in the following section.

3.3.2 Application of Finite Element Analysis to Plane Thermoelasticity

In an elastic system, the conditions of equilibrium are satisfied if the boundary conditions are satisfied and the total potential energy of the system is minimized. The total potential energy in an elastic system is

$$\Pi = \Lambda + W_p \tag{3.6}$$

where Λ is the strain energy and W_p is the potential of the applied loads (body forces, pressures, etc.). In the case of a thermal stress analysis of a tree trunk, there are no applied loads. Therefore, the term W_p can be deleted from our discussion.

The strain energy in the system is

$$\Lambda = \int_V \frac{1}{2} (\{\varepsilon\}^T \{\sigma\} - \{\varepsilon_0\}^T \{\sigma\}) dV \tag{3.7}$$

where

$\{\varepsilon\}$ = total strain vector

$\{\sigma\}$ = stress vector, and

$\{\varepsilon_0\}$ = initial strain vector.

The stress and strain are related by Hooke's law

$$\{\sigma\} = [D]\{\varepsilon\} - [D]\{\varepsilon_0\} \tag{3.8}$$

in which, for the case of plane strain in a cylindrical anisotropic system is

$$[D] = \frac{1}{(1 - \nu_{R\theta}\nu_{\theta R} - \nu_{\theta Z}\nu_{Z\theta} - \nu_{ZR}\nu_{RZ} - \nu_{R\theta}\nu_{\theta Z}\nu_{ZR} - \nu_{\theta R}\nu_{Z\theta}\nu_{RZ})}$$

$$\times \begin{bmatrix} E_R(1 - \nu_{Z\theta}\nu_{\theta Z}) & E_R(\nu_{\theta R} + \nu_{ZR}\nu_{\theta Z}) & 0 \\ E_\theta(\nu_{R\theta} + \nu_{Z\theta}\nu_{RZ}) & E_\theta(1 - \nu_{ZR}\nu_{RZ}) & 0 \\ 0 & 0 & G_{R\theta} \end{bmatrix} \tag{3.9}$$

Recalling the strain displacement relationships

$$\varepsilon_{xx} = \frac{\partial u}{\partial x} \, , \; \varepsilon_{yy} = \frac{\partial v}{\partial y} \, , \; \gamma_{xy} = \frac{\partial u}{\partial y} + \frac{\partial v}{\partial x} \tag{3.10}$$

and applying these to equation (3.4), the strain vector for any element can be written

$$\{\varepsilon^{(e)}\} = [B^{(e)}] \{U\} \tag{3.11}$$

where $[B^{(e)}]$ is formed by differentiating the shape function in equation (3.4) as indicated in equation (3.10). Substituting equations (3.11) and (3.8) into equation (3.6), we obtain

$$\begin{aligned} \Pi^{(e)} = \Lambda^{(e)} = \int_{V(e)} \frac{1}{2} \Big(& \{U\}^T [B^{(e)}]^T [D^{(e)}] [B^{(e)}] \{U\} \\ & - 2 \{U\}^T [B^{(e)}]^T [D^{(e)}] \{\varepsilon_0^{(e)}\} \\ & + \{\varepsilon_0\}^T [D^{(e)}] \{\varepsilon_0\} \Big) dV \end{aligned} \tag{3.12}$$

The last term in the brackets disappears during the minimization process because it is not a function of the displacements, and is deleted at this point. Summing equation (3.12) over the elements, differentiating with respect to $\{U\}$ and setting it equal to zero yields

$$\begin{aligned} \sum_{e=1}^{E} \left[\int_{V(e)} [B^{(e)}]^T [D^{(e)}] [B^{(e)}] \, dV \, \{U\} \right] \\ = \sum_{e=1}^{E} \left[\int_{V(e)} [B^{(e)}]^T [D^{(e)}] \{\varepsilon_0\} \, dV \right] \end{aligned} \tag{3.13}$$

where $\{\varepsilon_0\}$ defines the unrestrained thermal strain which is

$$\{\varepsilon_0\} = \begin{Bmatrix} (\nu_{ZR}\alpha_Z + \alpha_R)T \\ (\nu_{Z\theta}\alpha_Z + \alpha_\theta)T \\ 0 \end{Bmatrix} \tag{3.14}$$

for a cylindrical anisotropic material.

The integral on the left side of equation (3.13) is known as the element stiffness matrix

$$[k^{(e)}] = \int_{V^{(e)}} [B^{(e)}]^T [D^{(e)}] [B^{(e)}] \, dV \tag{3.15}$$

and the summation of the $[k^{(e)}]$ is the global stiffness matrix, [K]. The integral on the right side of equation (3.13) is known as the element force vector

$$\{f^{(e)}\} = \int_{V^{(e)}} [B^{(e)}]^T [D^{(e)}] \{\varepsilon_0\} \, dV \tag{3.16}$$

and the summation of the $\{f^{(e)}\}$ is the global force vector {F}. Equation (3.13) can be written as

$$[K]\{U\} = \{F\} \tag{3.17}$$

Equation (3.17) represents a system of equations which can be solved for the nodal displacements. There are twice as many equations as there are nodes. Fortunately, solution of these equations can be programmed for the digital computer. Substitution of the nodal displacements obtained by solving equation (3.17) into Hooke's law written in terms of displacements yields

$$\{\sigma\} = [D][B]\{U\} - [D]\{\epsilon_0\} \qquad (3.18)$$

which allows the stresses in each element to be calculated.

3.3.3 Computer Implementation

The implementation of the finite element method involves the performance of a large number of repetitive arithmetic operations. The digital computer can be programmed to perform these operations.

Available in the Department of Agricultural Engineering, Michigan State University, was a program, GRID, which, when provided with the geometry of a region to be subdivided into elements, and the spacing of nodes on the periphery of triangular segments of the region, generated the element grid for the region. The element grid used to represent a circular tree trunk is shown in Figure 3.20. The data for all nodes and elements were stored on tape for use in further computations and for CALCOMP plotting of the grid from which Figure 3.20 was derived. This element grid was placed on a light table over tree trunk temperature contour maps and the temperatures at all nodes were determined by visual interpolation.

Also available in the Department of Agricultural Engineering, Michigan State University, was a program, STRESS, for the solution of isotropic plane stress or plane strain problems. The program was modified for use with orthotropic materials. This required that provision be made for the input of the material properties for the three principal directions. Provision was also made for the input of more than one type of material so that a tree trunk made up of heartwood and sapwood could be modeled. Finally, the program was

modified to compute the stress in polar coordinates, so that the output would be in the form σ_{RR}, $\sigma_{\theta\theta}$, and $\sigma_{R\theta}$.

3.3.4 Input Data for the Analysis

The plane strain finite element model of the tree trunk required values for the material properties of the wood. Values were needed for three moduli of elasticity, six Poisson's ratios (only three of which were independent), three coefficients of thermal expansion, and one shear modulus. Sliker (1972, 1975, 1976) indicated that data for elastic moduli and Poisson's ratios are incomplete and somewhat unreliable. Values for the coefficients of thermal expansion in the radial and tangential directions were available from the experiments of this study, but the rest of the material properties had to be assumed on the basis of values from the literature.

Palka (1973) made a comprehensive review of the diverse data on the elastic properties of softwoods and proposed methods of predicting the elastic properties of a wood for which test data were not available. Kollmann and Côté (1968) have compiled the information available on the effects of moisture content, density and temperature on the elastic properties of woods. Bodig and Goodman (1973) used the data available at that time and developed prediction equations for the elastic moduli and Poisson's ratios based on wood density. Regression equations with high correlation coefficients were developed relating the moduli of elasticity and the shear moduli; prediction equations relating the various

Poisson's ratios could not be developed. In all cases, the data used was for air-dry rather than fresh wood.

Comben (1964) showed that, for ash in the green condition, both the longitudinal modulus of elasticity and longitudinal tensile strength were increased by approximately 15% when the wood was frozen. The same observation was made by Kollman and Côté (1968).

Moisture content affects the elastic parameters of wood (Kollman and Côté, 1968; Wood Handbook, 1974; Palka, 1973). In all cases, the modulus of elasticity decreases with increasing moisture content but this decrease stops at the fiber saturation point (30% moisture, d.b., approximately). In general, the decrease in modulus of elasticity is approximately 25% for an increase in moisture content from the air-dry to the "green" condition. Poisson's ratios change with moisture content as well, and most of the available information is for wood at moisture contents below the fiber saturation point. Palka (1973) indicates that $\nu_{\theta R}$, $\nu_{R\theta}$, and $\nu_{Z\theta}$ increase with increasing moisture content, whereas $\nu_{\theta Z}$, ν_{RZ}, and ν_{ZR} decrease with increasing moisture content. Regardless, the relationship $\nu_{ij}E_j = \nu_{ji}E_i$ for orthotropic materials must be satisfied. Since E_R and E_θ are much smaller than E_Z (Wood Handbook, 1974; Kollman and Côté, 1968), it follows that the values for ν_{RZ} and $\nu_{\theta Z}$ are very small; in fact, Sliker (1976) and Palka (1973) stated that these values cannot be measured and are simply calculated from values of the larger, more easily measured ratios.

Sliker (1976) stated that the Wood Handbook (1974) value of 1.31×10^6 psi for the longitudinal modulus of elasticity of black

cherry at 55% moisture (d.b.) would be a good starting point. Adjustment for moisture content, temperature and a degree of conservatism would be necessary. Sliker (1976) also indicated that the values of Poisson's ratios reported for black walnut (Wood Handbook, 1974) would be suitable, since the anatomy of cherry and walnut woods is reasonably similar. Again, adjustment for moisture content and temperature would be necessary.

From the above discussion, it is obvious that any set of assumed values for the material properties of cherry wood is open to challenge. Depending upon the method of prediction used, different sets of values can be generated. Therefore, using the recommendations of Palka (1973), Bodig and Goodman (1973), and Kollmann and Côté (1968) as guides, and keeping in mind the results of Kunesh (1968) and Kennedy (1968), the following set of material properties was assumed:

E_Z = 1,000,000 psi

E_R = 100,000 psi

E_θ = 50,000 psi

$G_{R\theta}$ = 15,000 psi

$\nu_{R\theta}$ = 0.76

$\nu_{\theta R}$ = 0.38

ν_{ZR} = 0.42

ν_{RZ} = 0.042

$\nu_{Z\theta}$ = 0.74

$\nu_{\theta Z}$ = 0.037

$\alpha_R = 0.000144\ °F^{-1}$

$\alpha_\theta = 0.000276\ °F^{-1}$

$\alpha_Z = 0.000028\ °F^{-1}$

The value for α_Z was assumed based on the above-freezing ratio of longitudinal to tangential coefficients of thermal expansion. The values for the elastic constants satisfy the relationship $\nu_{ij}E_j = \nu_{ji}E_i$; i = R, θ, Z; j = R, θ, Z.

3.3.5 Results of Finite Element Stress Analysis

The output from the program STRESS provided center-of-element values for strain and stress in cylindrical coordinates as well as principal stresses and principal directions. The nature of the trunk splitting problem suggested that the tangential stresses were of primary interest, but that the pattern of radial stresses should be checked as well. The values from the computer output were transcribed to each element on a grid identical to that shown in Figure 3.20. Lines of constant stress were then hand-plotted on the grid.

Figure 3.21 shows the lines of constant tangential stress predicted by the model for 9:00 P.M., 5 February 1969. (Temperature contours for this situation have been shown previously in Figure 3.5.) Positive values indicate tensile stress. Figure 3.21 shows that the model predicts tensile stress in all but a very small part of the tree at the center. The lines of constant stress form a pattern of nearly concentric rings with the highest values near the periphery and decreasing toward the center. The highest tensile

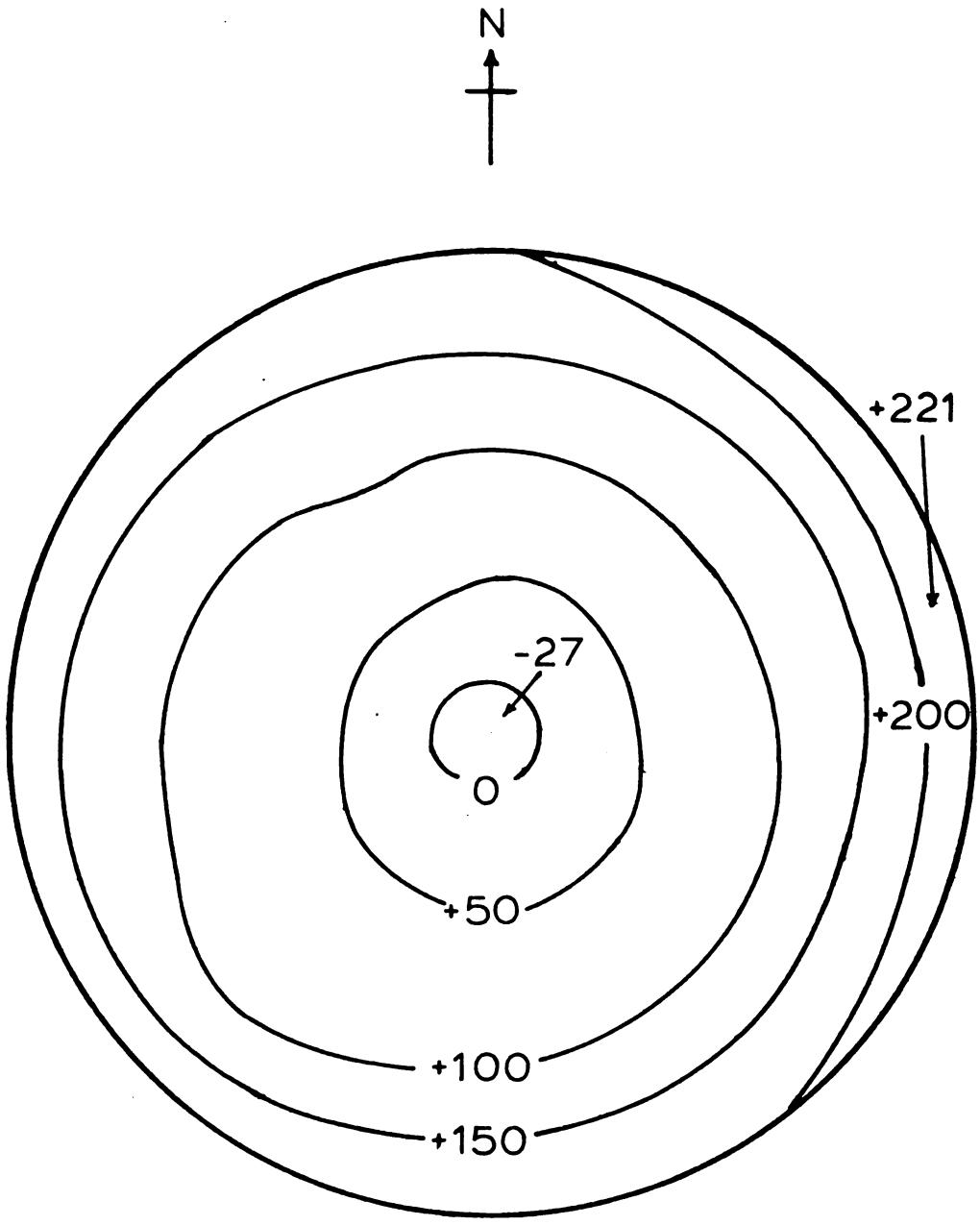

Figure 3.21.--Predicted tangential stress distribution in tree trunk, 9:00 P.M., 5 February 1969. (Scale 1.5X actual, stress values in psi.)

stress predicted was 221 psi in the position shown in Figure 3.21. The maximum predicted compressive tangential stress was 27 psi in an element at the center of the trunk.

The pattern of radial stresses which was predicted for 9:00 P.M., 5 February 1969, was interesting but not amenable to the contour style of presentation shown in Figure 3.21. The model predicted that the entire cross-section of the tree trunk would be in compression in the radial direction. The maximum compressive stress was predicted at the center of the trunk (-238 psi) but the value dropped quickly, as one moved outward along a radial line, to an almost constant value, then dropped to zero at the boundary. Figure 3.22 shows a plot of the predicted radial stresses along the East-West diameter of the trunk. Similar radial stress distributions were predicted for all cross-sections.

Figure 3.23 shows the predicted lines of constant tangential stress for 5:14 P.M., 14 January 1970. The isothermal map for this case is shown in Figure 3.9, Section 3.1.2. The results are quite similar to those in Figure 3.20 in that the maximum tensile stress (250 psi) occurs in a peripheral element and the tensile stress decreases as one moves toward the center. In this case, there is a larger area of compressive tangential stress predicted at the center of the trunk and a maximum value of -68 psi (compressive) occurs at the center.

Figure 3.24 shows the predicted tangential stresses for 7:42 P.M., 18 January 1970. The isothermal map for this case is shown in Figure 3.10, Section 3.1.2. On this particular evening,

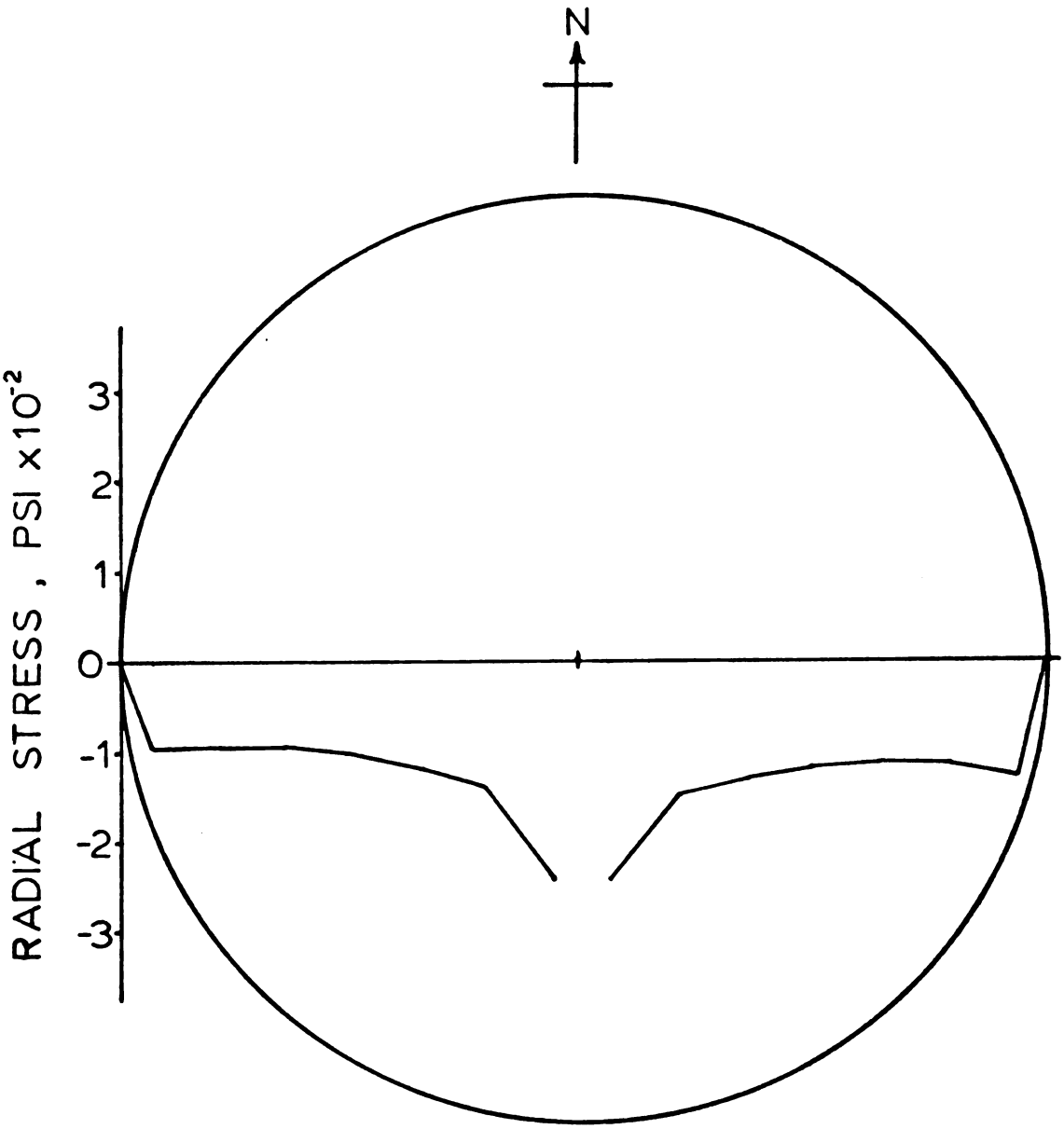

Figure 3.22.--Predicted radial stress distribution on East-West diameter of tree trunk, 9:00 P.M., 5 February 1969. (Scale 1.5X actual.)

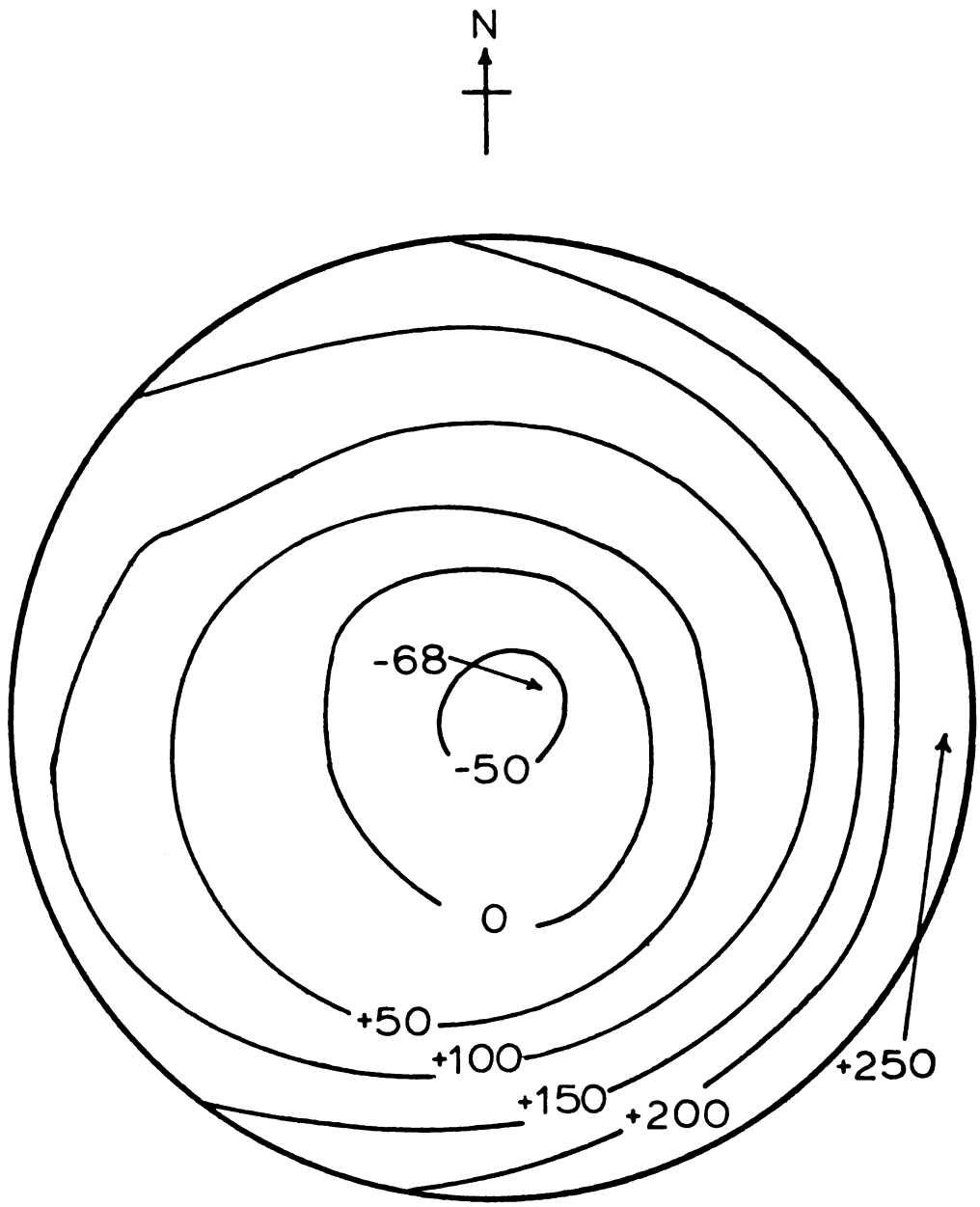

Figure 3.23.--Predicted tangential stress distribution in tree trunk, 5:14 P.M., 14 January 1970. (Scale 1.5X actual, stress values in psi.)

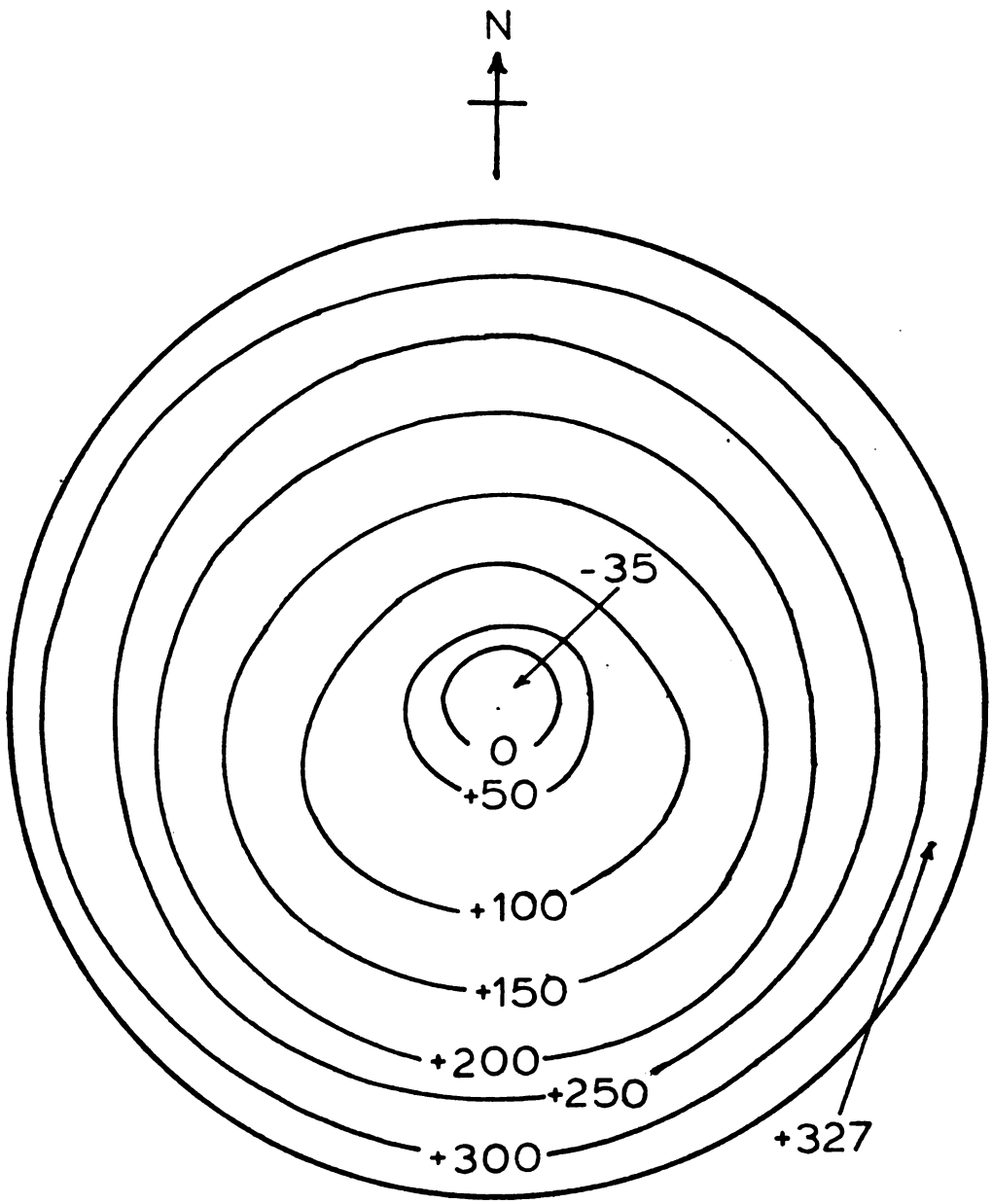

Figure 3.24.--Predicted tangential stress distribution in tree trunk, 7:42 P.M., 18 January 1970. (Scale 1.5X actual, stress values in psi.)

conditions were such that the tree trunk was cooling at very close to a uniform rate at all points on the circumference; that is, the temperature gradients along all radii were quite similar. As a result, the lines of constant tangential stress in Figure 3.24 are almost perfect concentric circles. Maximum predicted tensile stress was 327 psi in the position shown. A compressive stress of 35 psi was predicted at the center of the trunk.

The question of whether a tree trunk can split during rapid warming was raised by Parker (1963). The hypothesis was that rapid warming of one side of a frozen tree trunk would cause sufficient expansion at the surface to develop destructive tensile tangential stresses in the interior of the trunk. As a test of this hypothesis, temperature data for 9:00 A.M., 5 February 1969, was input to the finite element model. The isothermal map for this case is shown in Figure 3.4; the southeast side of the trunk was being warmed rapidly by the sun's radiation, while the northwest portion of the trunk had not yet experienced any appreciable temperature change. The predicted tangential stresses are shown in Figure 3.25. As expected, the model predicted compressive stresses at the heated surface (-223 psi); however, the maximum tensile tangential stress predicted in the interior is 39 psi. Therefore, this one test does not support the theory of internal splitting as a result of tangential expansion of the trunk periphery. However, the relatively high compressive stresses predicted in the area of rapid temperature rise may contribute to the failure of the trunk tissue by some other mechanism. For example, if the compressive stress exceeds the ultimate

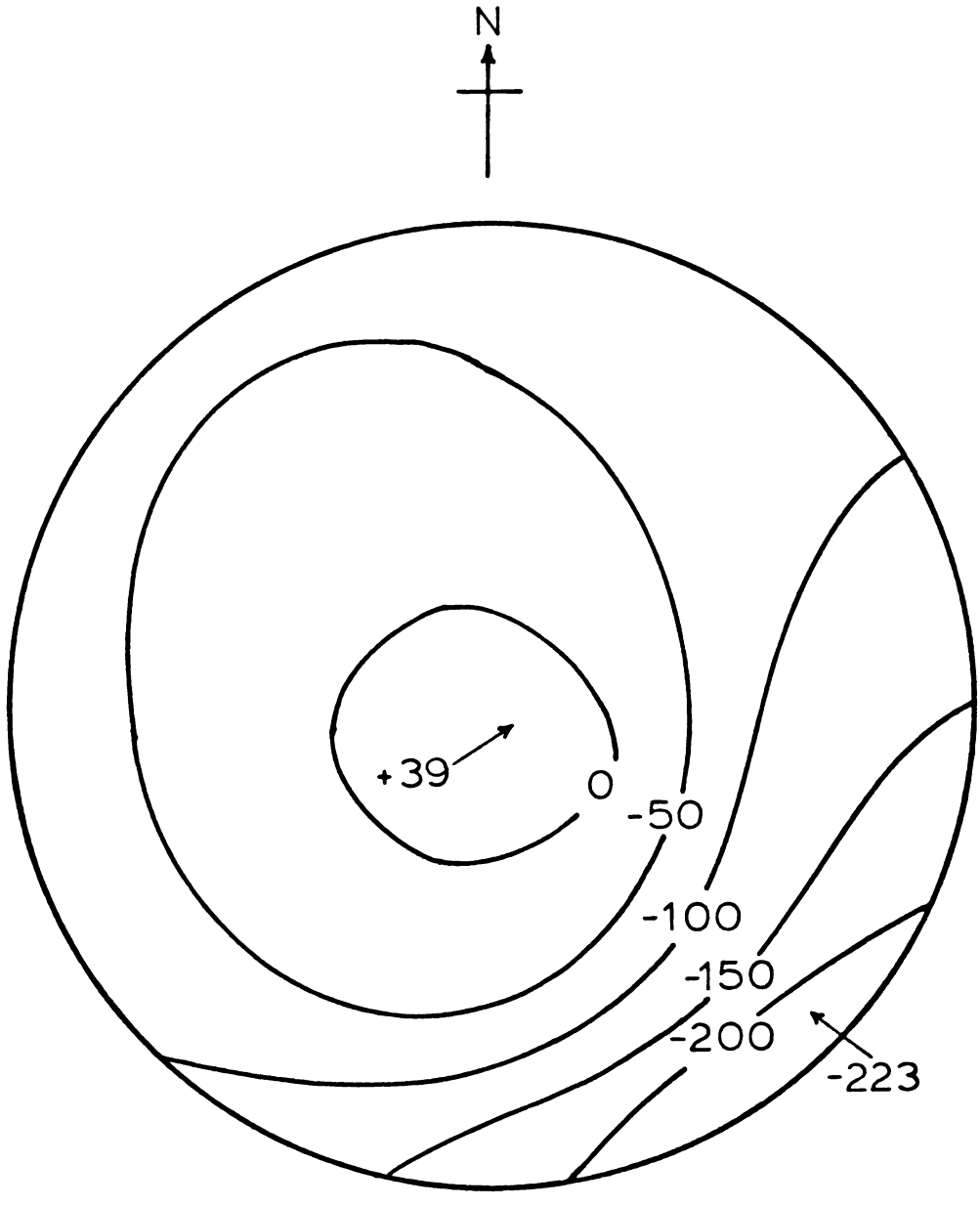

Figure 3.25.--Predicted tangential stress distribution in tree trunk, 9:00 A.M., 5 February 1969. (Scale 1.5X actual, stress values in psi.)

compressive stress, the crushing damage of the wood fiber structure would make the trunk more susceptible to tensile failure during subsequent temperature changes. Another possibility is that relaxation of the compressive stresses followed by heating and expansion of the internal trunk tissues could result in high tensile stresses in the area originally under severe compression.

Several facts must be kept in mind when considering the results of this section of the study. Firstly, the model was based on elastic theory and did not account for stress relaxation of the wood. However, the rather rapid temperature changes which were observed in the field study and reported in the literature would make it unlikely that stress relaxation could alleviate a major portion of the thermal stresses developed. For example, Bach and Rovner (1967) found that it took 100 minutes for the stresses in green Douglas fir to relax to 50% of original value. Therefore, stress relaxation will attenuate the stresses calculated but will not eliminate them.

The very positive fact which can be taken from the results of this analysis is that the order of magnitude of the tensile tangential stresses calculated is the same as for the few reported values of transverse strength of green wood presented in Section 2.2.1. Therefore, it only requires that somewhat more extreme temperature gradients occur in the tree trunk to result in destructive tensile stresses being developed.

4. DISCUSSION OF RESULTS

An overview of all four major portions of this study indicates that all results are consistent with a general pattern. The hypothesis that trunk splitting is the result of a thermal expansion phenomenon is supported by the data; however, there are certain special circumstances and occurrences which make this situation rather unique.

Firstly, consider the temperature patterns found in the field studies. The most interesting feature of these data is the temperature pattern which develops in a tree trunk in the evening of a cold, sunny day. These patterns are characterized by comparatively high temperatures near the center of the trunk and steep temperature gradients near the surface of the trunk. Cases were observed where the entire surface of the trunk was at a temperature below freezing while the inner portion was still above 32°F. This type of temperature field suggests a probable hoop stress situation, with the outer portion of the trunk trying to contract more quickly than the inner portion and developing a tensile tangential stress.

However, the situation is further complicated by the findings in the study of the coefficients of thermal expansion. At temperatures above 32°F, the magnitude of thermal strain is so small that concern about thermal stress is not justified. Below 32°F the picture changes abruptly. The coefficients of thermal expansion are

"large" compared to values for the coefficients above 32°F. Also, the thermal expansion characteristics show a marked anisotropy. The coefficients for bark, sapwood and heartwood are all significantly different from one another. Bark has the highest coefficient followed by sapwood; heartwood has the lowest coefficient. In the case of both sapwood and heartwood, the coefficients in the tangential direction were observed to be significantly greater than the coefficients in the radial direction. All of these phenomena tend to aggravate the hoop stress situation, when temperature is falling. First, it is possible to have a cylinder of material below 32°F surrounding an inner cylinder which is above 32°F. As temperature falls, this outer cylinder attempts to contract much more quickly than the inner cylinder. This aggravates the hoop stress system which normally would occur with the temperature gradient occurring in a homogeneous, isotropic material. Secondly, the anisotropic nature of the thermal expansion characteristics adds to the hoop stress situation; that is, the greater tendency to contract in the tangential direction compared to the radial direction is a condition which would induce a hoop stress in a cylinder with a decreasing, uniform temperature field. Therefore, the hoop stress is augmented by this phenomenon. Thirdly, if the tree is at a stage where heartwood has developed in its trunk center, the tendency of sapwood to contract faster than heartwood with decreasing temperature would set up a hoop stress in the sapwood. Finally, if the water in the trunk did supercool, only a matter of a few degrees, all of these effects could occur quite rapidly when crystallization did take place. This

is an important point, since wood is a viscoelastic material and the stresses developed undergo relaxation and will only reach dangerous levels if the temperature drops are relatively rapid (such as those shown in Figure 3.3) or if supercooling results in an abrupt crystallization and contraction.

The finite element model of the tree trunk subjected to the temperatures observed in the field served to verify the above discussion. The model was relatively simple in that only temperature fields entirely below 32°F were considered. The model did, however, consider the complex situation of plane strain in a body displaying cylindrical anisotropy. When data for the temperatures measured in rapidly cooling tree trunks was fed into the model, it predicted tensile tangential stresses near the surface of the tree trunk with the highest stress occurring at the point of highest temperature gradient.

These stresses were of the same order of magnitude as the few available values for ultimate tensile stress of wood in the tangential direction.

The model predicted compressive stresses in the radial direction for the entire trunk cross-section; this prediction is in line with the concept of a hoop-stress situation.

When the model was fed data for the case of rapidly rising trunk surface temperatures, the predicted internal tensile tangential stresses were an order of magnitude lower than any published values for ultimate tangential strength of fresh wood.

The microscopic investigation of frozen wood tissue shed some light on the mechanism by which the large sub-freezing coefficients of thermal expansion occur. Extracellular ice crystal formation results in progressive dehydration and shrinkage of the cells as temperature falls. The difference between the radial and tangential coefficients of thermal expansion is likely a function of anatomy, in that the ray cells tend to restrict the radial dimensional change of the tissues.

In summation, the data from this study indicate that a potentially destructive thermal stress situation may develop in tree trunks as the trunk cools in the evening of a cold, sunny day. This situation is aggravated by the high coefficients of thermal expansion, the anisotropy of thermal expansion properties of the wood and the different thermal expansion properties associated with heartwood and sapwood. Potential relief of high thermal stresses by the stress relaxation in the viscoelastic wood material is confounded if supercooling followed by abrupt crystallization occurs. The mechanism of the thermal contraction at sub-freezing temperatures is apparently a cell dehydration phenomenon with ice crystals forming in the intercellular spaces.

5. CONCLUSIONS

The data and analysis of this study lead to the following conclusions:

1. The coefficient of thermal expansion of Montmorency cherry wood is drastically increased at sub-freezing temperatures. This phenomenon is the result of cell dehydration with the formation of extracellular ice.

2. Thermal expansion in Montmorency cherry wood is anisotropic; the coefficient for the tangential direction is always greater than the coefficient for the radial direction. This is true for both sapwood and heartwood.

3. The coefficients of thermal expansion of Montmorency cherry bark, sapwood and heartwood are all different with bark exhibiting the greatest coefficient and heartwood exhibiting the smallest coefficient.

4. On a clear winter day, during which the ambient temperature is always sub-freezing, the majority of a tree trunk cross-section can reach temperatures above 32°F. Temperature differentials of 30°F or more between sunny and shaded sides of the tree can be observed.

5. Steep temperature gradients can occur near the surface of the tree trunk as the tree cools in the evening of a clear winter

day. Cases in which the unfrozen center of the tree is surrounded by frozen material have been observed.

6. A finite element model of the tree trunk cross-section predicts tensile tangential thermal stresses at the wood surface which are of the same order of magnitude as published values for the ultimate tensile tangential strength of fresh wood.

7. The same finite element model of the tree trunk predicts relatively low internal tensile tangential stresses in the tree trunk when subjected to the rapid heating of one surface as occurs in the morning of a clear winter day.

In summation, the data and analysis of this study support the hypothesis that low-temperature trunk splitting is the result of rapid thermal contraction of the surface of the tree trunk as it cools in the evening of a clear winter day.

6. SUGGESTED FUTURE RESEARCH

As in many research projects, more questions were raised than answered by this study. In order to answer these questions, many other research projects of the same or greater magnitude would have to be developed.

The first area in which this author found a real lack of information was the mechanical properties of fresh woody material. Those involved in research in the utilization of forest products have (understandably) focused their attention on the properties of dried lumber. It was most difficult to find reliable values for such parameters as modulus of elasticity or Poisson's ratio for fresh wood. The fact that wood is orthotropic served to make the problem even more difficult.

Secondly, information on the sub-freezing mechanical properties of fresh wood was even more difficult to find. Conclusions in this study were based on the assumption of similar mechanical properties of wood at temperatures below and above freezing. Considering the changes in moisture distribution within living wood tissue as the temperature goes below 32°F, one must suspect that assumption. Surely moisture migration will have a significant effect on the strength of the tissue; moreover, the viscoelastic nature of the material is almost certain to be altered by this movement and phase

change of the water within the material. To answer these questions alone implies a research program of considerable magnitude.

Another area which requires study is the effect of tree vigor and degree of winter hardiness on the problem of trunk splitting. The literature indicates that a vigorous, healthy tree will develop a greater degree of winter hardiness than an unhealthy tree. The development of winter hardiness entails physiological changes in the cell contents and cell wall. The protoplasm thickens, the vacuole decreases in size, and there is evidence to suggest that the permeability of the cell wall increases. All of these physiological changes can have profound effects on the physical processes which take place as the tissue is frozen. It would require a very comprehensive, interdisciplinary study to determine the effects of these physiological changes on the mechanism of trunk splitting.

APPENDICES

APPENDIX A

TEMPERATURE DATA:

1969

TABLE A.1.--Tree trunk temperatures,* 27 January 1969.

Thermocouple Number**	8:35 AM	9AM	10AM	11AM	12AM	1PM	2PM	3PM	4PM	5PM	6PM	7PM	8PM	9PM	10PM	11PM	12PM
1	2.0	7.4	17.2	26.5	31.6	34.5	39.4	39.4	40.8	31.3	29.0	25.5	20.0	17.5	16.5	15.0	14.3
2	1.0	4.8	15.8	25.5	30.0	32.5	35.4	37.0	38.5	34.7	33.6	30.2	22.8	18.9	17.2	15.5	14.4
3	1.2	4.0	14.4	24.2	29.4	32.4	34.5	37.0	38.7	35.4	33.7	30.7	23.3	19.0	17.5	15.6	14.5
4	1.5	4.1	15.5	25.1	29.6	32.4	34.5	36.3	37.0	34.8	33.8	30.5	23.3	19.0	17.5	15.7	14.6
5	1.5	4.5	16.4	25.8	29.8	32.4	33.3	34.0	34.0	33.5	33.5	39.4	23.0	19.0	17.5	15.8	14.5
6	1.5	2.5	11.7	21.1	26.2	30.0	30.9	32.2	34.4	34.2	33.5	30.0	23.4	19.1	17.5	15.7	14.6
7	1.5	3.2	14.5	24.0	28.2	30.7	32.0	33.0	34.3	33.7	33.9	29.5	23.5	19.2	17.7	15.9	14.7
8	1.7	3.5	14.5	23.5	27.5	30.0	30.7	31.5	31.9	32.2	32.0	28.0	22.6	19.2	17.8	16.0	14.7
9	2.5	6.1	16.3	24.0	26.5	28.5	29.4	30.0	30.5	30.0	28.8	24.6	20.5	18.2	17.5	15.9	14.7
10	3.0	9.4	22.5	30.5	32.0	33.7	34.5	34.3	33.6	32.2	31.2	26.3	20.6	18.5	17.5	15.9	14.7
11	2.3	3.2	11.7	20.5	25.2	28.1	29.5	30.8	32.0	32.4	32.0	28.4	22.9	18.9	17.5	15.8	14.7
12	8.0	15.5	28.0	34.5	36.5	38.2	38.8	37.5	34.0	28.5	26.5	23.0	18.9	17.3	16.8	15.3	14.5
13	11.0	22.0	33.7	33.5	34.0	32.4	32.0	31.1	29.8	28.0	26.4	22.0	18.5	17.2	16.7	15.3	14.5
14	6.4	8.7	16.0	22.0	29.0	26.0	27.1	28.1	28.0	26.5	24.3	20.5	18.0	16.8	16.4	15.0	14.1
15	3.9	5.5	13.1	20.2	29.5	27.0	29.0	30.0	31.8	31.0	28.3	24.9	20.3	17.4	16.4	15.0	14.1
16	3.7	5.5	14.0	22.5	27.2	31.6	37.7	41.8	42.7	35.1	29.2	26.6	21.0	17.4	16.4	15.0	14.1

*Temperatures in deg. F.

**Refer to Fig. 3.1

Meterological Data:
Maximum temperature 26°F
Minimum temperature -1°F
Wind (average) 8.3 mph E
Precipitation: 0.0 in. sleet, snow
0.0 in. water equivalent
Sunshine duration 9.8 hr. 100% of possible
Sky cover 0/10 (sunrise to sunset)
2/10 (midnight to midnight)

(Source: Environmental Science Service Administration, Capital City Airport, Lansing, Michigan.)

TABLE A.2.--Tree trunk temperatures,* 5 February 1969.

Thermocouple Number**	1AM	2AM	3AM	4AM	5AM	6AM	7AM	8AM	9AM	10AM	11AM	12AM	1PM	2PM	3PM	4PM	5PM	6PM	7PM	8PM	9PM	10PM	11PM
1	16.8	17.6	16.2	14.2	13.4	11.8	9.9	6.6	11.6	22.4	30.7	39.0	44.8	49.0	55.0	51.8	40.2	30.4	29.0	26.5	21.0	15.8	12.0
2	16.2	17.6	16.7	15.0	13.7	12.4	10.7	7.3	10.3	21.4	28.7	35.0	43.2	43.8	48.2	49.9	40.7	33.0	33.6	31.2	24.9	18.2	14.0
3	16.2	17.6	16.8	15.1	14.0	12.5	10.8	7.5	9.3	19.8	27.0	32.5	40.9	42.0	47.0	49.0	40.9	33.2	33.9	31.8	25.1	18.4	14.3
4	16.2	17.6	16.9	15.2	14.0	12.8	11.0	7.5	9.8	21.0	28.0	34.0	41.5	42.3	46.1	48.1	40.4	33.2	34.0	32.0	25.4	18.7	14.4
5	16.2	17.7	17.0	15.5	14.1	13.0	11.1	7.9	10.5	22.0	29.0	37.0	42.2	41.7	44.0	45.4	39.0	33.5	34.1	31.8	25.4	18.8	14.5
6	16.3	17.7	17.0	15.5	14.2	13.0	11.2	7.8	7.5	16.8	23.1	28.6	32.5	34.5	38.2	43.4	38.4	33.9	34.2	31.2	25.1	18.5	14.4
7	16.3	17.7	17.2	15.5	14.3	13.1	11.3	7.9	9.0	20.0	26.6	31.9	36.7	38.2	40.5	43.0	38.4	34.2	34.4	33.0	25.8	19.0	14.7
8	16.3	17.7	17.2	15.7	14.3	13.1	11.3	7.9	9.5	20.0	26.0	30.5	33.0	34.3	35.6	38.2	36.1	34.3	34.3	31.5	25.6	19.0	15.0
9	16.6	18.0	17.0	15.7	14.4	13.2	11.3	7.6	11.5	20.5	25.3	28.8	30.5	31.0	31.0	32.7	33.0	32.8	31.0	28.0	23.0	17.8	14.2
10	16.6	18.0	17.0	15.3	14.2	12.9	11.1	7.6	16.1	27.5	35.1	43.3	44.5	42.7	43.0	42.3	36.5	33.6	32.5	29.6	24.1	18.0	14.2
11	16.6	18.0	17.0	15.3	14.2	12.9	11.0	7.5	8.1	16.6	22.2	26.8	29.5	30.5	31.6	35.1	35.0	33.7	32.6	29.6	24.3	18.0	14.2
12	17.1	18.0	16.8	14.7	14.1	12.1	9.4	6.8	21.0	34.8	46.6	55.0	52.4	49.8	49.8	47.9	35.5	29.0	27.0	25.0	20.2	15.5	12.3
13	17.6	18.0	16.5	14.8	13.9	12.2	9.5	7.0	26.7	40.5	45.0	47.2	45.5	41.8	37.0	37.0	30.7	27.7	25.6	23.9	18.9	14.9	12.5
14	18.0	18.2	16.7	14.8	14.5	12.4	9.5	6.1	11.6	18.2	21.8	27.0	29.5	28.0	28.0	27.7	28.1	26.4	23.4	21.1	16.5	13.9	11.9
15	17.6	18.1	16.5	14.8	14.0	12.2	9.5	6.2	9.2	16.7	21.3	25.5	28.0	29.0	29.0	32.1	31.9	29.5	27.2	25.5	21.0	15.5	12.2
16	--	--	--	--	--	--	--	--	--	--	--	--	--	--	--	--	--	--	--	--	--	--	--

*Temperatures in deg. F.

**Refer to Fig. 3.1

Meterological Data:
Maximum temperature 25°F
Minimum temperature 4°F
Wind (average) 8.5 mph W
Precipitation: 0.0 in. snow, sleet
0.0 in. water equivalent

Sunshine duration 10.1 hr.
99% of possible

Sky cover 4/10 (sunrise to sunset)
3/10 (midnight to midnight)

(Source: Environmental Science Service Administration, Capital City Airport, Lansing, Michigan.)

APPENDIX B

TEMPERATURE DATA:

1970

TABLE B.1.--Tree trunk temperature* data, 14 January 1970.

Time	Thermocouple Number**											
	1	2	3	4	5	6	7	8	9	10	11	12
12:46 AM	3.3	2.8	2.8	3.0	3.8	3.2	5.0	5.2	5.2	4.9	5.2	5.2
1:38 AM	2.7	2.0	2.1	2.5	2.7	3.1	3.8	4.0	3.8	3.7	3.9	4.0
2:30 AM	3.5	2.9	2.8	3.1	3.9	4.2	3.2	3.2	3.2	3.2	3.3	3.6
3:22 AM	2.8	2.7	3.0	3.3	3.9	4.5	3.3	3.3	3.3	3.3	3.5	3.4
4:14 AM	4.3	4.7	4.5	4.8	5.5	5.5	3.8	3.7	3.7	3.8	4.2	4.2
5:06 AM	5.6	5.2	5.4	5.6	6.3	6.2	5.0	5.0	5.0	5.0	5.4	5.3
5:58 AM	3.7	3.5	3.3	3.7	4.0	3.9	4.9	4.9	4.7	4.7	4.8	4.8
6:50 AM	4.6	4.8	4.7	5.0	5.2	5.0	4.7	4.7	4.6	4.8	4.9	4.8
7:42 AM	4.4	4.7	4.9	5.0	5.1	4.5	4.9	4.9	4.8	4.8	5.0	4.9
8:34 AM	5.0	5.3	5.7	5.7	5.8	5.5	4.3	4.3	4.3	4.4	4.4	4.3
9:26 AM	7.1	8.0	8.6	8.1	8.1	7.8	6.0	6.0	6.0	6.2	6.2	6.2
10:18 AM	11.2	13.8	14.5	12.8	12.7	11.8	9.0	8.9	9.2	9.3	9.3	9.2
11:10 AM	16.2	21.6	19.4	16.7	16.6	16.0	14.9	14.7	14.9	14.6	13.8	13.8
12:02 PM	20.5	27.5	22.4	19.3	18.8	17.9	19.3	18.8	18.8	17.7	17.0	17.3
12:54 PM	24.8	27.3	26.4	24.3	22.0	23.0	23.6	23.0	23.0	21.4	20.4	21.1
1:46 PM	32.9	27.4	29.6	27.6	25.7	28.8	26.5	25.8	26.1	24.4	24.0	24.2
2:38 PM	36.3	28.8	25.3	27.5	26.3	32.0	29.0	28.2	27.8	25.9	26.2	27.6
3:30 PM	42.2	33.8	23.6	26.7	26.0	33.5	32.0	31.1	30.4	27.4	28.5	30.9
4:22 PM	41.0	24.2	19.5	23.1	22.5	30.0	32.5	31.7	30.6	26.0	27.8	30.6
5:14 PM	28.8	19.4	15.3	18.8	18.0	24.2	30.8	30.1	28.5	24.1	26.2	30.1
6:06 PM	26.9	17.7	13.5	14.6	15.0	21.3	27.3	26.7	24.1	20.5	22.9	26.8
6:58 PM	23.6	14.0	10.6	11.2	11.2	16.0	22.3	22.1	20.0	16.9	18.8	21.9
7:50 PM	14.3	10.9	8.3	8.6	9.1	11.8	16.4	16.3	15.2	12.9	14.0	15.7
8:42 PM	8.6	7.0	5.4	6.1	6.8	7.2	11.2	11.1	10.6	9.3	10.0	10.7
9:34 PM	5.9	4.8	4.5	5.1	5.2	5.4	8.0	8.1	7.9	7.1	7.4	7.6
10:26 PM	5.0	4.8	4.8	4.9	4.9	4.9	6.2	6.2	6.2	5.9	6.0	6.2
11:18 PM	4.3	4.9	5.1	4.8	4.7	5.0	5.1	5.1	5.2	5.0	5.0	5.1

*Temperature in deg. F.

**Refer to Fig. 3.8.

Meterological Data:
Maximum temperature 17 F
Minimum temperature -2 F
Wind (average) 4 mph, N.E.
Precipitation 0.0 in. snow, sleet
0.0 in. water equivalent
Sunshine duration 7.0 hr. (75 % of possible)
Sky cover 7/10 (sunrise to sunset
7/10 (midnight to midnight)

(Source: Environmental Science Services Administration, Capital City Airport, Lansing, Michigan.)

TABLE B.2.--Tree trunk temperature* data, 18 January 1970.

Time	Thermocouple Number **											
	1	2	3	4	5	6	7	8	9	10	11	12
12:38 AM	15.6	15.7	-	16.0	15.8	15.8	16.4	16.4	16.5	16.3	16.3	16.3
1:30 AM	15.4	15.5	-	15.6	15.5	15.6	16.3	16.2	16.2	16.2	16.2	16.2
2:22 AM	15.2	15.3	-	15.5	15.3	15.3	16.1	16.0	16.0	16.0	16.0	15.9
3:14 AM	14.9	14.8	-	15.1	15.1	15.0	15.8	15.8	15.7	15.6	15.7	15.6
4:06 AM	14.6	14.6	-	14.9	14.7	15.0	15.5	15.3	15.3	15.3	15.4	15.3
4:58 AM	14.4	14.2	-	14.4	14.4	14.5	15.3	15.2	15.3	15.0	15.1	15.1
5:50 AM	13.3	13.3	-	13.4	13.5	13.5	14.6	14.5	14.6	14.4	14.3	14.3
6:42 AM	13.0	12.9	-	13 0	13.2	13.1	13.8	13.8	13.8	13.6	13.6	13.6
7:34 AM	10.6	10.0	-	10.8	10.3	10.3	13.2	13.2	13.3	12.9	12.8	13.0
8:26 AM	7.6	11.7	-	10.1	7.9	7.9	10.3	10.3	10.7	10.6	9.9	10.0
9:18 AM	10.1	20.9	-	14.0	10.2	10.0	13.0	12.6	14.5	13.8	10.0	10.0
10:10 AM	16.6	32.4	-	19.4	15.1	14.5	19.1	18.4	20.4	18.9	13.9	14.2
11:02 AM	22.3	39.8	-	23.6	19.2	18.8	25.1	24.3	26.3	24.0	18.6	19.1
11:54 AM	28.7	47.5	-	25.4	21.8	22.8	29.5	28.6	30.3	27.4	22.3	23.4
12:46 PM	29.7	40.9	-	26.5	22.3	25.5	34.7	33.4	36.0	30.8	25.4	27.2
1:38 PM	33.2	34.6	-	26.9	23.5	26.4	35.3	34.5	36.1	31.7	27.4	29.3
2:30 PM	36.6	45.2	-	29.4	25.5	26.7	34.9	33.5	34.2	30.6	27.5	29.3
3:22 PM	48.5	46.5	-	27.6	24.0	33.5	37.0	35.6	35.3	31.4	28.7	31.2
4:14 PM	41.2	37.7	-	25.7	22.1	31.0	38.1	36.5	35.3	30.2	28.0	31.0
5:06 PM	29.0	26.5	-	21.5	18.7	24.5	35.0	35.0	34.8	29.0	27.9	30.6
5:58 PM	26.6	23.4	-	16.8	14.8	20.1	33.0	32.3	31.6	25.3	23.5	27.2
6:50 PM	22.3	18.6	-	13.3	12.3	16.0	29.0	28.0	26.7	20.7	20.0	23.0
7:42 PM	11.8	10.9	-	9.7	9.0	10.0	19.8	19.8	19.6	16.0	15.4	16.8
8:34 PM	5.6	5.5	-	5.7	5.3	5.3	11.3	11.7	12.0	10.4	9.9	10.1
9:26 PM	3.0	2.2	-	3.3	3.2	2.6	6.7	6.9	7.2	6.4	6.0	6.1
10:18 PM	-	-	-	0.5	0.2	-	3.4	3.5	3.9	3.4	3.0	2.8
11:10 PM	-	-	-	-	-	-	0.7	0.9	1.2	1.0	0.8	0.7

*Temperature in deg. F.

**Refer to Fig. 3.8.

Meterological Data:
Maximum temperature 17 F
Minimum temperature -14 F
Wind (average) 7.6 mph N.W.
Precipitation 0.0 in. snow. sleet
0.0 in. water equivalent
Sunshine duration 9.5 hrs (100 of possible)
Sky cover 1/10 (sunrise to sunset)
4/10 (midnight to midnight)

(Source: Environmental Science Services Administration, Capital City Airport, Lansing, Michigan.)

APPENDIX C

THERMAL EXPANSION DATA

TABLE C.1.--Data from coefficient of thermal expansion study, tree no. 1.

Sample Number	Moisture Content % w.b.	Dry Density lb/ft^3	Lowest Temp.	α Fall $\mu\varepsilon/°F$	α Rise $\mu\varepsilon/°F$
1 BT 1	46.8	34.1	+5	503	367
3	37.0	34.2	+4	364	271
4	41.9	33.8	-7	376	266
5	45.8	32.3	-7	373	222
6	43.7	32.8	-7	347	224
8	44.6	34.6	-4	307	177
1 XT 2	48.7	36.0	+7	243	237
3	40.7	33.7	-8	321	295
4	45.5	32.6	-8	250	--
5	43.0	32.2	-2	385	349
6	38.4	33.5	-2	339	307
7	36.9	35.3	-1	302	277
8	40.0	31.7	-2	281	260
1 XR 1	44.3	33.8	-8	130	--
2	42.3	34.1	-5	147	139
4	42.1	34.5	-8	125	116
5	42.4	34.8	-6	111	105
6	38.9	31.9	-6	135	126
7	35.2	33.3	-4	169	117
1 HT 1	33.1	30.6	+3	100	151
3	28.3	32.5	-8	106	122
5	26.5	30.9	-2	107	109
6	32.9	33.8	-2	146	158
7	35.4	32.9	-3	132	136
8	31.3	26.1	-3	129	129
1 HR 1	35.4	31.5	-4	77	76
3	37.2	31.2	-6	82	77
4	30.2	33.3	-6	89	90
5	29.5	34.0	-4	89	82
6	27.8	31.6	-4	91	84
7	30.2	34.0	-3	65	61
8	31.6	34.2	-2	58	71

TABLE C.2.--Data from coefficient of thermal expansion study, tree no. 2.

Sample Number	Moisture Content % w.b.	Dry Density lb/ft^3	Lowest Temp.	α Fall $\mu\varepsilon$/°F	α Rise $\mu\varepsilon$/°F
2 BT 1	46.5	34.9	-4	370	237
2	47.0	31.4	-4	338	208
5	47.4	32.4	+1	--	274
6	46.7	34.4	+1	--	316
7	47.2	28.2	+3	501	358
8	45.0	32.4	+3	393	222
2 XT 1	41.2	33.9	-7	244	227
2	41.3	34.0	-7	251	238
3	40.6	32.2	-1	292	272
4	39.1	32.6	-1	311	291
5	43.7	32.4	+1	253	294
6	41.7	31.5	+1	327	332
2 XR 1	39.5	34.4	-7	148	134
2	35.0	35.0	-7	109	99
3	39.7	26.4	-1	150	140
4	40.2	32.3	-1	142	92
5	39.7	34.6	+3	143	185
6	40.7	33.7	+3	192	176
2 HT 1	31.0	29.7	-2	193	183
2	30.6	25.0	-2	153	151
3	35.8	34.2	+1	181	159
4	36.3	33.9	+1	157	147
5	33.9	32.5	+3	170	151
6	35.4	34.7	+3	159	144
2 HR 1	32.6	34.3	-3	75	69
2	28.3	31.4	-3	85	79
3	27.5	28.6	-5	72	67
4	33.4	34.9	-5	81	73
5	31.2	33.3	-6	89	78

TABLE C.3.--Data from coefficient of thermal expansion study, tree no. 3.

Sample Number	Moisture Content % w.b.	Dry Density lb/ft^3	Lowest Temp.	α Fall $\mu\varepsilon$/°F	α Rise $\mu\varepsilon$/°F
3 BT 1	48.2	30.2	-3	352	171
2	47.2	30.8	-3	317	188
3	48.3	31.3	+3	326	192
4	48.5	29.1	+1	347	233
5	48.9	30.4	+1	402	234
6	47.1	29.8	+6	370	219
7	47.0	30.2	-1	355	171
8	46.6	30.3	-1	364	228
3 XT 1	44.4	34.4	+1	277	320
2	42.2	30.3	+1	365	391
3	43.6	32.2	+3	359	293
4	39.1	21.7	+3	256	298
5	38.6	29.9	-3	345	259
6	39.2	31.4	-2	270	243
3 XR 1	38.8	33.9	+1	--	179
2	39.4	34.1	+1	--	182
3	41.4	33.1	+2	105	192
4	40.1	33.2	+2	97	170
5	37.7	33.4	0	154	144
6	37.3	32.7	+1	173	164
3 HT 1	29.1	33.4	+3	120	144
2	28.9	31.0	+3	96	154
3	27.3	31.0	+2	139	129
4	26.3	32.2	+2	122	109
3 HR 1	27.0	31.9	0	72	64
2	26.3	32.1	0	57	48
3	29.7	33.6	+4	96	84
4	29.6	32.7	+4	71	63
6	28.9	33.7	-1	80	72

TABLE C.4.--Data from coefficient of thermal expansion study, tree no. 4.

Sample Number	Moisture Content % w.b.	Dry Density lb/ft^3	Lowest Temp.	α Fall $\mu\varepsilon$/°F	α Rise $\mu\varepsilon$/°F
4 BT 1	50.0	29.2	+4	435	256
2	50.0	--	+4	463	230
3	49.3	29.3	+1	380	189
4	49.0	31.0	+1	379	207
5	47.3	30.7	-1	323	189
6	47.2	28.6	+2	480	307
4 XT 1	44.7	32.4	-1	302	209
2	45.3	32.5	-1	227	248
3	43.9	32.9	+5	161	155
4	46.8	33.1	+5	147	143
5	41.3	33.1	+4	315	249
6	42.7	30.9	+5	258	252
4 XR 1	44.0	32.9	+1	169	--
2	44.8	31.9	+1	155	--
3	44.9	33.0	+6	148	142
4	43.4	31.8	+6	161	137
5	40.0	32.5	+5	159	156
6	39.6	31.1	+5	180	148
4 HT 3	31.6	33.2	+4	213	166
4	32.0	31.5	+4	182	170
5	31.8	33.3	+5	171	168
6	30.2	33.0	+3	138	169
4 HR 1	31.5	27.8	+4	80	75
3	30.4	--	+1	81	74
4	30.9	31.1	+1	76	66
5	31.0	30.3	+3	44	67

LIST OF REFERENCES

LIST OF REFERENCES

Anonymous. 1975 Michigan Agricultural Statistics, Michigan Crop Reporting Service, Michigan Department of Agriculture, Lansing, Michigan.

Anonymous. 1974 Wood Handbook. The Forest Products Laboratory, U.S. Dept. of Agriculture.

Anthony, R. D., R. H. Sudds and W. S. Clarke, Jr. 1936 Low temperature injury to orchards in Pennsylvania and adjoining states in the fall and winter of 1935-36. Proc. Amer. Soc. Hort. Sci. 34: 33-43.

A.S.T.M. 1968 Linear thermal expansion of rigid solids with a vitreous silica dilatometer. A.S.T.M. designation E 228-66aT, A.S.T.M. standards, part 31.

Bach, L. and B. Rovner. 1967 Stress relaxation in wood at different angles. Forest Products Laboratory, Vancouver, B.C. Information report VP-X-14.

Bach, L. and R. E. Pentony. 1968 Non-linear mechanical behavior of wood. For. Prod. J. 18 (3): 60-66.

Bodig, J. and J. R. Goodman. 1973 Prediction of elastic parameters for wood. Wood Sci. 5 (4): 249-264.

Boley, B. A. and J. H. Weiner. 1960 Theory of Thermal Stresses. John Wiley and Sons, New York.

Brierley, W. G., W. H. Alderman and T. S. Weir. 1950 Winter injury to apple trees in Minnesota, 1947-48. Proc. Amer. Soc. Hort. Sci. 55: 259-261.

Brown, M. S., E. S. B. Pereira and B. J. Finkle. 1974 Freezing of non-woody plant tissues II - Cell damage and the fine structure of the freezing curves. Plant Phys. 53: 709-711.

Choong, E. T. and P. J. Fogg. 1968 Moisture movement in six wood species. For. Prod. J. 18 (6): 66-70.

Comben, A. J. 1964 The effect of low temperatures on the strength and elastic properties of timber. Inst. of Wood Sci. J. 13: 44-55.

Derby, R. W. and D. M. Gates. 1966 The temperature of tree trunks--calculated and observed. Amer. J. of Botany 53 (6): 580-587.

Diener, R. G., F. H. Buelow and G. E. Mose. 1968-a Viscoelastic analysis of the behaviour and properties of cherry bark and wood under static and dynamic loading. Trans. Amer. Soc. Agr. Eng. 11 (3): 323-330.

Diener, R. G., J. H. Levin and B. R. Tennes. 1968-b Directional strength properties of cherry, apple and peach bark and influence of limb mass and diameter on bark damage. Trans. Amer. Soc. Agr. Eng. 11 (6): 788-791.

Eggert, R. 1944 Cambium temperatures of peach and apple trees in winter. Proc. Amer. Soc. Hort. Sci. 45: 33-36.

Erickson, H. D., R. N. Schmidt and J. R. Laing. 1968 Freeze-drying and wood shrinkage. For. Prod. J. 18 (6): 63-68.

Erickson, H. D. and R. W. Petersen. 1969 The influence of prefreezing and cold water extraction on the shrinkage of wood. For. Prod. J. 19 (4): 53-57.

Esau, K. 1965 Plant Anatomy. John Wiley and Sons, Inc., New York.

Evert, D. R. and C. J. Weiser. 1971 Relationship of electrical conductance at two frequencies to cold injury of Cornus stolinifera Michx. Plant Phys. 47: 204-208.

Gerhards, C. C. 1970 Further report on seasoning factors for modulus of elasticity and modulus of rupture. For. Prod. J. 20 (5): 40-41.

Glerum, C. 1973 Annual trends in frost hardiness and electrical impedance for seven coniferous species. Can. J. of Plant Sci. 53: 881-889.

Hammerle, J. R. 1968 Failure in a thin viscoelastic slab subjected to temperature and moisture gradients. Unpublished Ph.D. thesis, Pennsylvania State University.

Harvey, R. B. 1923 Cambial temperatures of trees in winter and their relation to sunscald. Ecology 4: 261-265.

Herrington, L., J. Parker and E. B. Cowling. The coefficient of
1964 expansion of wood in relation to frost cracks. Phytopathology 54: 128.

Hoyle, R. Introduction to thermal stress and strain. Thermal
1964 Stress. P. P. Benham and R. Hoyle, editors. Sir Isaac Pitman and Sons Ltd., London.

Ishmukhametova, N. N. and L. P. Khokhlova. Use of the dielcometric
1971 method to study the state of water in leaves of winter plants. Sov. Plant Phys. 18 (1): 139-144.

Jensen, R. E., E. F. Savage and R. A. Hayden. The effect of certain
1970 environmental factors on cambium temperatures in peach trees. J. Amer. Soc. Hort. Sci. 95 (3): 286-292.

Johns, D. J. Thermal Stress Analysis. Pergamon Press, Oxford, U.K.
1965

Joule, J. P. On some thermodynamic properties of solids. Phil.
1859 Trans. Roy. Soc. 149: 91-131.

Kass, A. J. Shrinkage stresses in externally restrained wood.
1965 For. Prod. J. 15 (6): 225-232.

Kennedy, R. W. Wood in transverse compression. For Prod. J.
1968 18 (3): 36-40.

Kollmann, F. F. P. and W. A. Côté, Jr. Principles of Wood Science
1968 and Technology. Springer-Verlag, New York.

Konstantinov, L. K. Effect of sharp temperature fluctuations on
1971 apple bark and cambium during the winter-spring period. Sov. Plant Phys. 18 (2): 352-355.

Konstantinov, L. K. and V. V. Batalov. Light and thermal regime
1972 of woody plants during the winter and its effect on the frost resistance of tissues. Sov. Plant Phys. 19 (1): 40-44.

Krasavtsev, O. A. Amount of unfrozen water in woody plants at
1968 different temperatures. Sov. Plant Phys. 15 (2): 191-198.

Krasavtsev, O. A. Rate of water outflow from cells of frost
1970 resistant plants at negative temperatures. Sov. Plant Phys. 17: 417-422.

Krasavtsev, O. A. Microscope data on content and distribution
1973 of water in frozen cells. Sov. Plant Phys. 20 (2): 194-200.

Krasavtsev, O. A. and G. I. Tutkevich. Electron microscope
1970 investigation of freezing and frost death in woody plants. Sov. Plant Phys. 17: 317-323.

Krasavtsev, O. A. and G. I. Tutkevich. Ultrastructure of bark
1971 parenchyma cells in woody plants in connection with their frost resistance. Sov. Plant Phys. 18 (3): 507-513.

Kübler, H. Shrinkage and swelling of wood by coldness. Holz
1962 al Roh-und-Werkstoff 20 (9): 364-368.

Kunesh, R. H. Strength and elastic properties of wood in
1968 transverse compression. For. Prod. J. 18 (1): 65-72.

Larsen, P. Out on a limb. American Fruit Grower 88 (6): 28.
1968

Larsen, P. Personal communications, East Lansing, Michigan,
1968 July 19.

Lekhnitskii, S. G. Theory of Elasticity of an Anisotropic Elastic
1963 Body. Holden-Day, Inc., San Francisco.

Marks, L. S., editor. Mechanical Engineer's Handbook, sixth
1964 edition. McGraw-Hill, New York.

Martin, R. E. Interim volumetric expansion values for bark.
1968 For. Prod. J. 18 (4): 52.

Martin, R. E. and J. B. Crist. Selected physical-mechanical
1968 properties of eastern tree barks. For. Prod. J. 18 (11): 54-60.

McLeester, R. C., C. J. Weiser and T. C. Hall. Multiple freezing
1969 points as a test for viability of plant stems in the determination of frost hardiness. Plant Phys. 44: 37-44.

Nowacki, W. Thermoelasticity. Addison-Wesley Publishing Co.,
1962 Reading, Massachusetts.

Olien, C. R. Freezing processes in the crown of Hudson barley.
1964 Crop Sci. 4: 91-95.

Palka, L. C. Predicting the effect of specific gravity, moisture
1973 content, temperature and strain rate on the elastic properties of softwoods. Wood Sci. and Tech. 7: 127-141.

Parker, J. 1963 Cold resistance in woody plants. The botanical review 29 (2): 137-147.

Perry, J. H., editor. 1950 Chemical Engineer's Handbook, third edition. McGraw-Hill Publishing Co., New York.

Pogosyan, K. S. 1971 Effect of freezing rate on survival of grapevine tissues. Sov. Plant Phys. 18 (1): 145-150.

Pogosyan, K. S. and A. Sakai. 1972 Effect of thawing speed on survival of grapevine plants. Sov. Plant Phys. 19 (6): 1023-1028.

Quamme, H., C. Stushnoff and C. J. Weiser. 1972 The relationship of exotherms to cold injury in apple stem tissues. J. Amer. Soc. Hort. Sci. 97 (5): 608-613.

Quamme, H., C. J. Weiser and C. Stushnoff. 1973 The mechanism of freezing injury in xylem of winter apple twigs. Plant Phys. 51: 273-277.

Rawlings, C. O. and G. F. Potter. 1936 Unusual and severe winter injury to the trunks of McIntosh apple trees in New Hampshire. Proc. Amer. Soc. Hort. Sci. 34: 44-48.

Rubenstein, L. I. 1971 The Stefan Problem. Translations of mathematical monographs, 27. American Mathematical Society, Providence, Rhode Island.

Sakai, A. and K. Otsuka. 1967 Survival of plant tissue at super low temperature, V. An electron microscope study of ice in cortical cells cooled rapidly. Plant Phys. 42: 1680-1694.

Schirp, M. and H. Kübler. 1968 Investigations on dimensional changes of small wood samples during cooling. Holz al Roh- und Werkstoff 26 (9): 335-341.

Segerlind, L. J. 1976 Applied Finite Element Analysis. John Wiley and Sons, Inc., New York.

Simons, R. K. 1970 Phloem tissue development in response to freeze injury to trunks of apple trees. J. Amer. Soc. Hort. Sci. 95 (2): 182-190.

Skaar, C. and W. Simpson. 1968 Thermodynamics of water sorption by wood. For. Prod. J. 18 (7): 49-58.

Sliker, A. 1972 Measuring Poisson's ratios in wood. Experimental mechanics 12: 239-242.

Sliker, A. 1975 Young's modulus of wood as affected by strain rate, grain angle and stress level. Wood Sci. 7 (3): 223-231.

Sliker, A. 1976 Personal communications. East Lansing, Michigan, May 11.

Stamm, A. J. 1969 Wood and Cellulose Science. Ronald Press, New York.

Sylvester, F. D. 1966 Mechanical Properties of Timber. Pergamon Press, New York.

Tingley, M. A. 1937 Case history of two winter injured Baldwins. Proc. Amer. Soc. Hort. Sci. 35: 135.

Vorreiter, V. 1938 Bending strength and resistance to compression of frozen spruce timber. Thar. For. Jahrb. 89: 491-510.

Wangaard, F. F. 1950 The Mechanical Properties of Wood. John Wiley and Sons, Inc., New York.

Weatherwax, R. C. and A. J. Stamm. 1947 The coefficients of thermal expansion of wood and wood products. Trans. Amer. Soc. Mech. Eng. 69 (4): 421-432.

Weiser, C. J. 1970 Cold resistance and injury in woody plants. Science 169: 1269-1278.

Yokota, T. and H. Tarkow. 1962 Changes in dimension on heating green wood. For. Prod. J. 12 (1): 43-45.

Youngs, R. L. and B. A. Bendtsen. 1964 Tensile, compressive and shearing stresses developed in red oak as it dries. For. Prod. J. 14 (3): 113-118.